A Hydrodynamic Model of the Atchafalaya Basin

EVALUATING RESTORATION ALTERNATIVES PHASE 2

Moffatt and Nichol started the development of a 2-D hydrodynamic model of the Atchafalaya Basin, capable of informing and testing proposals for improving environmental management of sediment, water and renewable resources within the Basin. This report documents the model development, calibration, validation and a set of possible application scenarios to aid in management optimization and evaluation.

moffatt & nichol

One American Place
301 Main Street, Suite 800
Baton Rouge, LA 70825
www.moffattnichol.com

August 2012

ATCHAFALAYA BASIN MODEL

A HYDRODYNAMIC MODEL OF THE ATCHAFALAYA BASIN

EVALUATING RESTORATION ALTERNATIVES PHASE 2

FINAL REPORT
Prepared for:

Audubon

ATCHAFALAYA BASIN MODEL

FINAL REPORT

A HYDRODYNAMIC MODEL OF THE ATCHAFALAYA BASIN

Rev No	A	B	–	–	–
Issue Purpose	Client Approval	Final Report			
Date	May 15th 2012	August 1st 2012			
By	MK	KH			
Checked		MK			
Approved		JH			

TABLE OF CONTENTS

1.0 INTRODUCTION 15

1.1 Project Background 15
1.2 Atchafalaya Basin and Bay - Study Area 16
1.3 Study Objectives 19
1.4 Study Approach 19

2.0 DATA COLLECTION AND DATA INVENTORY 21

2.1 Introduction 21
2.2 Hydraulic data 21
2.2.1 Available Data 21
2.2.2 2011 Field Campaign 25
2.3 Bathymetric and topographic data 26
2.4 Synopsis Data collection and inventory 26

3.0 MODEL DEVELOPMENT 29

3.1 Model Domain and Boundary conditions 29
3.1.1 Model domain and grid 29
3.1.2 Bathymetry 34
3.1.3 Water Level Boundaries 36
3.1.4 Discharge Boundaries 36
3.2 Roughness Settings 37
3.3 Assumptions and limitations 39
3.4 Model Parameters settings 40
3.4.1 Eddy viscosity 40
3.5 Output parameters and locations 40
3.6 Model Implementation 42

4.0 MODEL CALIBRATION 43

4.1 Introduction 43
4.2 Water Level Calibration 45
4.2.1 Measured and Calculated Time Series Comparisons 45
4.2.2 Spatial Distribution of Water Level Calibration Results 58
4.2.3 Flood Arrival Timing 60
4.2.4 Tidal Constituent Analysis 60
4.3 Discharge and Current Calibration 65
4.3.1 Measured and Calculated Discharge Comparison 66
4.3.2 Measured and Calculated Current Comparison 69
4.3.3 Rating Curves and Discharge Distribution through Outlets 72
4.4 Synopsis of Model Calibration 75

5.0 VALIDATION 77

5.1 Introduction 77
5.2 Water Level Validation 78
5.2.1 Measured and Calculated Time Series Comparisons 78
5.2.2 Spatial Distribution of Water Level Validation Results 88
5.3 Discharge and Current Validation 90
5.3.1 Measured and Calculated Discharge Comparisons 90
5.3.2 Measured and Calculated Current Comparisons 92
5.3.3 Discharge Distribution through Outlets 94
5.4 Synopsis of Model Validation 95

6.0 HYDRODYNAMIC PRE-SCREENING SCENARIO RUNS 97

6.1 Introduction 97
6.2 Pulse Flood 97
6.2.1 Scenario Description.....97
6.2.2 Boundary Conditions 98
6.2.3 Scenario Results and Analysis 99
6.3 Atchafalaya River at 15% Latitude Discharge.....104
6.3.1 Scenario Description.....104
6.3.2 Boundary Conditions 104
6.3.3 Scenario Results and Analysis 105
6.4 Synopsis of pre-screening runs 109

7.0 CONCLUSIONS AND RECOMMENDATIONS 111

7.1 Introduction 111
7.2 Conclusions.....111
7.3 Recommendations 113

8.0 REFERENCES..... 115

APPENDIX A DATA SOURCES PROCESSED

A.1 Water Level Data 118
A.1.1 USACE Hourly Data 118
A.1.2 USACE Daily Data.....121
A.1.3 USGS Data.....121
A.1.4 CRMS data 124
A.2 Current Velocity and Discharge Data 126
A.2.1 USGS Data.....126
A.2.2 USGS Synoptic Data 126
A.2.3 NAS Data.....129
A.2.4 NAS Synoptic Data.....129
A.3 Salinity Data.....132
A.3.1 CRMS Data.....132
A.3.2 ENCOS NAS Data.....132
A.4 All ENCOS Continuous Data 132

APPENDIX B ATCHAFALAYA BASIN WATER MANAGEMENT UNITS

APPENDIX C MODEL CALIBRATION STATISTICS

LIST OF FIGURES

Figure 1-1: Atchafalaya Model Domain in South-Central Louisiana 17

Figure 1-2: Historic and Projected Land Loss and Gain along the Central Louisiana Coast (Lake Pontchartrain Basin Foundation and Coalition to Restore Coastal Louisiana, 2007) 19

Figure 2-1: Atchafalaya Basin gages and model output locations - Upper Basin 23

Figure 2-2: Atchafalaya Basin gages and model output locations - Lower Basin 24

Figure 2-3: 2011 Field Campaign Stations 25

Figure 2-4: Timeline of data source collection periods and model simulations. The bars for each category given on the y-axis represent the range of time over which data was collected (for the data sources) or the period of time simulated by the model (for the calibration and validation model simulations). Note that the time axis scale changes at January, 2010 so that years of most interest to the study can be shown in greater detail. 28

Figure 3-1: Model mesh and bathymetry 30

Figure 3-2: Detail of model mesh and bathymetry: use of triangular and quadrilateral elements 31

Figure 3-3: Detail of model mesh and bathymetry: use of triangular and quadrilateral elements 32

Figure 3-4: Important features in upper portion of the Atchafalaya Basin model 33

Figure 3-5: Important features in lower portion of the Atchafalaya Basin model 34

Figure 3-6: Bathymetry Sources 35

Figure 3-7: Avoca Island Cutoff artificial siphon location 37

Figure 3-8: Manning's M distribution over model domain 38

Figure 3-9: Selected gage locations/ output points used in model calibration and validation 41

Figure 4-1: Simmesport discharge boundary condition for the calibration period in m^3/s 43

Figure 4-2: Morganza Spillway discharge boundary condition for the calibration period in m^3/s 44

Figure 4-3: Model calibration results for 2011 flood with calculated and measured water levels [m] for Simmesport (03045), Mellevile (03060)and Krotz Springs (03075) 46

Figure 4-4: Model calibration results for 2011 flood water levels [m] for Butte La Rose (03120), Grand Lake At Charenton (03550), and Keelboat Pass (03615) 47

Figure 4-5: Model calibration results for 2011 flood water levels [m] for Six Mile Lake (03645), Sweet Bay Lake (03820), and Bayou Latenache (43500) 48

Figure 4-6: Model calibration results for 2011 flood water levels [m] for WABPL Borrow Pit (46375), Bayou Courtableau Outlet (46750), and WABPL at Lower Grand Bayou (49195) 49

Figure 4-7: Model calibration results for 2011 flood water levels [m] for upper Grand river (49570), EABPL Borrow Pit (49630), and the Intracoastal Waterway (49690) 50

Figure 4-8: Model calibration results for 2011 flood water levels [m] for Bayou Boeuf Lock, (76400), Wax Lake Outlet at Calumet (07381590), and Lower Atchafalaya River at Morgan City (07381600)..... 51

Figure 4-9: Model calibration results for 2011 flood water levels [m] for GIWW at Bayou Sale (07381670), Vermilion Bay near Cypremont Point (07387040), and Chico Pass (073815450)..... 52

Figure 4-10: Model calibration results for 2011 flood water levels [m] for Crewboat Channel (073815925), Bell Isle (USGS_AB2932), and Pontoon Bridge Canal (USGS_AB3016)..... 53

Figure 4-11: Model calibration results for 2011 flood water levels [m] for Lake Pelba (USGS_AB3020), Southwest Pass near Porpoise Pt. (NAS12V), and Eugene Island (NAS1H) 54

Figure 4-12: Model calibration results for 2011 flood water levels [m] for East Cote Blanche Bay (NAS2H), West Cote Blanche Bay (NAS3H), and Vermilion Bay (NAS4H) 55

Figure 4-13: Model calibration results for 2011 flood water levels [m] for Old River (NAS67), Bayou Sorrell (NAS89), and Little Bayou Sorrell (49725)..... 56

Figure 4-14: Mean absolute error between calculated and measured water levels at particular gage locations in the basin as a geographical representation of values presented in Table 5-1 59

Figure 4-15: Difference between calculated and measured flood stage arrival times (time in GMT)..... 60

Figure 4-16: NAS12V (Southwest Pass near Porpoise Pt.) calculated and measured tidal constituent amplitude comparison 61

Figure 4-17: 07387040 (Cypremont Point) calculated and measured tidal constituent amplitude comparison 62

Figure 4-18: 07385835 (East Cote Blanche Bay) calculated and measured tidal constituent amplitude comparison 63

Figure 4-19: 88800 (East Cote Blanche Bay) calculated and measured tidal constituent amplitude comparison 64

Figure 4-20: 8764227 (Amerada Pass) calculated and measured tidal constituent amplitude comparison 65

Figure 4-21: Model calibration results for 2011 flood with calculated and measured discharges - upper basin outlets [m3/s] at Wax Lake Outlet at Calumet (07381590) and Morgan City (07391600) 67

Figure 4-22: Model calibration results for 2011 flood with calculated and measured discharges [m3/s] - NAS gages at Bayou Sorrel (NAS89) and Old River (NAS67) 68

Figure 4-23: Model calibration results for 2011 flood with calculated and measured channel-averaged current speeds [m/s] - at Wax Lake Outlet at Calumet (07381590) and Morgan City (07391600) 70

Figure 4-24: Model calibration results for 2011 flood with calculated and measured channel-averaged current speeds [m/s] –NAS gages at Bayou Sorrel (NAS89) and Old River (NAS67) 71

Figure 4-25: Measured and calculated rating curve at the Wax Lake Outlet at Calumet 73

Figure 4-26: Measured and calculated rating curve at the Atchafalaya River at Morgan City 74

Figure 4-27: Measured and calculated proportion of discharge flowing through Morgan City vs. the total discharge through both outlets during calibration period 75

Figure 5-1: Simmesport discharge boundary condition for the validation period 77

Figure 5-2: validation results for 2011 low-flow period with calculated and measured water levels[m] for Simmesport (03045), Melville (03060) and Krotz Springs (03075) 79

Figure 5-3: Model validation results for 2011 low-flow period with calculated and measured water levels [m] for Butte La Rose (03120), Six Mile Lake (03645), and Sweet Bay Lake (03820) 80

Figure 5-4: Model validation results for 2011 low-flow period with calculated and measured water levels [m] for Upper Grande River (49570), EABPL Borrow Pit (49630), and Bayou boeuf Lock (76400) 81

Figure 5-5: Model validation results for 2011 low-flow period with calculated and measured water levels [m] for Wax Lake Outlet at Calumet (07381590), Lower Atchafalaya River at Morgan City (07381600), and GIWW at Bayou Sale (07381670) 82

Figure 5-6: Model validation results for 2011 low-flow period with calculated and measured water levels [m] for Vermilion Bay (07387040), Chicot Pass (073815450), and Crewboat Channel (073815925) 83

Figure 5-7: Model validation results for 2011 low-flow period with calculated and measured water levels [m] for Southwest Pass near Porpoise Pt. (NAS12V), Eugene Island (NAS1H) andEast Cote Blanche Bay (NAS2H) 84

Figure 5-8: Model validation results for 2011 low-flow period with calculated and measured water levels [m] for West Cote Blanche Bay (NAS3H), Vermilion Bay (NAS4H), and Old River (NAS67) 85

Figure 5-9: Model validation results for 2011 low-flow period with calculated and measured water levels [m] for Bayou Sorrell (NAS89), and Little Bayou Sorrell (49725)..... 86

Figure 5-10: Mean absolute error between calculated and measured water levels over the entire validation period at particular gage locations in the basin [m] 89

Figure 5-11: Model validation results for 2011 flood with calculated and measured discharges [m^3/s] for Wax Lake Outlet at Calumet (07381590), Lower Atchafalaya River at Morgan city (07381600), and Bayou Sorrel (NAS89)..... 91

Figure 5-12: Model validation results for 2011 flood with calculated and measured channel-averaged velocities [m/s] for Wax Lake Outlet at Calumet (07381590), Lower Atchafalaya River at Morgan city (07381600), and Bayou Sorrel (NAS89) 93

Figure 5-13: Measured and calculated proportion of discharge flowing through Morgan City vs. the total discharge through both outlets during validation period 95

Figure 6-1: Schematic of preliminary model application to a high discharge pulse during a period of low flow (scenario A) 98

Figure 6-2: Simmesport discharge boundary conditions for scenario A0 (steady state low flow discharge) and scenario A1 (high discharge pulse)..... 99

Figure 6-3: Comparison between scenario A0 and scenario A1 water level time series at selected upstream, mid-basin, and coastal stations 100

Figure 6-4: Spatial variation of differences between calculated peak water levels [m] for scenarios A0 and A1. Text in the figure gives values at indicated points. 102

Figure 6-5: Spatial variation of differences between calculated peak current speeds [m/s] for scenarios A0 and A1. Text in the figure gives values at indicated points. 103

Figure 6-6: Schematic of preliminary model application scenario B 104

Figure 6-7: Simmesport discharge boundary conditions for scenario B0 (symmetric typical flood hydrograph) and scenario B1 (50% reduction in flow during falling limb) 105

Figure 6-8: Comparison between scenario B0 and scenario B1 water level time series [m] at selected upstream, mid-basin, and coastal stations 106

Figure 6-9: Spatial variation of differences between mean water levels [m] during the falling limb of scenarios B0 and B1 hydrographs. Text in the figure gives values at indicated points. 107

Figure 6-10: Spatial variation of differences between mean current speeds [m/s] during the falling limb of scenarios B0 and B1 hydrographs. Text in the figure gives values at indicated points. 108

Figure A-1: USACE hourly gages 120

Figure A-2: USGS water level gages 123

Figure A-3: Selected CRMS gages 125

Figure A-4: Selected USGS synoptic measurement locations 128

Figure A-5: ENCOS synoptic transects 131

Figure A-6: NAS1H Measured Data 133

Figure A-7: NAS2H Measured Data 133

Figure A-8: NAS3H Measured Data 134

Figure A-9: NAS4H Measured Data 134

Figure A-10: NAS67 Measured Data 135

Figure A-11: NAS67new Measured Data 136

Figure A-12: NAS89 Measured Data 137

LIST OF TABLES

Table 3-1: Manning's M to n value conversion 39

Table 3-2: Selected typical Manning's n values for floodplains and channels 39

Table 4-1: Summary of Water Level Calibration Results 57

Table 4-2: Summary of Discharge Calibration Results 68

Table 4-3: Summary of Current Calibration Results 71

Table 5-1:Summary of Water Level Validation Results 87

Table 5-2:Summary of Discharge Validation Results 90

Table 5-3: Summary of Current Speed Calibration Results 92

Table A-1: USACE Hourly Gages 118

Table A-2: USACE water level stations 119

Table A-3: USACE daily gages 121

Table A-4: USACE daily gage datum adjustments 121

Table A-5:USGS water level gage datum information 122

Table A-6:Selected CRMS gages 124

Table A-7:USGS current velocity and discharge gages 126

Table A-8: Selected USGS synoptic measurement locations 127

Table A-9: ENCOS synoptic transects 130

UNIT CONVERSION FACTORS

Divide	By	To Obtain
square meters	4,046.873	acres
cubic meters	1,233.5	acre-feet
cubic meters	0.02831685	cubic feet
cubic meters	1.6387064 E-05	cubic inches
cubic meters	0.7645549	cubic yards
radians	0.01745329	degrees (angle)
degrees Celsius	(F-32)/1.8	degrees Fahrenheit
meters	1.8288	fathoms
meters	0.3048	feet
meters	0.0254	inches
newton meters	0.1129848	inch-pounds (force)
meters per second	0.5144444	knots
meters	1.0 E-06	microns
meters	1,852	miles (nautical)
meters	1,609.347	miles (U.S. statute)
kilograms	14.59390	slugs
square meters	0.09290304	square feet
square meters	0.8361274	square yards
meters	0.9144	yards

EXECUTIVE SUMMARY

The most downstream portions of the Atchafalaya Basin are currently one of the few areas of the Louisiana coast that are actively building land. The increasing flow and sediment loads discharging through the basin over the past century have established two prograding bayhead deltas in the Atchafalaya Bay whose continued growth has offset to a small degree the pervasive land loss of the surrounding coast.

Despite the basin's environmental value as the largest contiguously forested swamp in North America and potential to further enhance land-building at the eroding Louisiana Coast, the management of the basin has been largely driven by flood management and navigation issues on the Mississippi River. The massive sedimentation throughout the entire basin has rapidly filled-in shallower open water lakes and reduced low-water circulation, creating challenges with respect to maintaining water quality. The inflow discharge into the basin is fully controlled so that a U.S. law-specified 30% of the combined Mississippi River and Red River inflows is discharged through the basin. Over time there has been increasing interest in exploring alternative management scenarios that could enhance the environmental and restoration functions of the basin. A dependable hydrodynamic model of the Atchafalaya Basin is critical to making decisions that affect water and sediment movement throughout the basin. Under contract to the National Audubon Society, Moffatt and Nichol has been tasked to start the development of a 2-D hydrodynamic model of the Atchafalaya Basin, capable of informing and testing proposals for improving environmental management of sediment, water and renewable resources within the Basin. This report documents the model development, calibration, validation and a set of possible application scenarios to aid in management optimization and evaluation.

A previous report prepared by Moffatt & Nichol (2010) identified the locations of the numerous existing measurement stations in the vicinity of the Atchafalaya Basin as well as the various state and federal agencies from which the data could be obtained. In addition to streamlining the eventual processing and use of measured data, that report also begins the initial effort to identify significant gaps in the data that could affect model development and inform the planning of a field measurement campaign, including hydraulic parameters to be collected and instruments to be used. In line with the outlined plan, field stations were deployed in the spring of 2011 in the months leading up to a record flood. The Mississippi River flood in April and May 2011 was among the largest and most damaging of those recorded along this U.S. waterway in the past century, comparable in extent to the major floods of 1927 and 1973. The Mississippi River and many of its tributaries, including the distributary Atchafalaya River, rose to record levels by the beginning of May. The unprecedented wealth of hydraulic and hydrologic information collected during this event and subsequent low flow periods was used to calibrate and validate the model to a high level of accuracy.

The hydrodynamic model of the Atchafalaya Basin was developed using the DHI MIKE21-FM modeling system. The MIKE21 flexible mesh model is a cell-centered, finite volume, 2D/3D, hydrostatic, shallow water hydrodynamic model with coupled baroclinic salinity and temperature transport. The model domain encompasses the full Upper and Lower Atchafalaya Basins, the shallow bay system into which the Wax Lake Outlet and Atchafalaya River discharge, and a portion of the Gulf of Mexico offshore of the coastal

bay limits. The domain land boundaries were located to coincide with the extensive levee systems that bound the upstream Atchafalaya channel, the Morganza floodway, the upper basin, and the urbanized areas of St. Mary parish that separate the upper and lower portions of the basin.

The model was calibrated using the measured data recorded during the historic 2011 flood period. This period encompassed some of the highest observed discharges in decades and included only the second diversion of Mississippi River flow into the basin through the Morganza Spillway in the structure's history. The focus of the calibration effort was on accurate simulation of water levels in the upper basin and the discharge through the two outlets into the lower basin. Though comparisons were made for other model hydrodynamic parameters including channel averaged current speed, tidal constituents, and flood stage arrival time, their accurate simulation did not drive the model alterations through the calibration process.

The model simulates water levels very well at most gages, with average absolute differences typically on the order of 10 cm over a 4 month period. The small differences between measured and modeled water level time series at most of the measurement locations over such a large and complex domain indicate high performance in modeling the flood hydrodynamics. Discharge comparisons were made at only a few locations in the model domain; however, the distribution of discharge through the two upper-basin outlets was very accurately simulated with normalized Root Mean Squared (RMS) errors of less than 10% at both gages.

The model was subsequently validated for a period from early September to late December 2011. This simulation period was chosen because of its low flows that are typical of the basin in non-flood conditions. Comparisons with measured data confirmed the model's ability to accurately simulate real basin behavior over the full range of possible flow magnitudes. Despite the increased influence of tidal fluctuations during the lower flows, measured water levels throughout the domain were still very well represented in the calculations. The normalized RMS errors for most gages still remain very low even with the much lower water levels. Water level validation results were consistent with the calibration results in that the few gages where results did not agree as well have the higher error values in both simulations. Overall, the validation results for both water levels and discharges are very good and confirm the model's ability to accurately simulate the hydrodynamics of the basin even during low-flow conditions.

Finally, two model application scenarios were presented; along with accompanying comparison scenarios, they demonstrate the calibrated and validated model's capability to evaluate the various management scenarios. Basin-wide effects are easily evaluated from rather simple water level and current speed comparisons, and the model platform supports the development of more in-depth evaluation tools (use of tracers, etc.). These preliminary scenarios and results can support the development of more specific management alternatives for which the model can then aid in optimization and evaluation.

1.0 INTRODUCTION

1.1 Project Background

Coastal and freshwater wetlands in southern Louisiana are being lost at an alarming rate, and serious measures to restore deltaic sediment and water distribution are needed to arrest the current environmental and social catastrophe. In response to the situation, federal, state, local, and private interests have proposed or undertaken a variety of projects aimed at reversing or at least slowing these losses. These efforts have ranged from small-scale efforts to plug dredged canals and repair breaches in man-made or natural levees to small- and large-scale freshwater diversions such as Myrtle Grove of the Louisiana Coastal Protection and Restoration Authority (CPRA) and the Corps of Engineers' Davis Pond project.

Various model studies have been conducted or suggested to explore the effectiveness and impacts of proposed alternatives to retard wetland loss, restore marshes, and facilitate project design. The two-dimensional (2D) model of Barataria Basin conducted by Moffatt & Nichol (M&N) for CPRA is such an example (Moffatt & Nichol, 2000). The most downstream portions of the Atchafalaya Basin are currently one of the few areas of the Louisiana coast that are actively building land. The increasing flow and sediment loads discharging through the basin over the past century have established two prograding bayhead deltas in Atchafalaya Bay whose continued growth has offset to a small degree the pervasive land loss of the surrounding coast.

Despite the basin's environmental value as the largest contiguously forested swamp in North America and potential to further enhance land-building at the eroding Louisiana Coast, the management of the basin has been largely driven by flood management and navigation issues in the Mississippi. The massive sedimentation throughout the entire basin has rapidly filled-in shallower open water lakes and reduced low-water circulation, creating challenges with respect to maintaining water quality. The inflow discharge into the basin is fully controlled so that a U.S. law-specified 30% of the combined Mississippi River and Red River inflows is discharged through the basin. Over time there has been increasing interest in exploring alternative management scenarios that could enhance the environmental and restoration functions of the basin. A dependable hydrodynamic model of the Atchafalaya Basin is critical to making decisions that affect water and sediment movement throughout the basin. To date, there have been limited initiatives to develop a numerical model of the existing hydrodynamics of the Atchafalaya Basin, with most efforts having primarily concentrated on the lower, coastal portions. Under contract to the National Audubon Society, Moffatt and Nichol (M&N) has been tasked to start the development of a 2-D hydrodynamic model of the Atchafalaya Basin, capable of informing and testing proposals for improving environmental management of sediment, water and renewable resources within the Basin.

The Mississippi River flood in April and May 2011 was among the largest and most damaging of those recorded along this U.S. waterway in the past century, comparable in extent to the major floods of 1927 and 1973. Record levels of rainfall on the Mississippi watershed combined with the a late springtime thaw of record accumulations of snow in the upper Mississippi watershed caused the Mississippi River and many of its tributaries, including the distributary Atchafalaya River, to swell to record levels by the beginning of

May. The unprecedented wealth of hydraulic and hydrologic information collected during this event and subsequent low flow periods was used to calibrate and validate the model to a high level of accuracy.

1.2 Atchafalaya Basin and Bay - Study Area

The Atchafalaya River is located in south central Louisiana. At 895,000 acres, the Atchafalaya Basin (AB) is the nation's largest swamp wilderness, containing nationally significant expanses of bottomland hardwoods, swamplands, bayous and back-water lakes. The basin is approximately 20 miles wide and 170 miles long with the Atchafalaya River being the primary feature. The location of the present study area, roughly corresponding to the USACE Atchafalaya Basin Floodway boundary, is given below in Figure 1-1. Additionally, the locations of the water management units (WMU) that make up the basin are given in Appendix B. The WMU names are used throughout the report to refer to specific locations within the basin. While the Floodway comprises approximately 595,000 acres of the full basin, the inclusion of the Atchafalaya Bay system and a portion of the Gulf in the model domain brings the total modeled area to over 2,863,000 acres.

The Atchafalaya River is a distributary of the Mississippi and Red rivers. It is navigable and provides a significant industrial shipping channel for the state of Louisiana. The river is formed near Simmesport at the Red River/Mississippi River confluence. The Atchafalaya River receives the water of the Red as well as an average of 25% of the water of the Mississippi River as measured from 2008-2010. Although no more than 30% of the Mississippi River flows into the Atchafalaya River, an average of 17% of the sand load and 40% of the fine sediment load passed into the Atchafalaya River over the same measurement period (Allison, et al., 2012). The Atchafalaya River meanders south, through extensive levees and floodways, past Morgan City, and empties into the Gulf of Mexico in Atchafalaya Bay approximately 15 miles south of Morgan City. The river is now forming a new delta in the bay, which is the only place on the Louisiana coastline that is gaining ground.

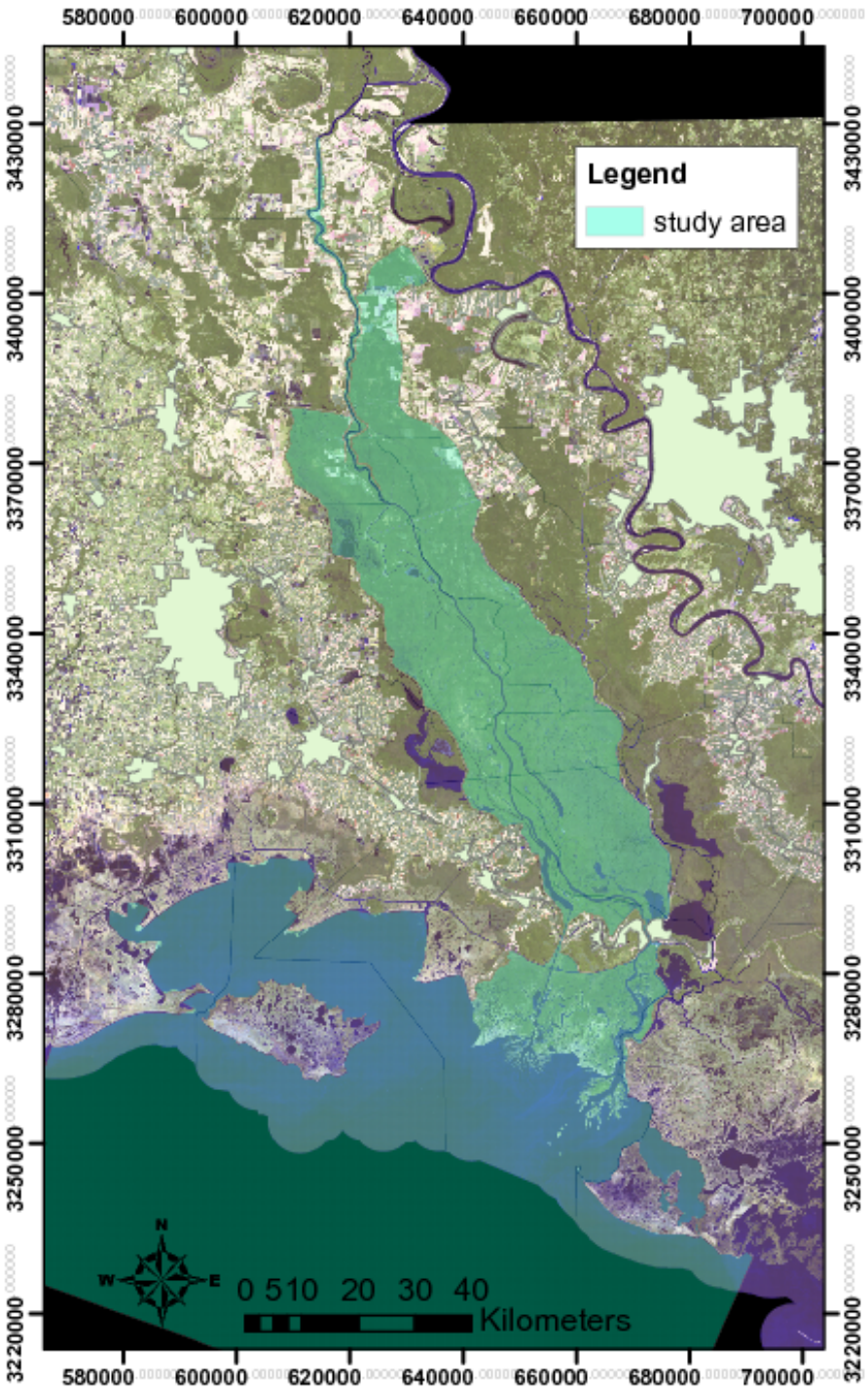

Figure 1-1: Atchafalaya Model Domain in South-Central Louisiana

Roughly half of the migratory species in the North American flyway use the area each year, and the basin yields 23 million pounds of crawfish annually. The AB contains one of the largest fish crops in the US, and is an Everglades-scale natural resource that

deserves the same national attention to its preservation. However, it is largely unprotected, with the Atchafalaya National Wildlife Refuge comprising only 15,000 acres. The AB has four ecological sections. To the north are woodlands and farmlands. The middle section contains North America's largest river basin swamp. Farther south is marshland. The fourth section is comprised of the Atchafalaya Bay. The AB is home to 200 species of birds and includes endangered species, such as the peregrine falcon, Bachman's warbler, pallid sturgeon, and Louisiana Black Bear. Many species of neo-tropical songbirds use Louisiana wetlands for resting and feeding habitat during migration.

A large portion of the AB is privately held. Most of the old cypress trees were logged out by the late 1920's, and much of the northwest part of the basin has been turned into soy bean and corn fields. Vast stretches of the swamp remain in the southern portions of the basin. Beginning in the late 1920's, the Corps of Engineers turned the Atchafalaya River into a floodway between levees to divert Mississippi River floodwaters away from Baton Rouge and New Orleans. In 1985, Congress approved a compromise flood control plan developed by the Corps, state agencies, landowners, timber interests, fishermen, and conservation groups.

Compared with the rest of the Louisiana coast, the central portion that encompasses the Atchafalaya Bay system and the developing deltas has the greatest extent of sustainable wetlands along the Louisiana coast. Historic and projected land loss and gain for the area are given below in Figure 1-2:. There is historic and ongoing land loss and currently a net land loss, but loss is offset approximately 60% by the land gain associated with the Atchafalaya and Wax Lake Outlet Deltas. However, there are localized areas that are experiencing great loss of wetlands. The largest area of historically high loss and ongoing loss is the Penchant Basin area southeast of Morgan City (Figure 1-2:). Break-up of the floating marsh present in the area is a frequent occurrence and contributes to the land loss as open water areas expand.

The Wax Lake Outlet receives approximately 1/3 of the Atchafalaya River discharge (~90,000 cfs), with the Atchafalaya Delta receiving most of the remainder (~180,000 cfs). The Wax Lake Delta is a naturally forming delta fed by a man-made diversion channel initially dredged in the early 1940s. Atchafalaya river water flows through Six Mile Lake into the Wax Lake Outlet. There has been little human manipulation of the Wax Lake Delta which is building land naturally. In contrast, the Atchafalaya Delta has developed under significant anthropogenic influence, with frequent dredging of the main navigation channel through the delta.

The total Atchafalaya River discharge has increased dramatically from the 1800's due primarily to the dredging of a channel between the Red River and the Mississippi River (now the site of the Old River Control Structure) and clearing of massive log jams on the Atchafalaya River. The Old River Control Structure was built in 1963 to control the flow between the Mississippi River and the Atchafalaya River to prevent the Mississippi River from seeking a shorter route to the Gulf and by-passing New Orleans. The discharge was fixed at an upper limit of 30% of the total Mississippi River and Red River discharge. Though the Atchafalaya was not diverting the full 30% after the control structure construction, the gradually increasing discharge reached this level by the early 1950s. This higher discharge has resulted in significant deposition in the Atchafalaya Basin with infilling by lacustrine delta formations and subsequent sediment deposition into

Atchafalaya Bay (Lake Pontchartrain Basin Foundation and Coalition to Restore Coastal Louisiana, 2007). The 1973 flood introduced 640,000 cfs through the channel and resulted in the emergence of the sand-dominant delta in Atchafalaya Bay, although it is estimated that most of the delivered sediment (90%) is not actively contributing to land building but is instead being distributed as suspended load to the downdrift Gulf shoreline (Lake Pontchartrain Basin Foundation and Coalition to Restore Coastal Louisiana, 2007). There has also been a shift from more brackish to more freshwater habitat and a lack of re-growth of historic oyster reefs that were once prominent in Atchafalaya Bay.

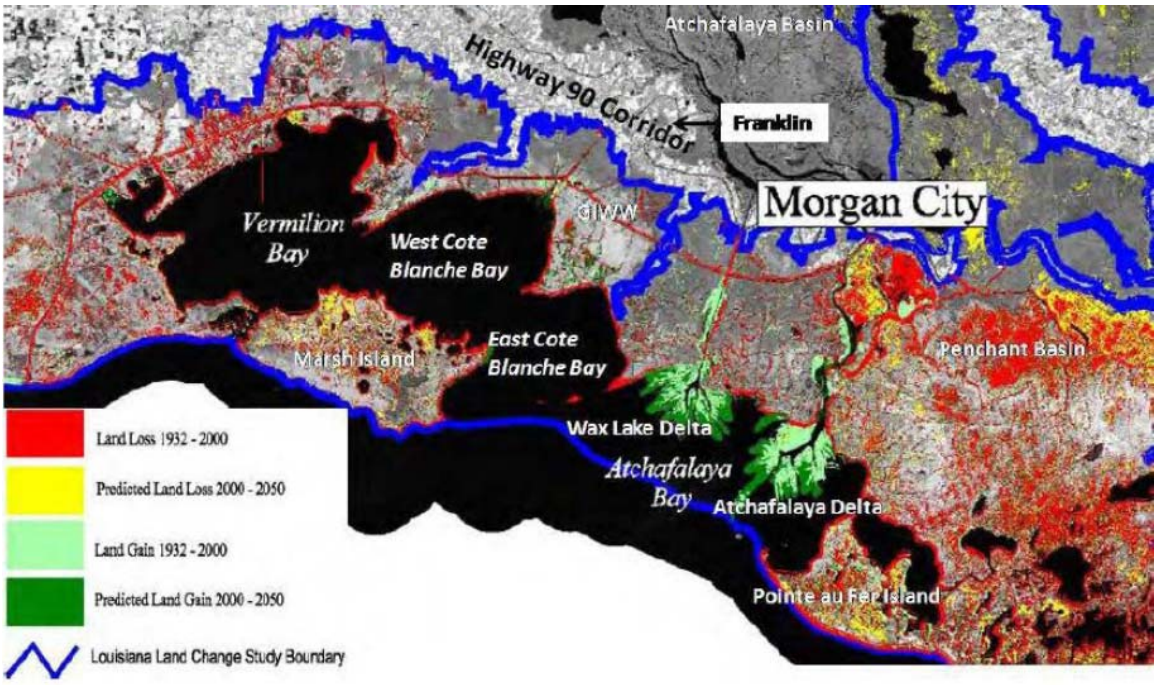

Figure 1-2: Historic and Projected Land Loss and Gain along the Central Louisiana Coast (Lake Pontchartrain Basin Foundation and Coalition to Restore Coastal Louisiana, 2007)

1.3 Study Objectives

The objective of this study is to develop a comprehensive hydrodynamic model of the full Atchafalaya Basin for use as a simulation tool for predicting water flow rates, velocities, circulation patterns, depths, and stages resulting from various water management strategies and possible restoration alternatives.

1.4 Study Approach

This report describes the initial data collection effort and subsequent development of the hydrodynamic model, including descriptions of bathymetry compilation, computational mesh construction, selection of roughness and other model parameters, and boundary condition derivation. Additionally, the calibration and validation process is detailed. To ensure accurate representation of the hydrodynamics of the basin during the full range of possible discharges, the model was calibrated to the historic 2011 flood and validated

using a subsequent period of much lower discharges. Finally, a preliminary set of scenarios that demonstrate model capabilities and applications are applied using the calibrated and validated model.

2.0 DATA COLLECTION AND DATA INVENTORY

2.1 Introduction

Prior to and in anticipation of the modeling phase, substantial effort was made to identify, locate, and obtain relevant data for use in model development and later in the calibration and validation process. An initial report, *Preliminary Data Gaps Analysis for Development of a Hydrodynamic and Salinity Model of the Atchafalaya Basin for Evaluating Restoration Alternatives,* was prepared to identify the sources of measured data in the planned model domain (Moffatt & Nichol, 2010). The report identifies the locations of the fairly numerous measurement stations in the vicinity of the Atchafalaya Basin as well as the various state and federal agencies from which the data could be obtained. In addition to streamlining the eventual processing and use of measured data, this report also begins the initial effort to identify significant gaps in the data that could affect model development and inform the planning of a field measurement campaign. The next stage in the data collection process included obtaining all relevant data and evaluating the quality and potential for use in the model. Substantial information on all available data has already been presented in previous reports so will not be presented here. Instead, the following sections will address the additional data collection as part of the modeling effort, especially from the 2011 field campaign, and how the data was processed for use.

2.2 Hydraulic data

If the hydrodynamic model of the Atchafalaya basin is to be successfully used to evaluate alternative management strategies and potential project effects, it must to the greatest extent possible mimic the behavior of the real basin under the same circumstances. This is accomplished by simulating a historical event for which important hydrodynamic parameters have been measured and adjusting the model to minimize the error between calculated and measured values. The measured values obtained in the data collection phase were used to evaluate model performance in simulating the 2011 flood hydrodynamics and then to validate the calibrated model for the 2011 low-flow period. Additionally, the measured data was important in developing discharge and water level boundaries during model development.

2.2.1 Available Data

Numerous existing measurement stations are located throughout the Atchafalaya Basin. Operated by federal and state agencies, measured hydrodynamic data was generally available for large portions of the model domain. Measured water level data was the most widespread, with data available at continuous monitoring stations operated by the USACE, the USGS, and the Louisiana Department of Natural Resources. Figure 2-1: and Figure 2-2: present an overview of all stations with the study area that collect continuous data for different hydraulic parameters. The most current data was retrieved for the 2011 simulation period and, if needed, was adjusted by various means to the model vertical datum of NAVD88 (see Appendix A for details). Datum adjustments for several important stations that lacked reliable previously-determined adjustments were established for this project by survey; however, these new values have not been

incorporated into the current study (John Chance Land Surveys, 2012). Continuous discharge and current measurements were only available at a few measurement stations (operated by the USACE and USGS) in the model domain; however, they are generally located in important areas of the model including the upstream boundary at Simmesport, the Morganza spillway structure, and the Wax Lake Outlet at Calumet and the Atchafalaya River at Morgan City, the main outlets of flow from the upper basin. Despite the many available data sources within the basin, it was determined that measurements in certain areas of the model that lacked adequate station coverage would be beneficial understanding of the basin's hydrodynamics and thus to model development. A field measurement campaign involving continuous water level and discharge station installation and synoptic discharge measurements was commissioned in early April 2011.

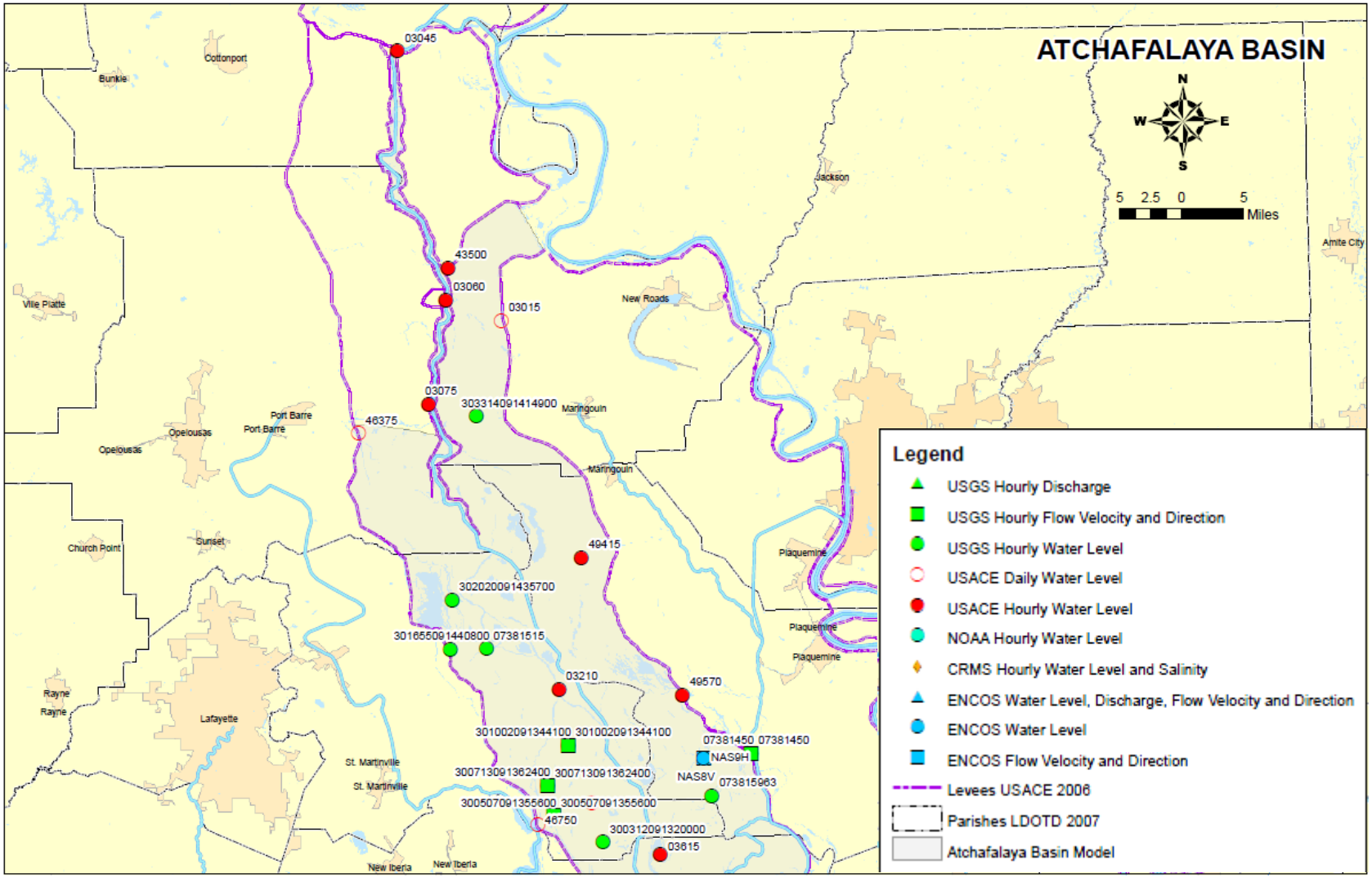

Figure 2-1: Atchafalaya Basin gages and model output locations - Upper Basin

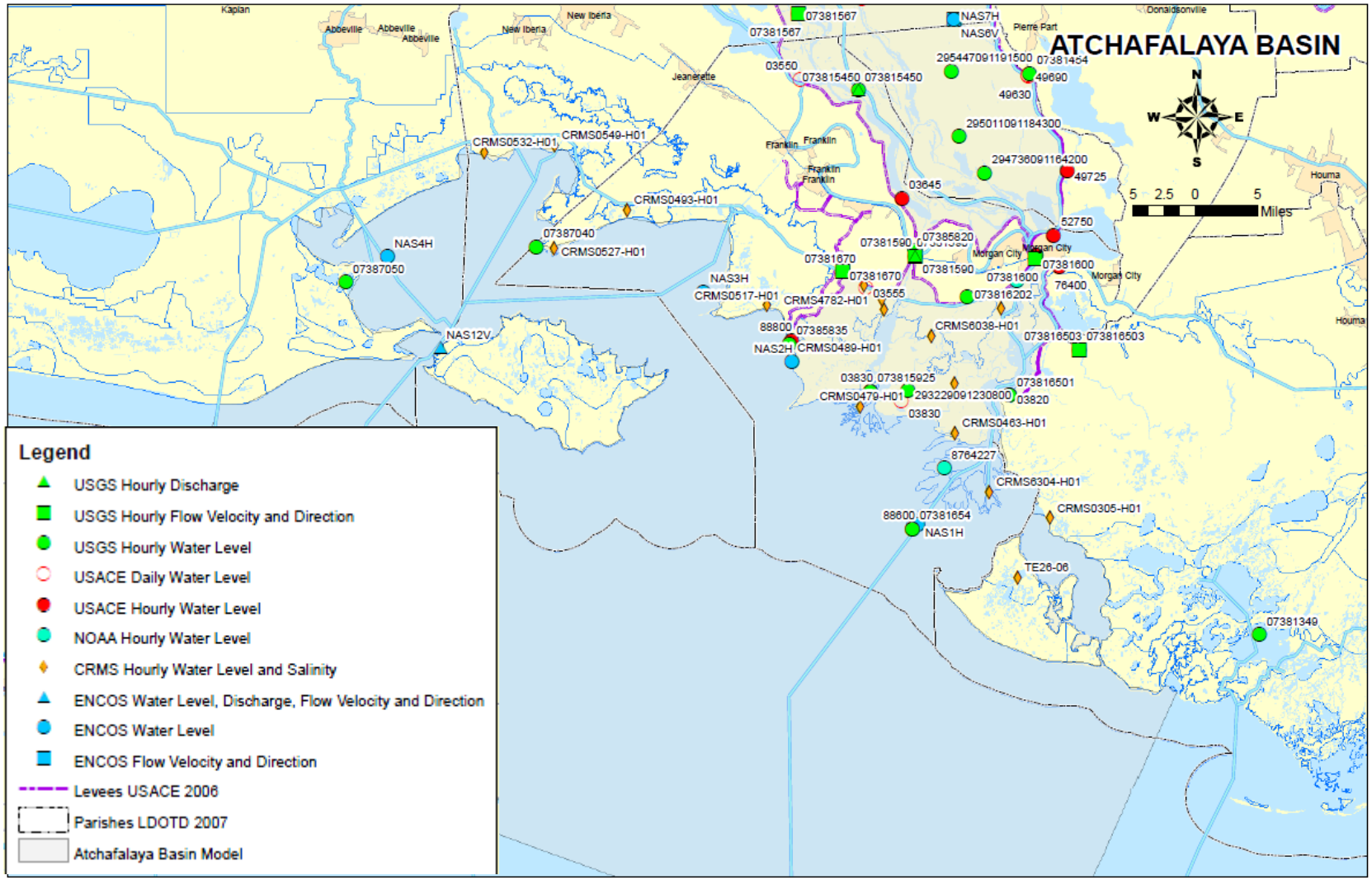

Figure 2-2: Atchafalaya Basin gages and model output locations - Lower Basin

2.2.2 2011 Field Campaign

Several water level gages and ADCP current meters were deployed from approximately late April through late December, 2011 to augment the measured data for model calibration and validation (ENCOS, 2012). The water level gages were mostly located in coastal areas of the model, with the exception of two co-located water level/ current stations in important channels in the Upper Bell River region. These two stations, NAS89 located in Bayou Sorrell and NAS67 located in Old River, were able to provide needed information on the flow in this complex area of the basin and significantly increase the measurement data available for discharge calibration. The locations of the water level, salinity, and discharge gages deployed during the 2011 field campaign are given below in Figure 2-3:.

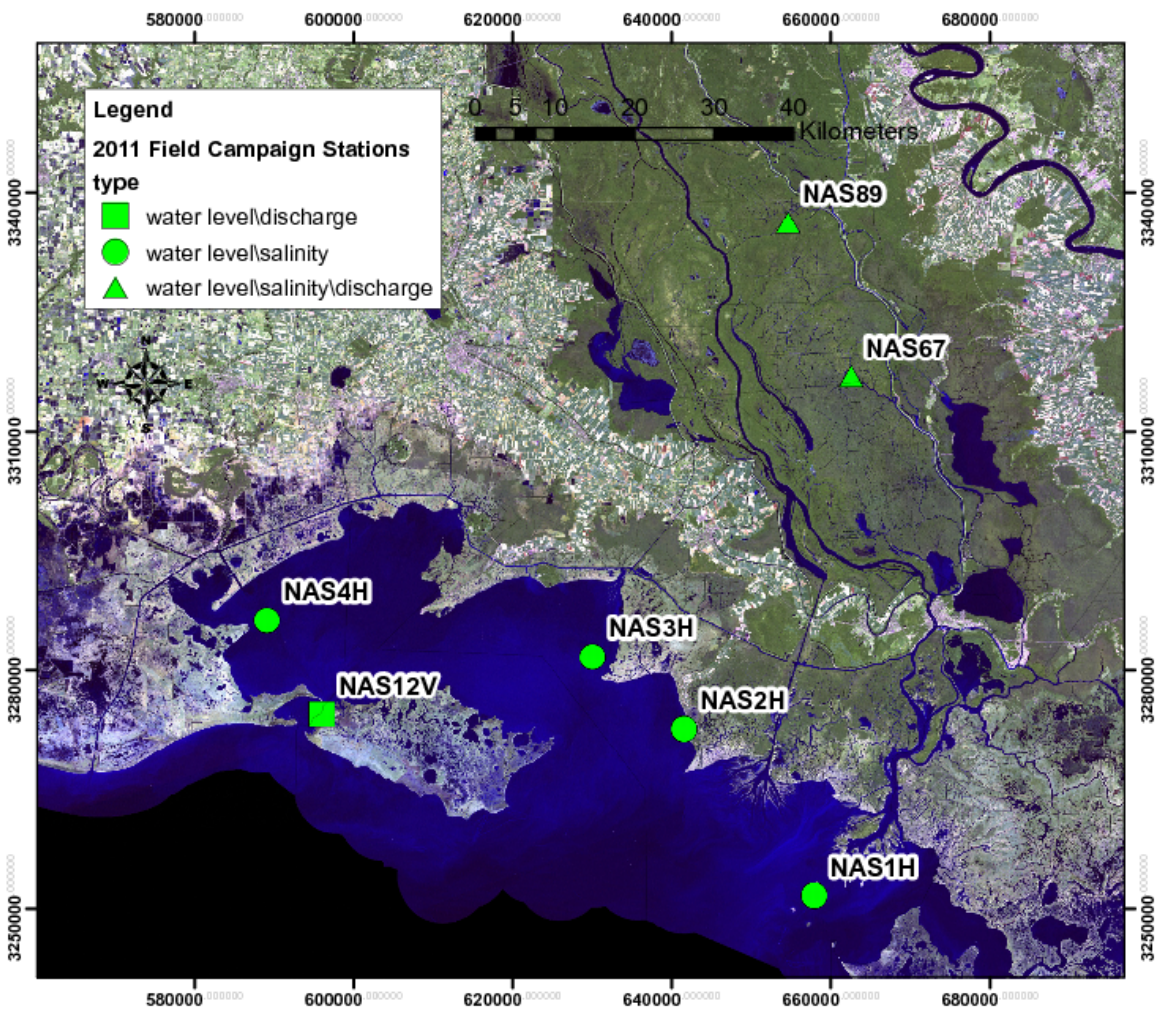

Figure 2-3: 2011 Field Campaign Stations

Processing water level data from the seven stations (identified with NAS- prefixes) was straightforward, as adjustments between gage datums and the NAVD88 vertical datum were determined at installation. Calculating useful discharge values across the full channel transects from ADCP measurements required a more involved process,

including substantial assumptions, that is described in more detail in section A.2.3 in Appendix A. The gage NAS12V, located in Southwest Pass out of Vermillion bay, was able to directly measure discharge; however, the instrument could only measure over a small portion of the full pass and returned discharges of such a low magnitude (order of 1 m^3/s) as to be unusable.

2.3 Bathymetric and topographic data

The preliminary data gaps report referenced earlier also identified potential bathymetry and topography sources for development of the model grid bottom elevations (Moffatt & Nichol, 2010). In many cases, the data sets that were obtained and processed as part of this initial effort were able to be superseded by more recent surveys. The sources that were finally utilized in the model grid development are described in greater detail in section 4.2.2 in the Model Development chapter.

While high quality, recent bottom elevation and topographic information was available for many areas in the model domain, specifically the main river channel, several hydrodynamically important channels still lacked reliable sources. Though smaller in scale than the major channels of the Atchafalaya River and the Wax Lake Outlet, these secondary channels, including Upper Grand River, Bayou Sorrel, Old River, Bayou Garotier, Bayou L'Embarras, Grand Bayou and Lake Fausse Pointe Cut, parts of East Grande Lake, and the Gulf Intracoastal Waterway (GIWW), are still large enough to convey significant flow and affect the large-scale hydrodynamics of the basin. In these areas, a synthesized bathymetry based on engineering judgment had to be created so that the channel would still be adequately represented in the model grid bathymetry.

The process of creating the full channel bathymetry involved interpolating high resolution transects along the channel centerline between two or more source transects at the upstream and downstream ends. The channel centerlines and approximate bank locations were first located from aerial photography. If these channels lacked a bottom track measurement from ADCP synoptic transects, then the source transects were created fully from engineering judgment, taking into account bathymetry of similarly sized channels and the estimated discharge capacity. If, however, a synoptic discharge measurement had been taken in the channel at some point, a series of real depth measurements across the channel was available. Based on surrounding water level measurements, an estimated water surface elevation at the time and location of the transect measurement was derived which allowed for conversion of the depth values into vertically-referenced bottom elevations. If sufficient source transects still did not exist to represent the upstream and downstream ends of the channel, the derived ADCP bottom transect elevations were copied and adjusted based on estimated channel slope to establish bounds for the interpolation. The interpolated transect points were located at a sufficiently-fine cross-channel and along-channel resolution to ensure that the full channel cross-sectional area was represented in the much coarser computational grid.

2.4 Synopsis Data collection and inventory

The timeline in Figure 3-2 graphically depicts the measurement periods for the various data sources and their temporal relation to one another. It furthermore shows the relation between the dates of collection of data-sets used for model development and the model

Calibration and Validation simulation periods (further elaborated on in Chapter 4, 5 and 6).

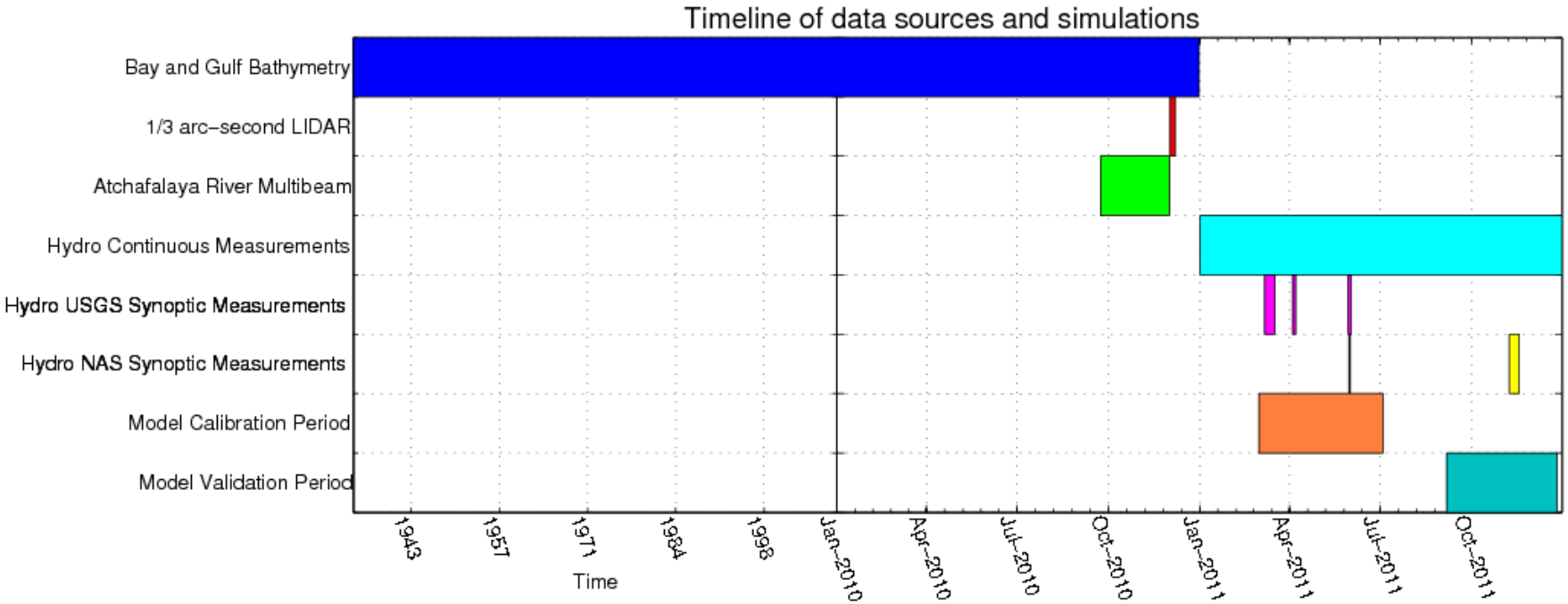

Figure 2-4: Timeline of data source collection periods and model simulations. The bars for each category given on the y-axis represent the range of time over which data was collected (for the data sources) or the period of time simulated by the model (for the calibration and validation model simulations). Note that the time axis scale changes at January, 2010 so that years of most interest to the study can be shown in greater detail.

3.0 MODEL DEVELOPMENT

In several previous reports (Moffatt & Nichol, 2009a), a number of hydrodynamic modeling packages were assessed for applicability to the Atchafalaya Basin. The MIKE21-FM software was the preferred modeling system, mostly due to its ability to simulate the important processes of the very different upper and lower basin and bay area using a single computational grid, eliminating the need to use different but coupled models for both areas. While the current model only simulates depth-averaged hydrodynamics, the ability to easily extend model capabilities and applications was an important consideration. The MIKE21-FM system allows simulation of complex, density driven flows with 3D grids that could better represent salinity dynamics in the coastal areas of the model. Additionally, both cohesive and non-cohesive sediment transport and resulting morphological change can also be simulated. Finally, the flexible mesh can be easily refined in a particular area without affecting the mesh resolution in the rest of the model, allowing for a more detailed assessment in small areas of interest while still efficiently integrating with the full domain to assess basin-wide effects.

The hydrodynamic model of the Atchafalaya Basin was developed using the DHI MIKE21-FM modeling system. The MIKE21 flexible mesh model is a primitive variable (i.e., flow velocities are primary dependent variables), cell-centered, finite volume, 2D/3D, hydrostatic, shallow water hydrodynamic model with coupled baroclinic salinity and temperature transport. The horizontal grid uses unstructured triangles or quadrilaterals, while the vertical grid (utilized for 3D simulations) uses structured sigma coordinates.

The following sections detail various aspects of the model development.

3.1 Model Domain and Boundary conditions

3.1.1 Model domain and grid

The model domain encompasses the full Upper and Lower Atchafalaya Basins, the shallow bay system into which the Wax Lake Outlet and Atchafalaya River discharge, and a portion of the Gulf of Mexico offshore of the coastal bay limits. The domain land boundaries were located to coincide with the extensive levee systems that bound the upstream Atchafalaya channel, the Morganza floodway, the upper basin, and the urbanized areas of St. Mary parish that separate the upper and lower portions of the basin. It was assumed that these boundary levees were sufficiently high to hydraulically isolate the model domain from the areas to the east and west.

The flexible mesh computational grid consists of 27114 nodes and 43604 elements. Element areas range from the order of 100 m^2 in shallow, narrow bayous to the order of km^2 in the bays and offshore areas. These element areas correspond to length scales on the order of 100 m in channels and on the order of kilometers in the largest offshore elements. The entire model mesh is shown in Figure 3-1: below.

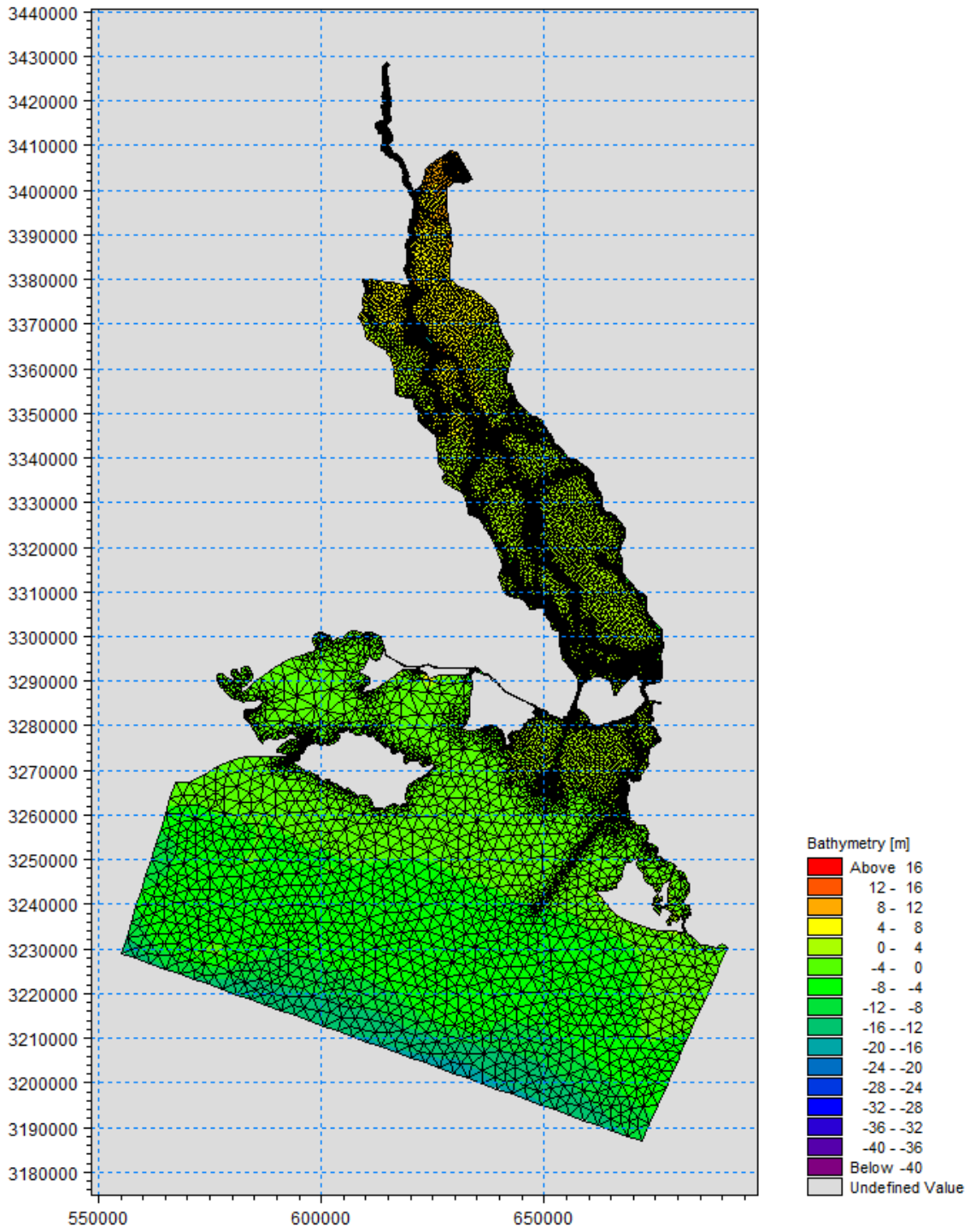

Figure 3-1: Model mesh and bathymetry

The MIKE21-FM hydrodynamic model is capable of using meshes that combine triangular elements with quadrilateral elements. The use of flexible meshes composed of triangular elements is generally preferred for coastal modeling applications because complex shorelines and bathymetries can be adequately represented without forcing high resolutions for areas where it is unnecessary. Alternatively, quadrilateral elements

are ideal for discretization of river channels and navigation canals where cross-channel depth gradients are much higher than the along-channel gradients. In these situations the channel bathymetry and flow patterns can be adequately represented with higher aspect ratio quadrilaterals, reducing the required number of elements and increasing computational efficiency. The Atchafalaya Basin, with its highly irregular coastline, complex floodplain geometry, and numerous interconnected channels is ideally modeled with a mix of these two element types. In general, channels were modeled with quadrilateral elements, with transversal resolution roughly corresponding to channel width and discharge capacity; however, floodplains and coastal areas where modeled with triangular elements. The geometries of some smaller channels and complex areas of larger channels (tight river bends, junctions, etc.) were sometimes still spatially discretized with triangles. Figure 3-2: and Figure 3-3: below exemplify the alternative uses of the two element types.

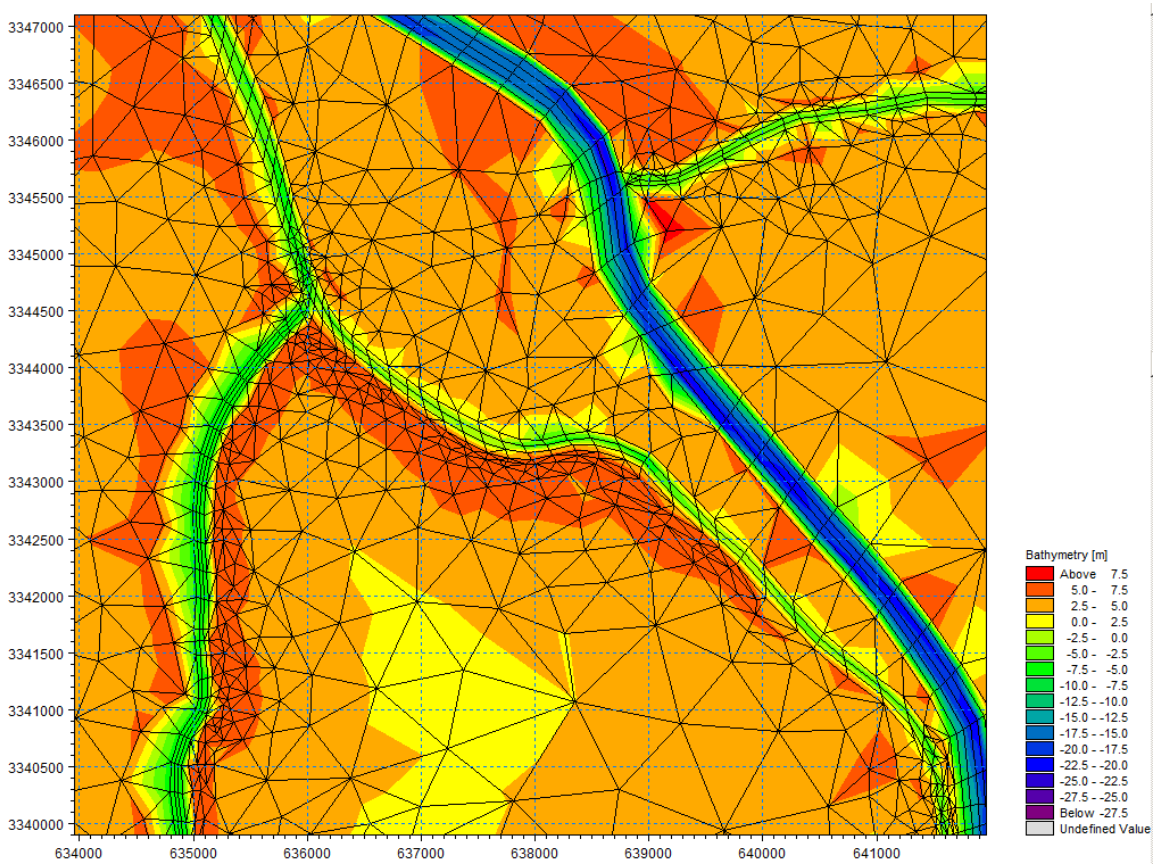

Figure 3-2: Detail of model mesh and bathymetry: use of triangular and quadrilateral elements

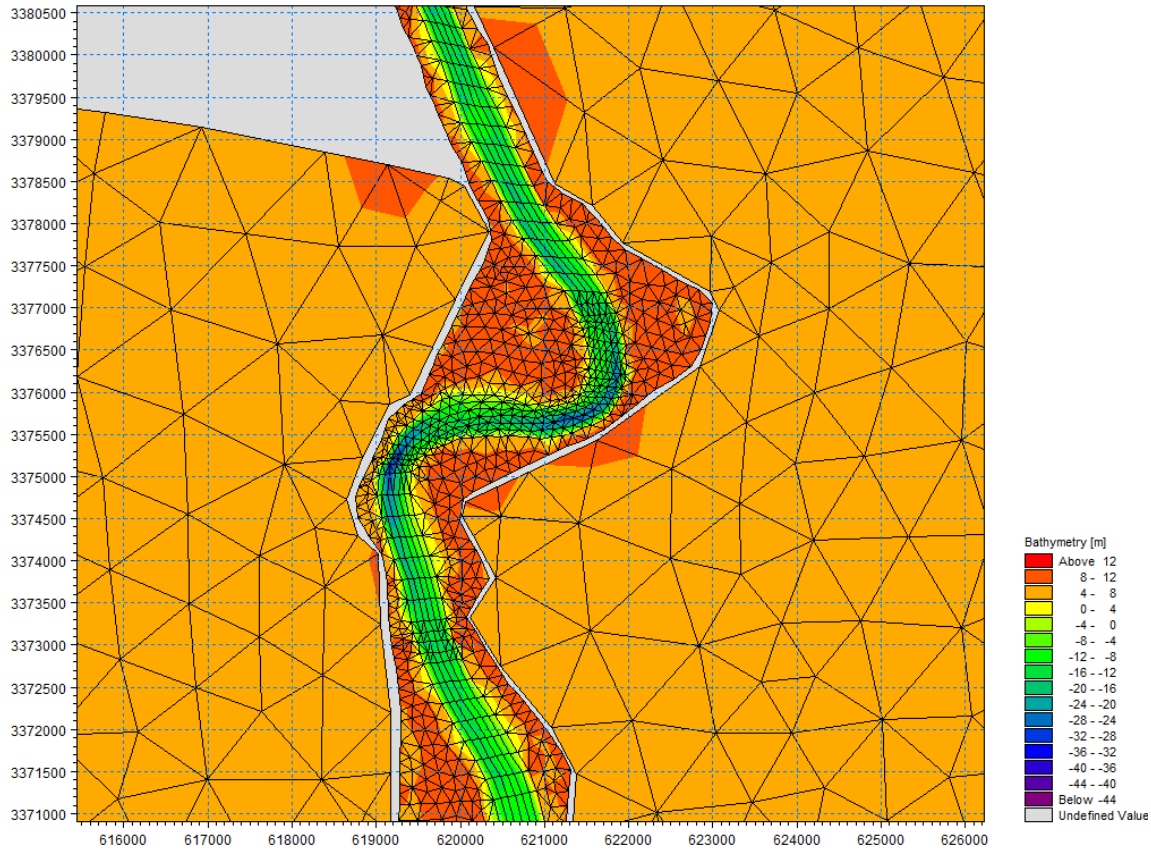

Figure 3-3: Detail of model mesh and bathymetry: use of triangular and quadrilateral elements

The desired simulation of a full flood season with reasonable run times required a balance of including detail while limiting element number and resolution. The large scale of the model domain, complexity of the basin channel network, and varying scales of connecting channel conveyance capacity required the exclusion of many smaller features without significant influence on basin-wide hydrodynamics from representation in the model. Effort was made to include channels where discharges above approximately 100 m^3/s had been measured or where trial simulations revealed significant influence on the distribution of water within the basin. Figure 3-4: and Figure 3-5: highlight the important included features represented in the model.

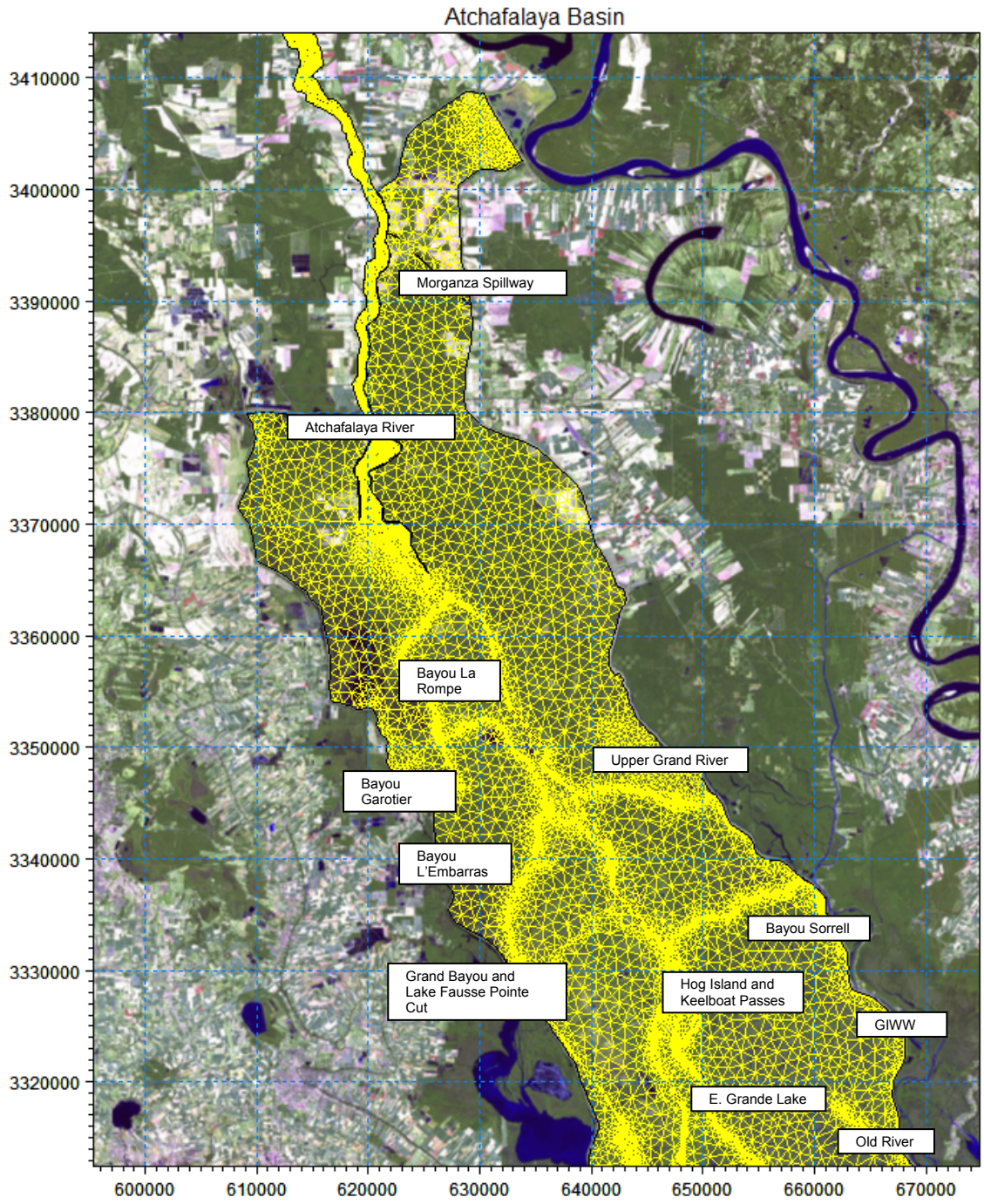

Figure 3-4: Important features in upper portion of the Atchafalaya Basin model

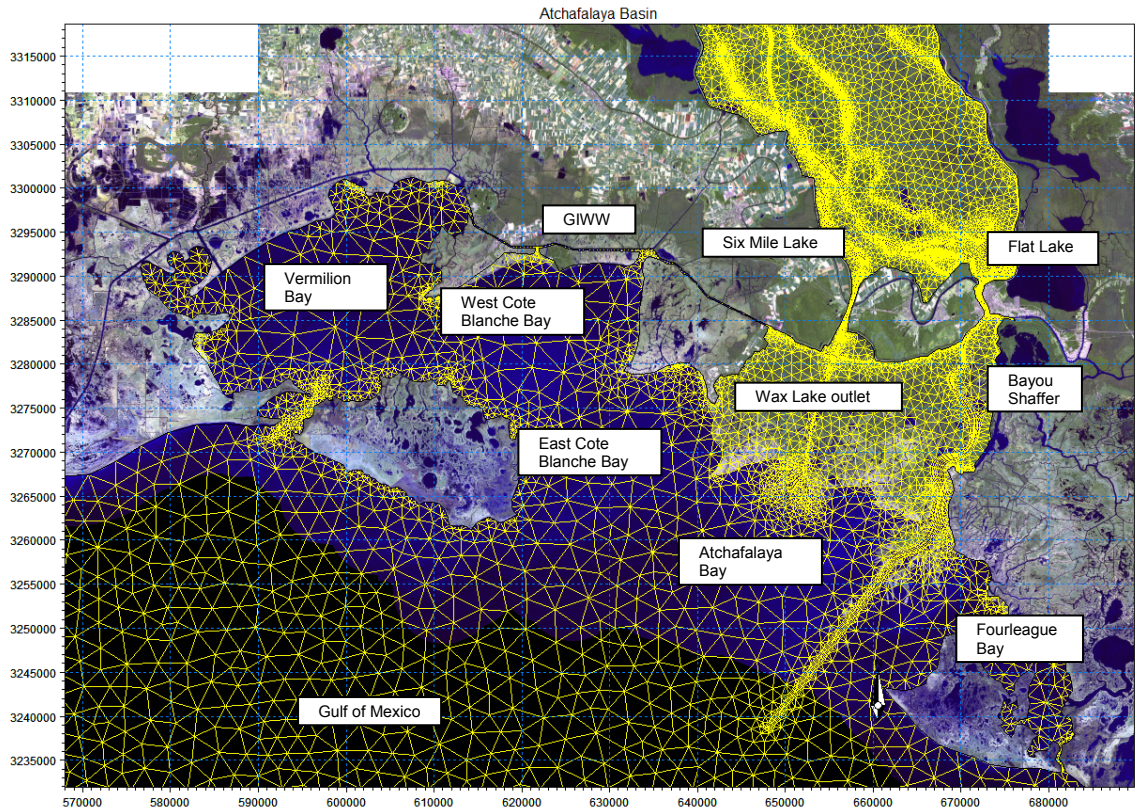

Figure 3-5: Important features in lower portion of the Atchafalaya Basin model

3.1.2 Bathymetry

Model bathymetry was compiled from a number of sources. In most cases, the most recent and highest resolution data available for each model area was utilized. The spatial extent of the data used from each source is given in Figure 3-6:. Recent multi-beam survey data at extremely high resolution (order of 1 meter) was available for certain areas but was first systematically reduced to a lower resolution for ease of use. All bathymetry was converted from its original coordinate system to UTM Zone 15 (meters, NAD83) coordinate system. The elevation values from sets not already referenced to NAVD88 were also all converted to NAVD88 vertical datum to establish a consistent vertical reference. The areas of the model domain labeled “expert judgment/ ADCP bottom tracks” lacked adequate, high resolution, bathymetry sources, so synthesized bathymetry point scatter sets were created according to the procedure discussed in Section 2.3. Additionally, grey areas of the model domain lacked more recent sources, so bathymetry from the initial “rolling chassis” model was used. The portions of this bathymetry set used in the current model development combined sources including the 1997 USACE Atchafalaya Hydrosurvey, older NOAA NOS survey data sets for areas of Atchafalaya Bay and the Gulf, and expert judgement/ADCP bottom track-derived bathymetry for several areas including parts of E. Grande Lake.

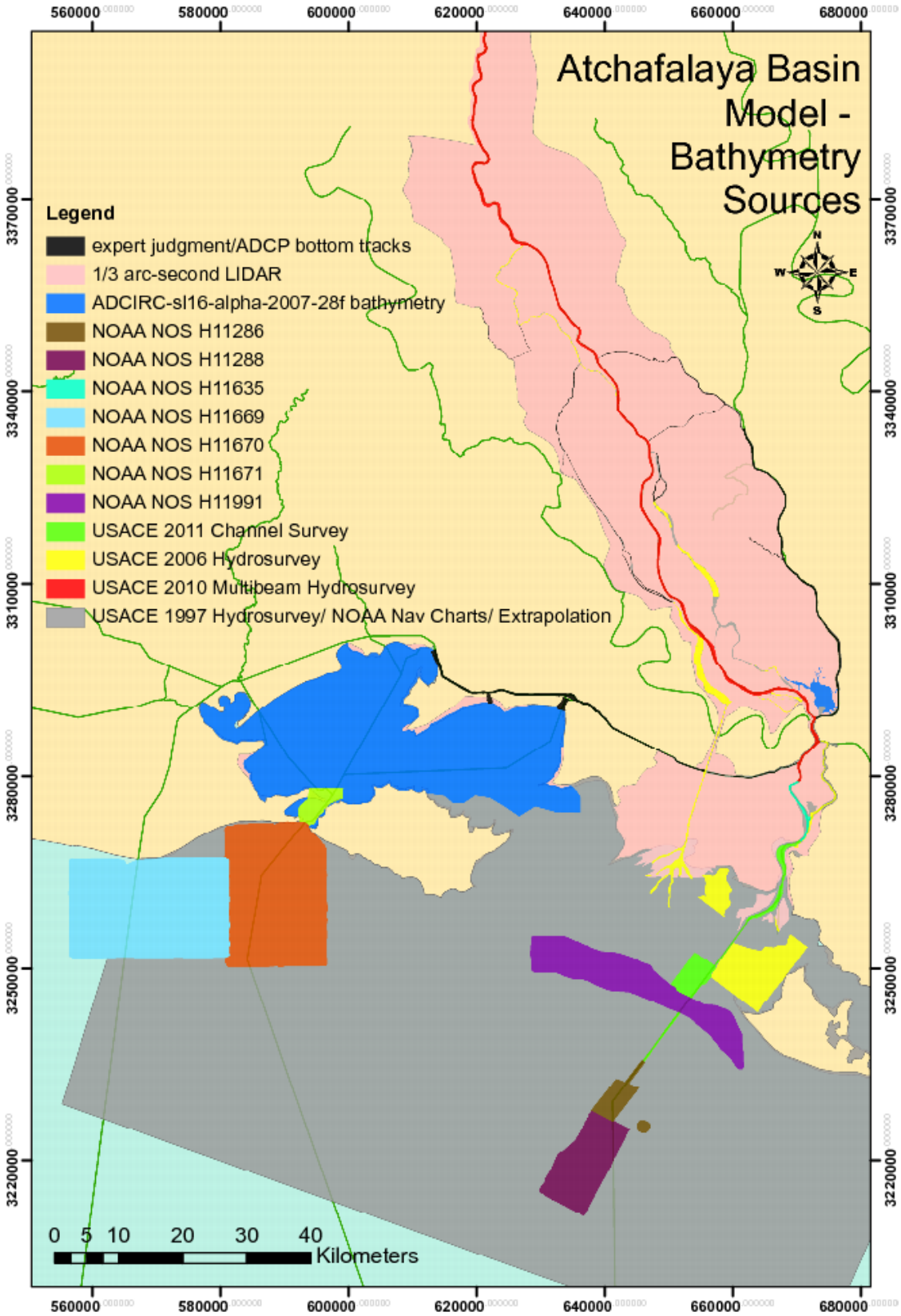

Figure 3-6: Bathymetry Sources

3.1.3 Water Level Boundaries

The model domain was specified to extend into the Gulf of Mexico, encompassing the full Atchafalaya Bay system and extending a sufficient distance both offshore and along the coast to free the open boundaries from the influence of river discharges and upstream water level variation. The model offshore boundary thus consists of two cross-shore oriented and one along-shore oriented boundary sections that together extend out to approximately the -15 (m NAVD88) contour. Here the model is forced with an astronomical tidal signal composed of both water level and velocity fluctuations (a combination known as a Flather boundary condition that promotes numerical stability near the boundaries) derived from the most important tidal constituents.

Constituents at the model boundary were extracted from the OSU Regional Tidal Solutions for the Gulf of Mexico (Egbert & Erofeeva, 2010). Additionally, a 0.2 m/s steady alongshore current flowing from East to West was superimposed at the offshore boundaries to mimic the large scale circulation present in the northern Gulf of Mexico.

Though meteorological forcings can have significant influence on water levels in the Atchafalaya Bay, especially with the passage of warm-weather tropical systems and winter cold fronts, their effect on the upper-basin hydrodynamics is limited. As the precise reproduction of measured lower basin water levels was not a priority for this phase of the modeling effort, no residual tidal water levels or other meteorological forcings were imposed at the boundaries.

3.1.4 Discharge Boundaries

Additional open boundaries were specified in the model domain to apply discharge inflow boundary conditions. The most upstream boundary of the model was defined to coincide with the Simmesport USGS streamflow gage. At this point, the Atchafalaya River is narrowly confined between two flood protection levees so that the flow measured through this transect represents the full inflow to the basin from the combined Atchafalaya and Red River discharges.

The Morganza floodway forms a connection between the Mississippi River and the upper Atchafalaya Basin a short distance downstream of the Atchafalaya/Mississippi bifurcation at the Old River Control Structure. Flow through this connection is regulated by the Morganza Spillway control structure, which can be operated to relieve pressure on downstream Mississippi River levees by diverting flow into the Atchafalaya Basin. The spillway is only operated during the most extreme flood events, and has been opened only twice since its construction. During the 2011 flood event, the spillway was opened for a total of 45 days, diverting a peak discharge of 5098 m^3/s. A second upstream flow boundary was specified at the spillway control structure location so that this additional inflow into the basin during the 2011 flood could be applied.

The southern extent of the Atchafalaya Basin flood control levees reaches to the Avoca Island Cutoff levee, south of which the flow is no longer confined. To represent the flow that could possibly leave the domain through the channel connection immediately

downstream of the levee limit, a simple source was used to extract water at a specified flow rate. The location of the applied artificial siphon is given in Figure 3-7:. The time series of this rate was determined by correlating a single synoptic measurement of discharge at the connection location with the much more complete record of discharges through the Atchafalaya River at Morgan City. Several other connections exist that could promote exchange of water between the model domain and surrounding bayous and channels; however, they are controlled by locks, so it was assumed that no flow exchange would actually occur.

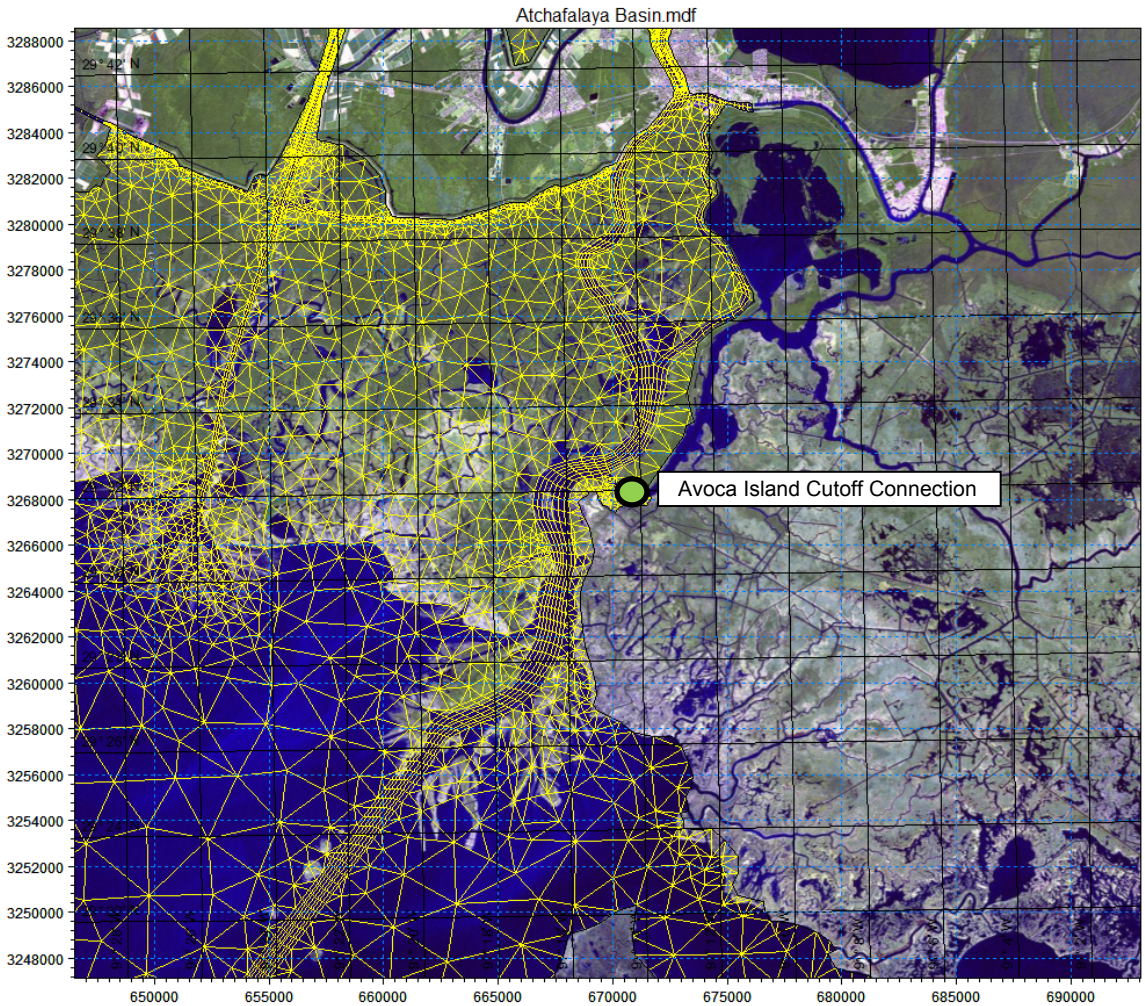

Figure 3-7: Avoca Island Cutoff artificial siphon location

3.2 Roughness Settings

In the MIKE21-FM Hydrodynamic model, the stress generated as water flows over the bottom is formulated using a quadratic friction law with a drag coefficient that is defined as a function of bed roughness. The roughness is parameterized by setting a Manning's M value that can either be constant over the full domain or vary to represent the natural variation in bed roughness of different environments. The variation in Atchafalaya Basin bed roughness was represented by defining several regions of varying Manning's

number. Figure 3-8: shows how the bed roughness values are distributed over the domain. In the implement formulation, higher M values correspond to smoother beds, so the most difference exists between the deep main channel of the Atchafalaya River and the heavily vegetated overbank floodplains. Table 3-1: Manning's M to n value conversion gives the conversion from model domain M values to the more-typically used Manning's n values. Table 3-2: gives some selected ranges of n values for various floodplain and channel types to show the validity of calibrated model values.

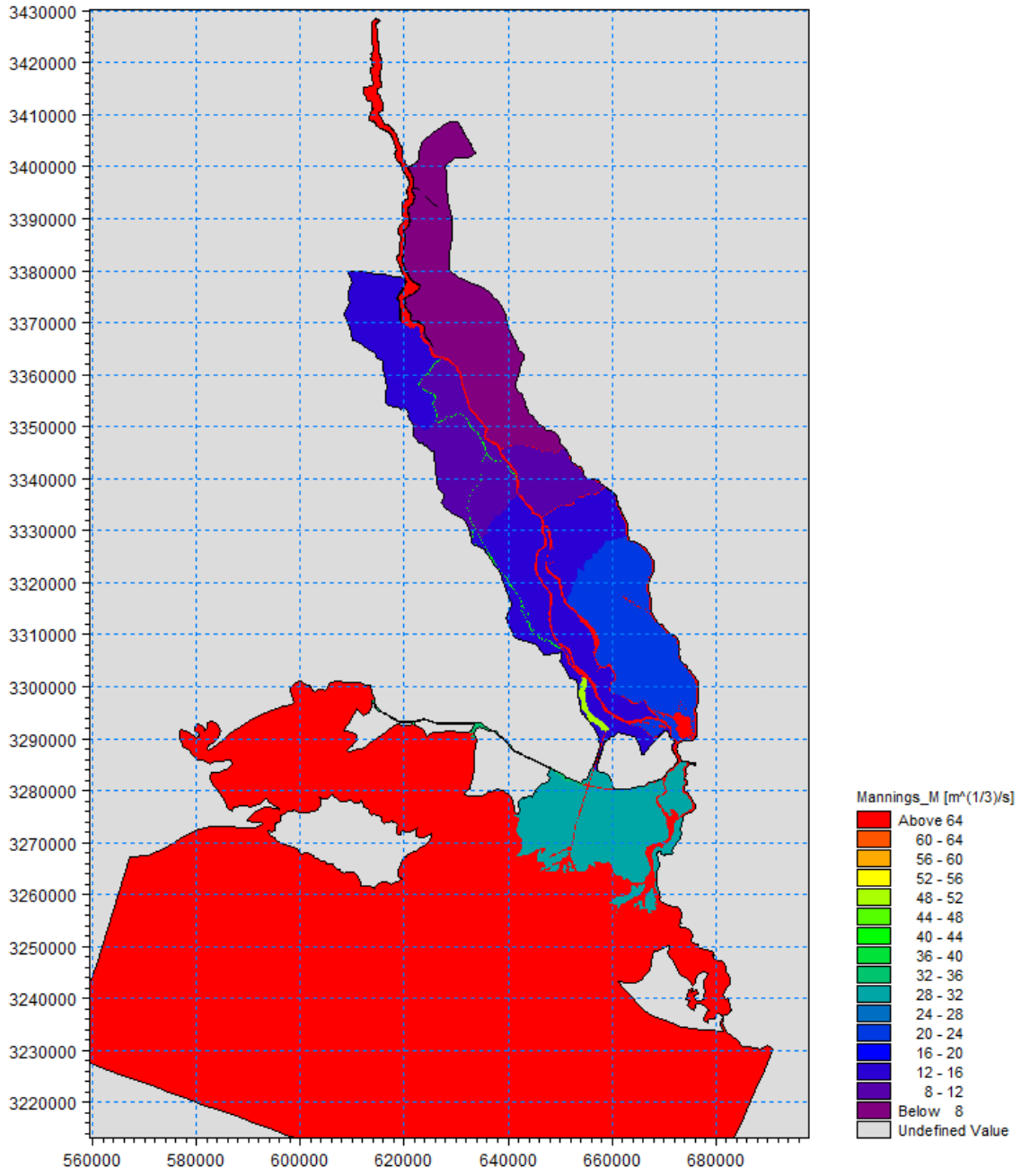

Figure 3-8: Manning's M distribution over model domain

Table 3-1: Manning's M to n value conversion

M (m^(1/3)/s)	Manning's n (s/m^(1/3))
5	0.200
10	0.100
15	0.067
20	0.050
30	0.033
35	0.029
40	0.025
50	0.020
65	0.015

Table 3-2: Selected typical Manning's n values for floodplains and channels

Floodplains	range of n values	representative M
Heavy stand of timber, a few downed trees, little undergrowth	0.12 - 0.16	7
dense willows, summer, not bent over by current	0.15 - 0.2	6
heavy weeds, scattered brush	0.05 - 0.07	17
Channels		
minor stream, regular section	0.03 - 0.035	31
major streams	0.028 - 0.033	33
excavated, unlined, channel	0.016 - 0.018	59

source: Chow, V.T.,1959, Open Channel Hydraulics, McGraw-Hill, New York, NY

3.3 Assumptions and limitations

The MIKE21-FM modeling suite is able to incorporate coupled salinity and temperature transport within the HD model and is expandable to include the modeling of cohesive and non-cohesive sediment transport, morphological change, and three-dimensional hydrodynamics. Though the use of this particular modeling software was partly driven by the potential use of these expanded capabilities, the present phase of the model only incorporates simulation of depth-averaged hydrodynamics. As such, the large amount of pre-processed salinity data and salinity and sediment inflow boundary conditions were not used or implemented. In its present form, the model was not calibrated to simulate any density driven or three-dimensional flows which could have importance in estuarine conditions.

3.4 Model Parameters settings

3.4.1 Eddy viscosity

Though the MIKE21-HD module incorporates many user-editable variables to control simulation parameters, default values and formulations were used for all cases except for the turbulence closure scheme. In the model, turbulent stresses representing the unresolved fluctuations are dependent on velocity gradients and an eddy viscosity term. In the default implementation, spatially varying eddy-viscosity values are calculated according to each element's characteristic length and local velocity gradients. Through test simulations, it was found that this formulation contributed to highly elevated water levels where flow was heavily influenced by adjacent land boundaries. Instead, a constant eddy viscosity of .002 m^2/s was applied over the full model domain. Subsequent sensitivity testing found that model results were not heavily dependent on the chosen constant value, with even order of magnitude changes producing no appreciable differences in results.

3.5 Output parameters and locations

In order to evaluate model results in comparison to prototype measured values, calculated time series of the parameters of interest were generated at many points throughout the domain. Figure 2-1: and Figure 2-2:, presented in section 3.2.1 above, give an overview of all the gages located in the Atchafalaya Basin and the required model output point locations. At each gage location where water level was measured, calculated water levels were generated from the model results every fifteen minutes of simulation runtime. For gages at which discharge and/or channel-averaged current velocity were measured, output transects that approximated the prototype measurement transect extents were set up in the model to return discharges through each transect and total water depth at equally-spaced points along the transect for purposes of channel-averaged velocity calculation. At each output time step, the returned discharge was divided by the calculated flow area of the transect to determine velocity.

As evidenced by the above figures, a wealth of information was available at many locations throughout the model domain for comparison of calculated results to measured values. However, the quality of the measured water level data was not uniform across every gage. The model bathymetry, water level boundary conditions, and resulting calculated values were all referenced to the NAVD88 vertical datum. For useful comparisons to be made, measured water levels must also be referenced to the same datum. Water level comparisons for calibration and validation were thus limited to the gages that were confirmed to be already referenced to NAVD88 or for which reliable conversion values from the gage datum to NAVD88 had been provided by the responsible agencies. Established methods do exist to convert elevations referenced to the NGVD29 datum to NAVD88; however, their applicability in coastal Louisiana is limited due to the relatively high rates of subsidence. Figure 3-9: gives the locations within the model domain and ID's of the output locations selected for model performance evaluation.

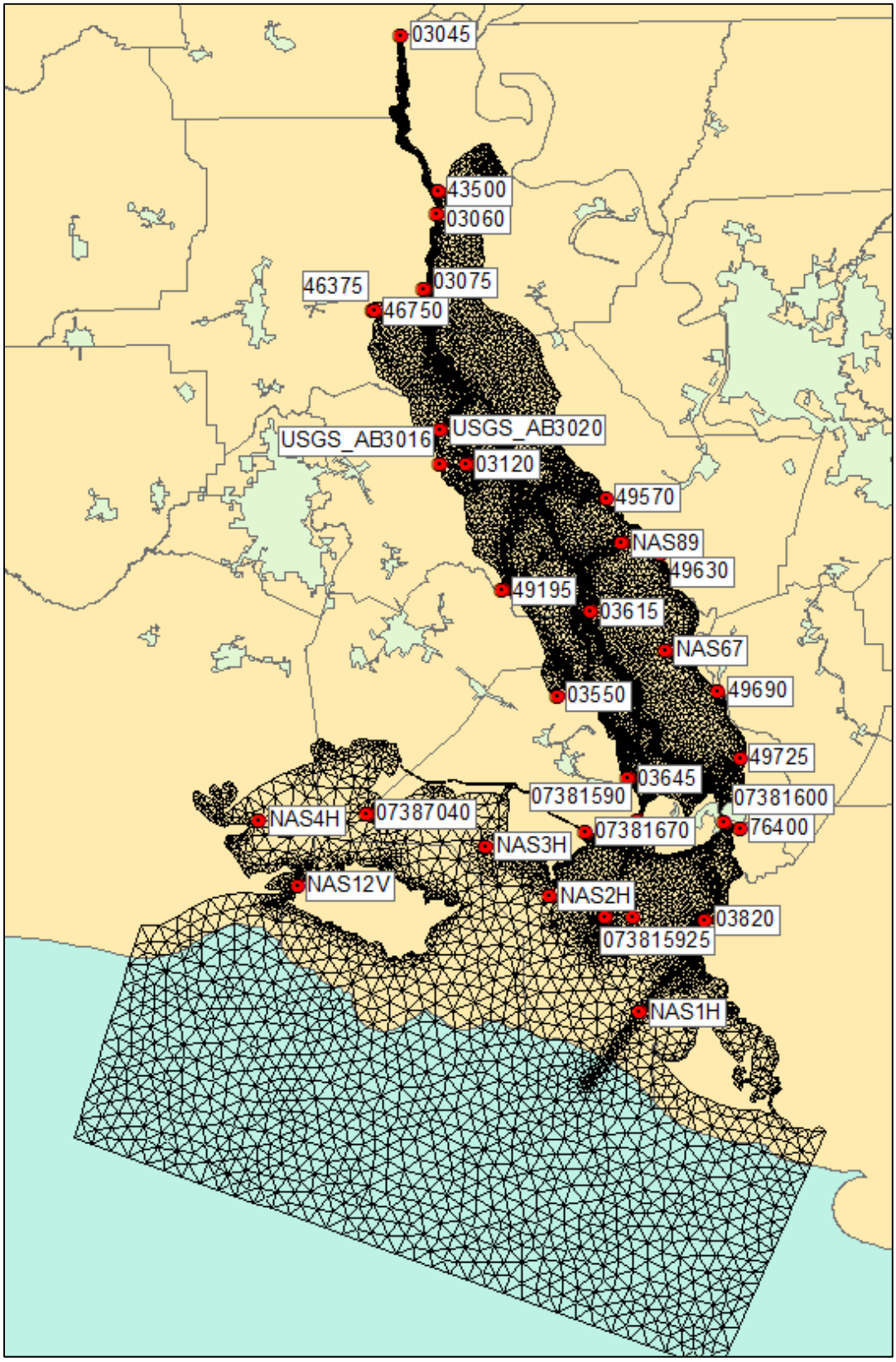

Figure 3-9: Selected gage locations/ output points used in model calibration and validation

3.6 Model Implementation

The model was run using a time step of 60 s. The MIKE-21FM HD code was implemented in parallel on an 8-core machine, giving typical run-times for the roughly 4-month calibration simulation of 20 hours. This run-time corresponds to approximately 150 hours of simulation time per hour of computer run time.

4.0 MODEL CALIBRATION

4.1 Introduction

A time period corresponding to the 2011 flood season was used for calibration of the model. The 2011 flood had one of the highest observed peak discharges through the basin and required only the second diversion in the Morganza spillway's history. In addition to the large number of continuously operating monitoring gages already present in the basin, a number of water level and discharge gages were deployed to capture the peak flood in certain areas that were lacking measurements. Ranging from March 1, 2011, to July 4, 2011, the model calibration simulation period encompasses the rising limb, peak, and falling limb of the flood as well as the full period of the discharge through the Morganza floodway. Figure 4-1: and Figure 4-2: below give the imposed discharge boundary conditions at the upstream limits of the model domain at Simmesport and the diversion input at Morganza (based upon USACE data). Other hydraulic structures which allow for inflow into the Basin were analyzed but were considered insignificant for the model calibration effort due to highly irregular operation and relatively low inflow discharges.

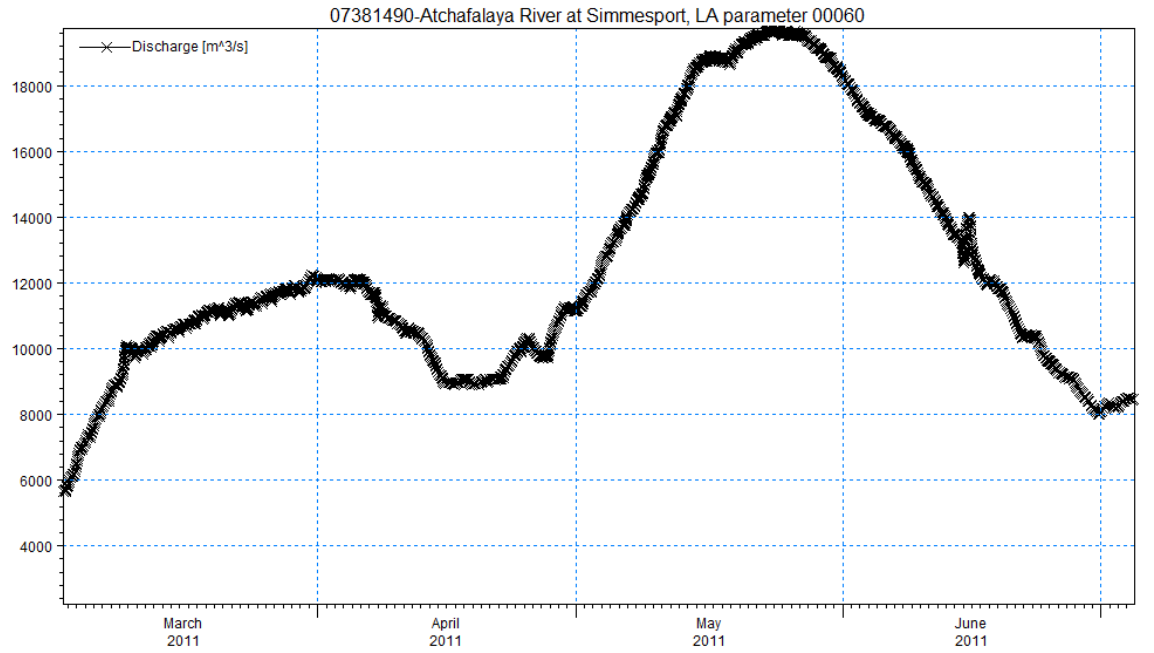

Figure 4-1: Simmesport discharge boundary condition for the calibration period in m^3/s

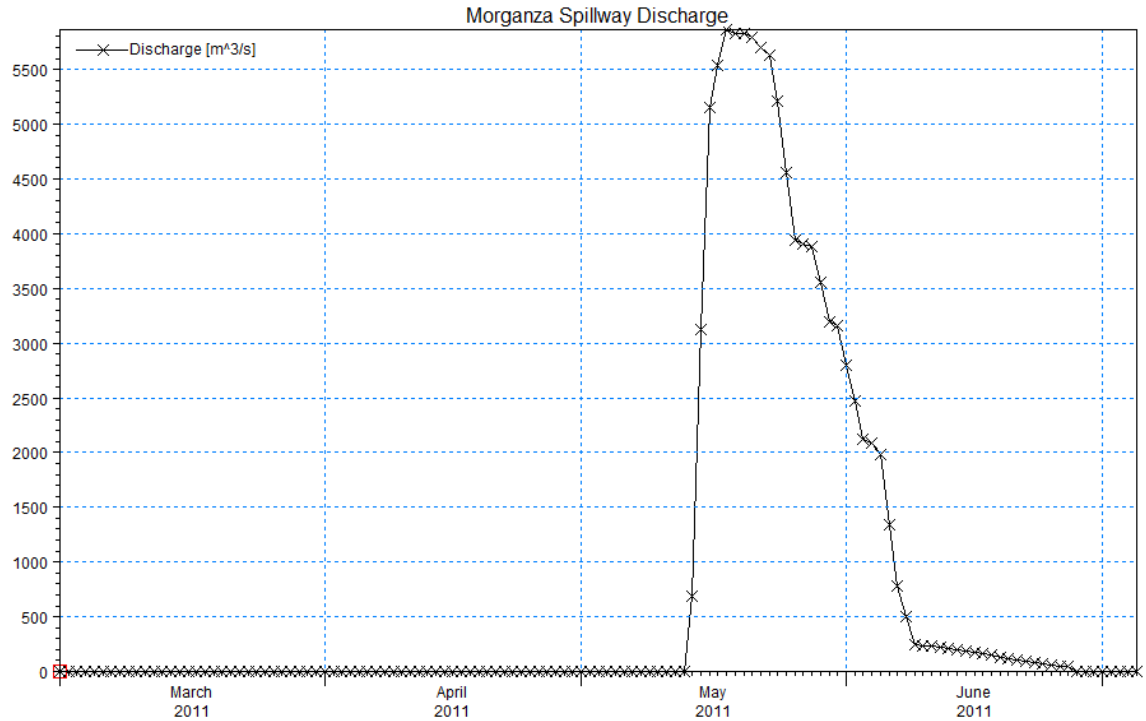

Figure 4-2: Morganza Spillway discharge boundary condition for the calibration period in m^3/s

The main goal of the current phase of modeling was to develop a hydrodynamic model of the full basin that accurately predicted water levels mostly in the upper basin and the distribution of discharge through the two outlets to the lower basin, the Wax Lake Outlet and the Atchafalaya River at Morgan City. Although attempts were made to accurately model the water level variation at the tidally-influenced gages, agreement among calculated and measured values at more upstream gages and achieving valid discharge distributions was the primary focus of calibration.

The primary performance metrics used for calibration include the average difference between measured and calculated (modeled) values over the full period of simulation. Additionally, the normalized root mean squared error between measured and calculated values was also computed to give another indication of model performance. Observations of agreement between flood hydrograph shape and the difference in arrival time of the peak flood also aided in calibration.

The following sections present comparisons between measured and calculated water levels and discharges at various gages/output points (locations given in Figure 3-9:), including discussions of the model's success in simulating the hydrodynamics of the flood calibration period.

4.2 Water Level Calibration

4.2.1 Measured and Calculated Time Series Comparisons

Figures 5-3 to 5-13 below present comparisons between calculated and measured water levels at the selected output gage locations for the 2011 flood calibration period. In each plot, values are given for the root mean squared error (ε_{rms}), normalized root mean squared error (ε_{norm}), mean absolute error (calc-meas), correlation coefficient (R), and several other performance measures (see Appendix C for a detailed description of their calculation). In general, the model simulates water levels very well, with most mean absolute errors on the order of ± 10 cm over the 4 month calibration period. Table 4-1 presents a summary of the errors between calculated and measured water levels at selected stations. The model performs particularly well in the upstream channelized section of the model (gage 03045), the Butte la Rose area (gage 03120), the outlets into the lower basin at Calumet and Morgan City (gages 07381590 and 07381600 respectively), and most coastal gages where the flood discharge may or may not influence water levels (gages 03820 and NAS1H, respectively)[1]. The accurate simulation of water levels in the upper basin was the primary goal of the calibration process, so the small differences at most of the measurement locations over such a large and complex domain indicate high performance in modeling the flood hydrodynamics. Though mean absolute error values do vary among individual gages, the flood hydrograph shape is also well simulated for most areas of the model.

Water levels in some specific areas of the basin, however, are not as well predicted, and the differences in the calculated and measured hydrograph shapes could indicate that local physical processes may not be adequately represented. Gages in the region known as Upper Bell River, bounded by East Grande Lake to the west and the GIWW to the east, and the area to the north encompassing the Bayou Sorrell and Upper Grande River connections from the main Atchafalaya Channel to the GIWW show somewhat increased deviation from measured values compared to gages in other areas. Model performance in these areas will be further discussed in the following section.

[1] See Appendix A for a full overview of measurement locations and their ID numbers

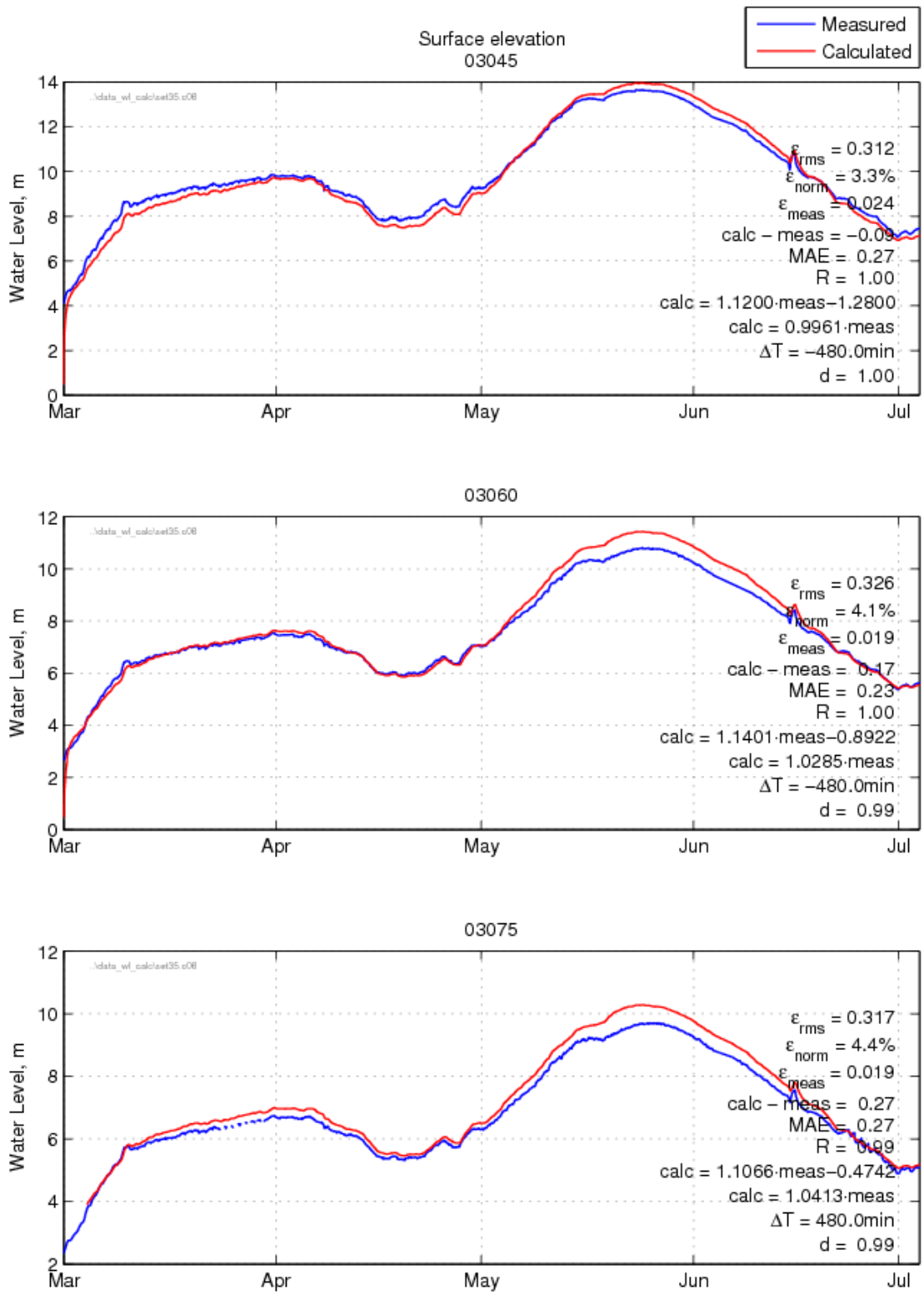

Figure 4-3: Model calibration results for 2011 flood with calculated and measured water levels [m] for Simmesport (03045), Mellevile (03060)and Krotz Springs (03075)

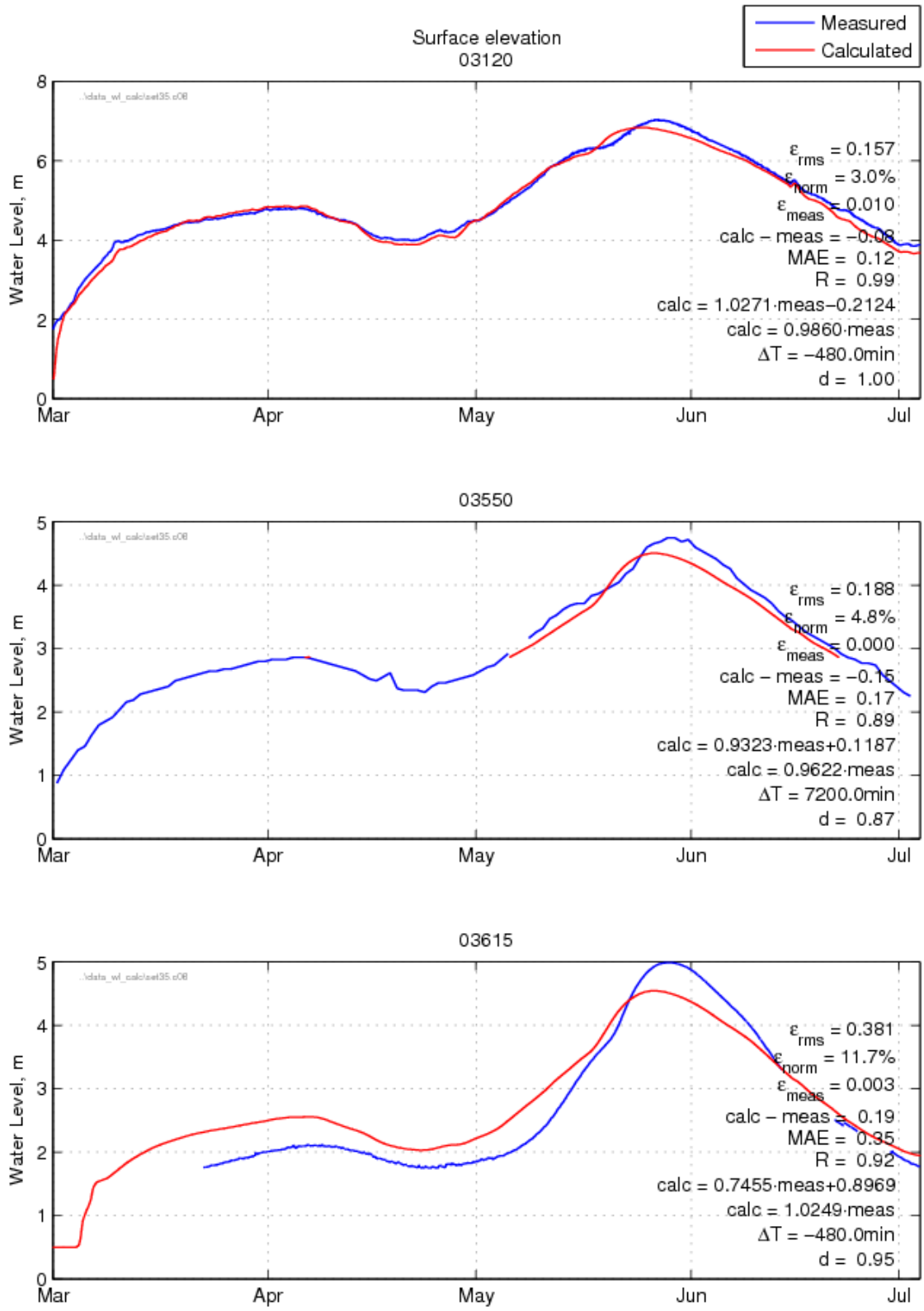

Figure 4-4: Model calibration results for 2011 flood water levels [m] for Butte La Rose (03120), Grand Lake At Charenton (03550), and Keelboat Pass (03615)

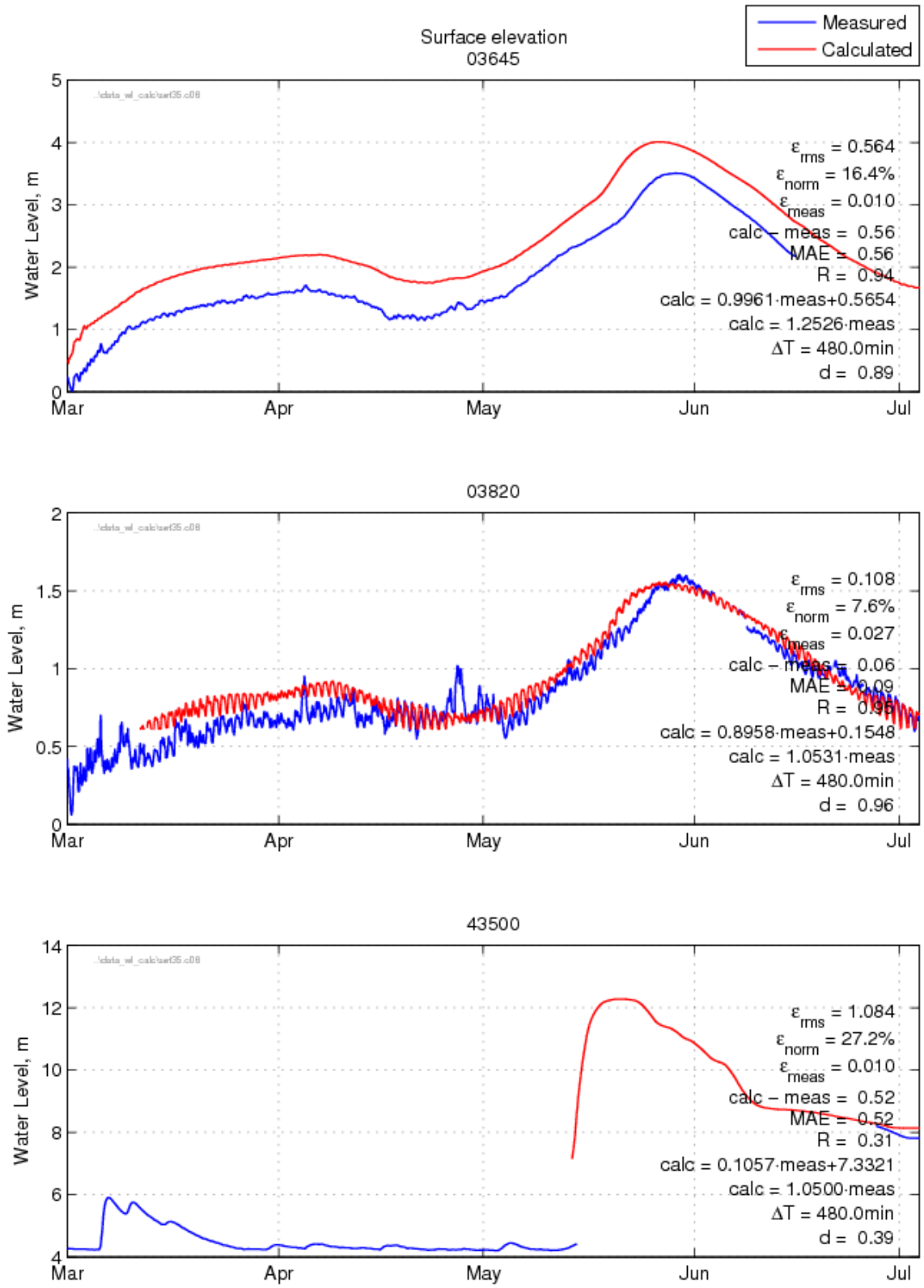

Figure 4-5: Model calibration results for 2011 flood water levels [m] for Six Mile Lake (03645), Sweet Bay Lake (03820), and Bayou Latenache (43500)

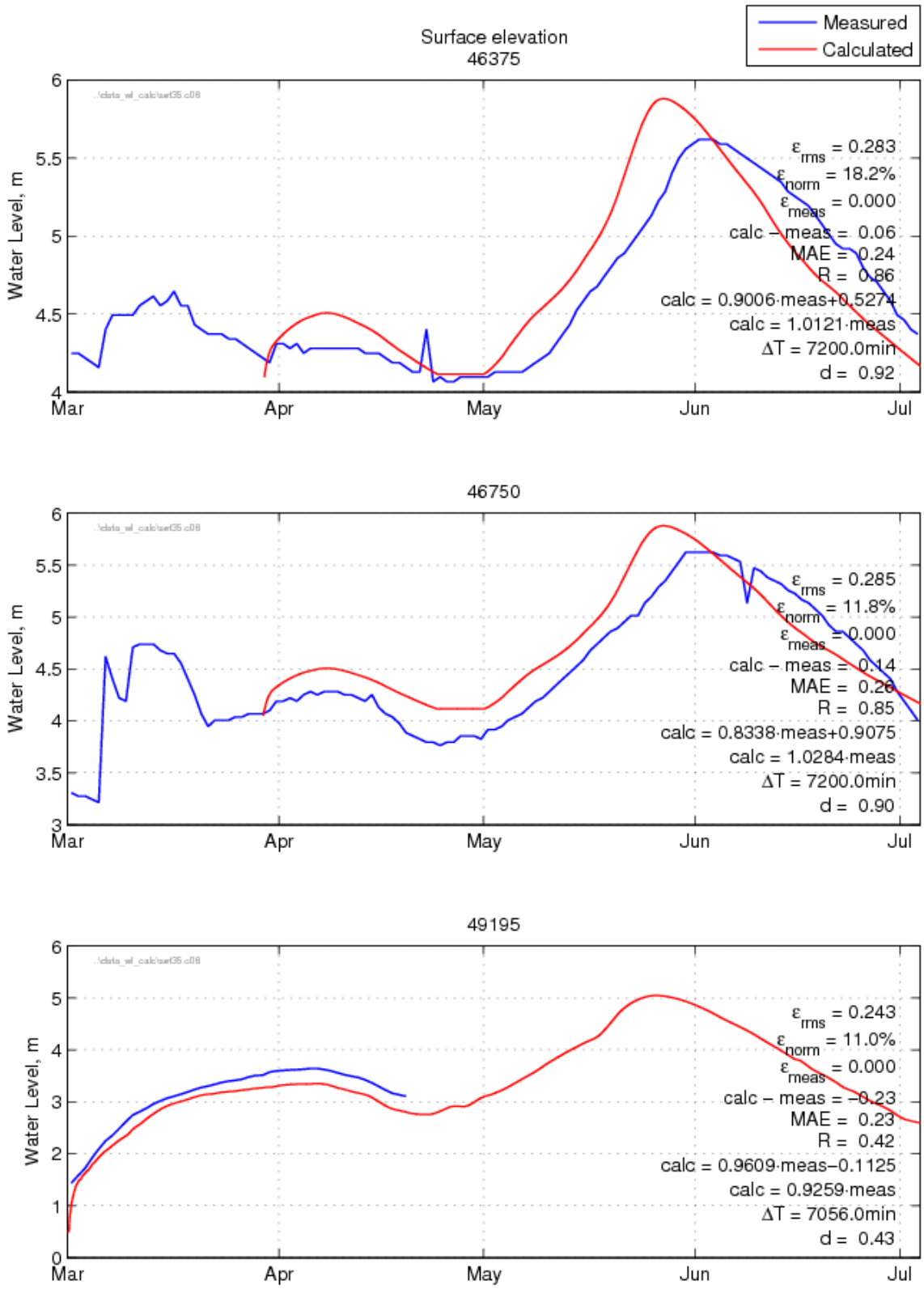

Figure 4-6: Model calibration results for 2011 flood water levels [m] for WABPL Borrow Pit (46375), Bayou Courtableau Outlet (46750), and WABPL at Lower Grand Bayou (49195)

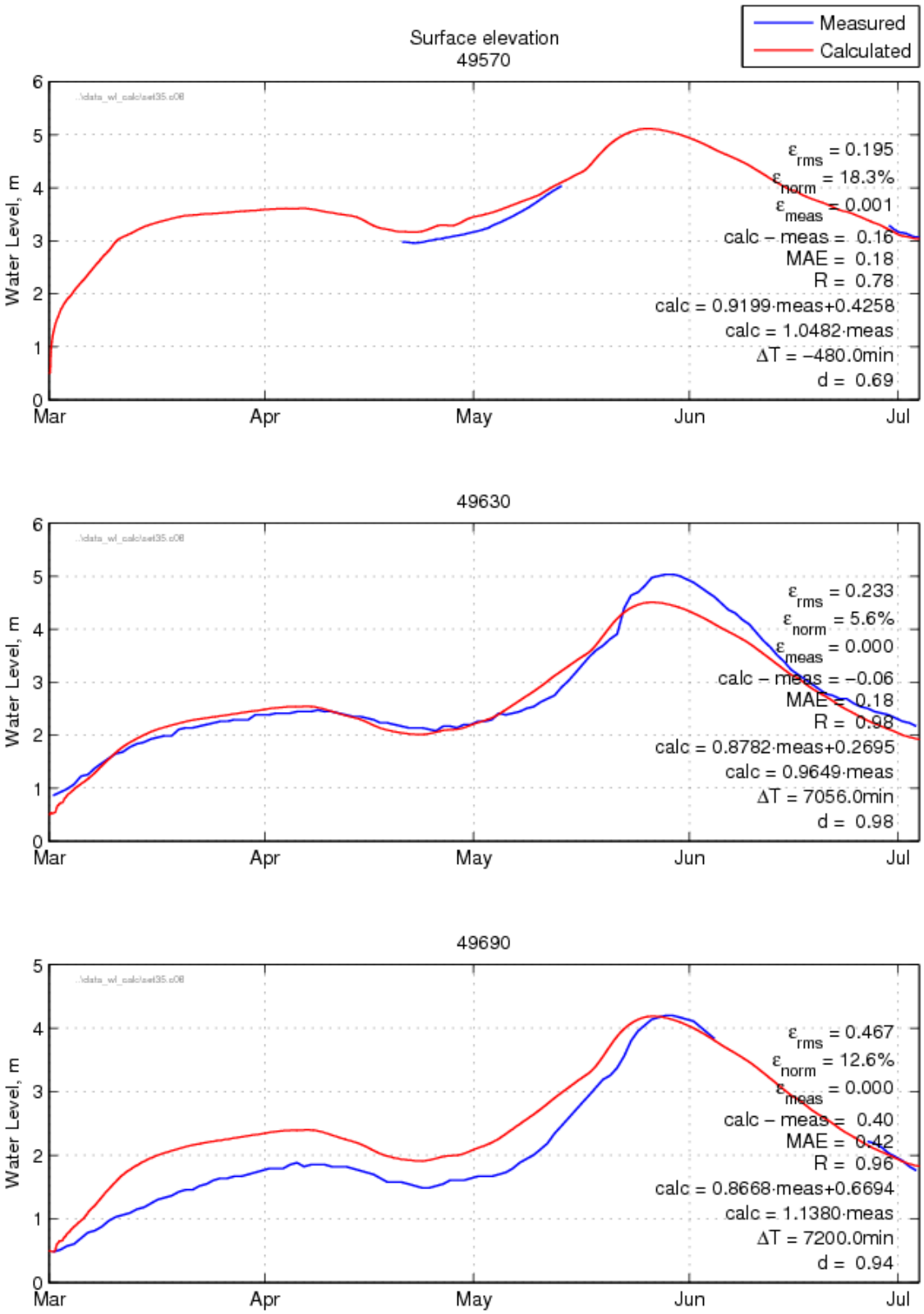

Figure 4-7: Model calibration results for 2011 flood water levels [m] for upper Grand river (49570), EABPL Borrow Pit (49630), and the Intracoastal Waterway (49690)

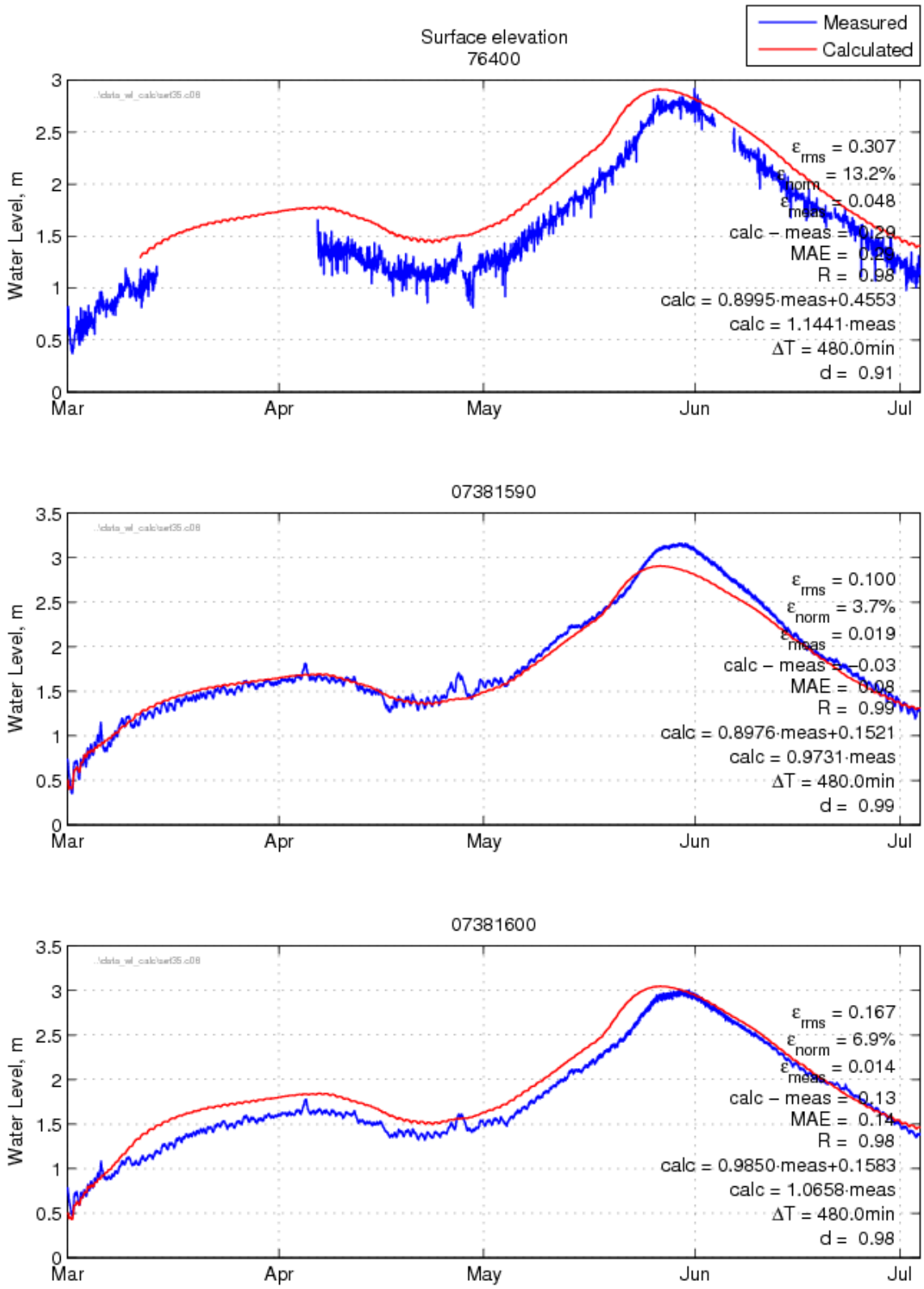

Figure 4-8: Model calibration results for 2011 flood water levels [m] for Bayou Boeuf Lock, (76400), Wax Lake Outlet at Calumet (07381590), and Lower Atchafalaya River at Morgan City (07381600)

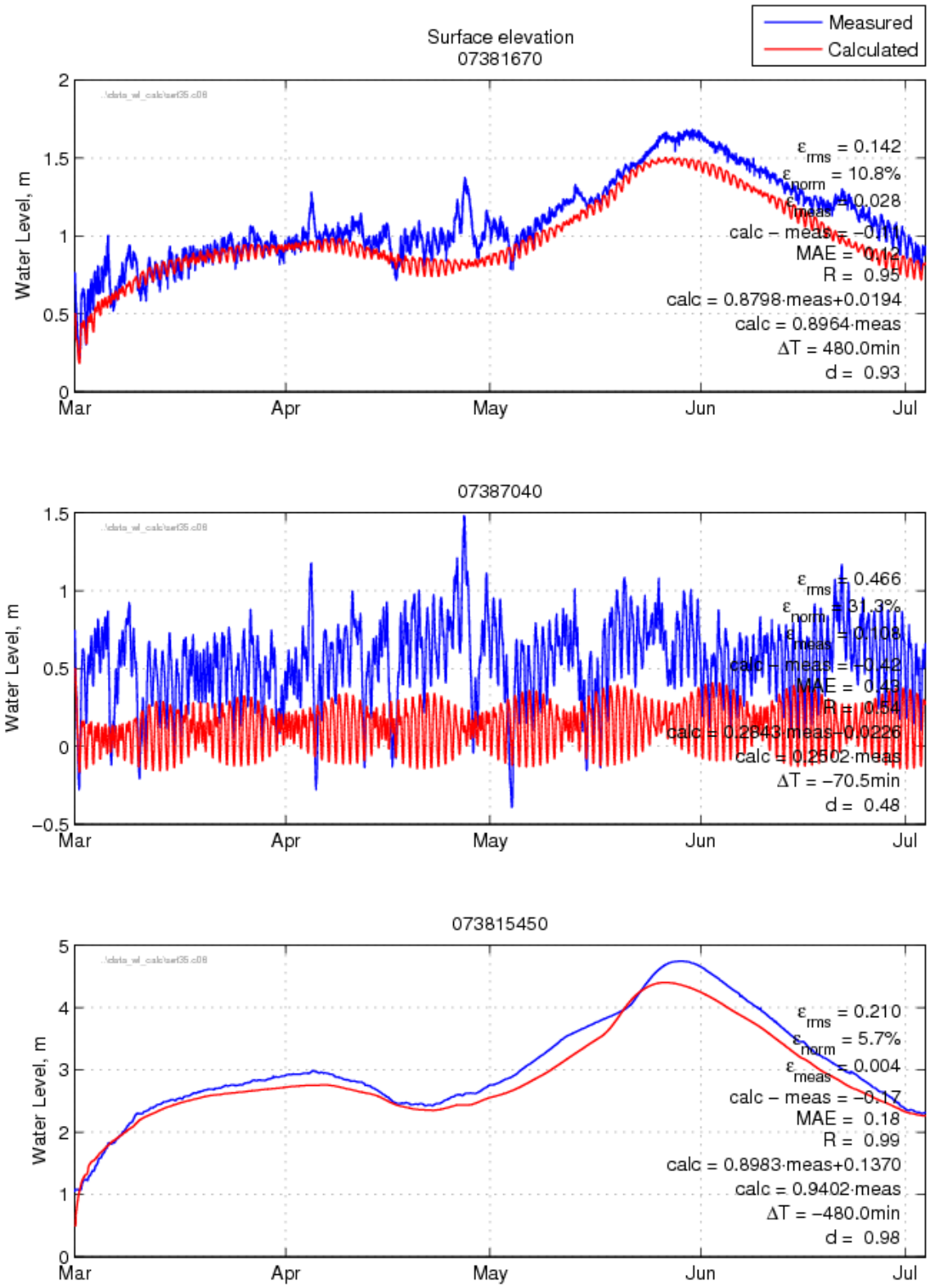

Figure 4-9: Model calibration results for 2011 flood water levels [m] for GIWW at Bayou Sale (07381670), Vermilion Bay near Cypremont Point (07387040), and Chico Pass (073815450)

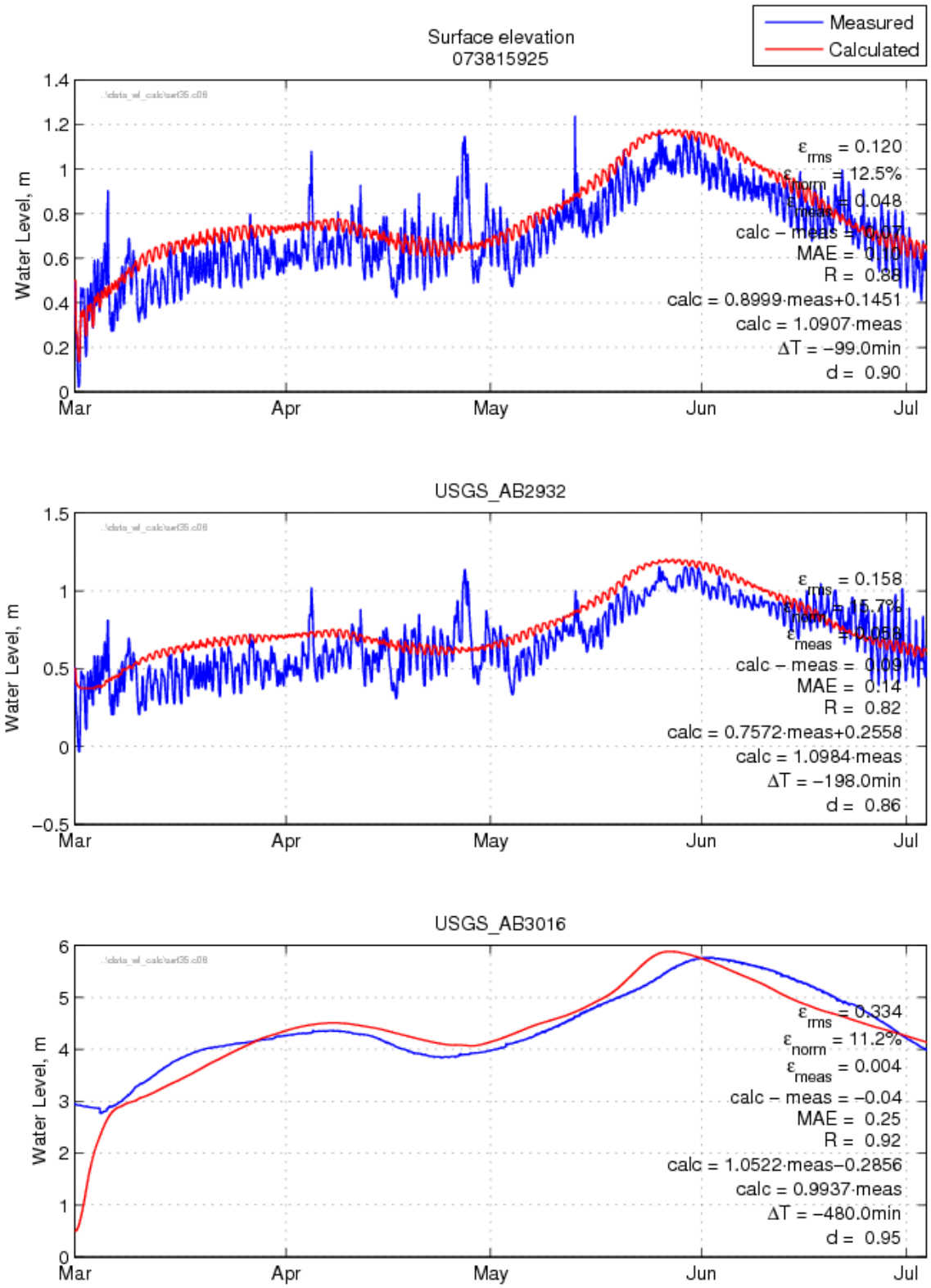

Figure 4-10: Model calibration results for 2011 flood water levels [m] for Crewboat Channel (073815925), Bell Isle (USGS_AB2932), and Pontoon Bridge Canal (USGS_AB3016).

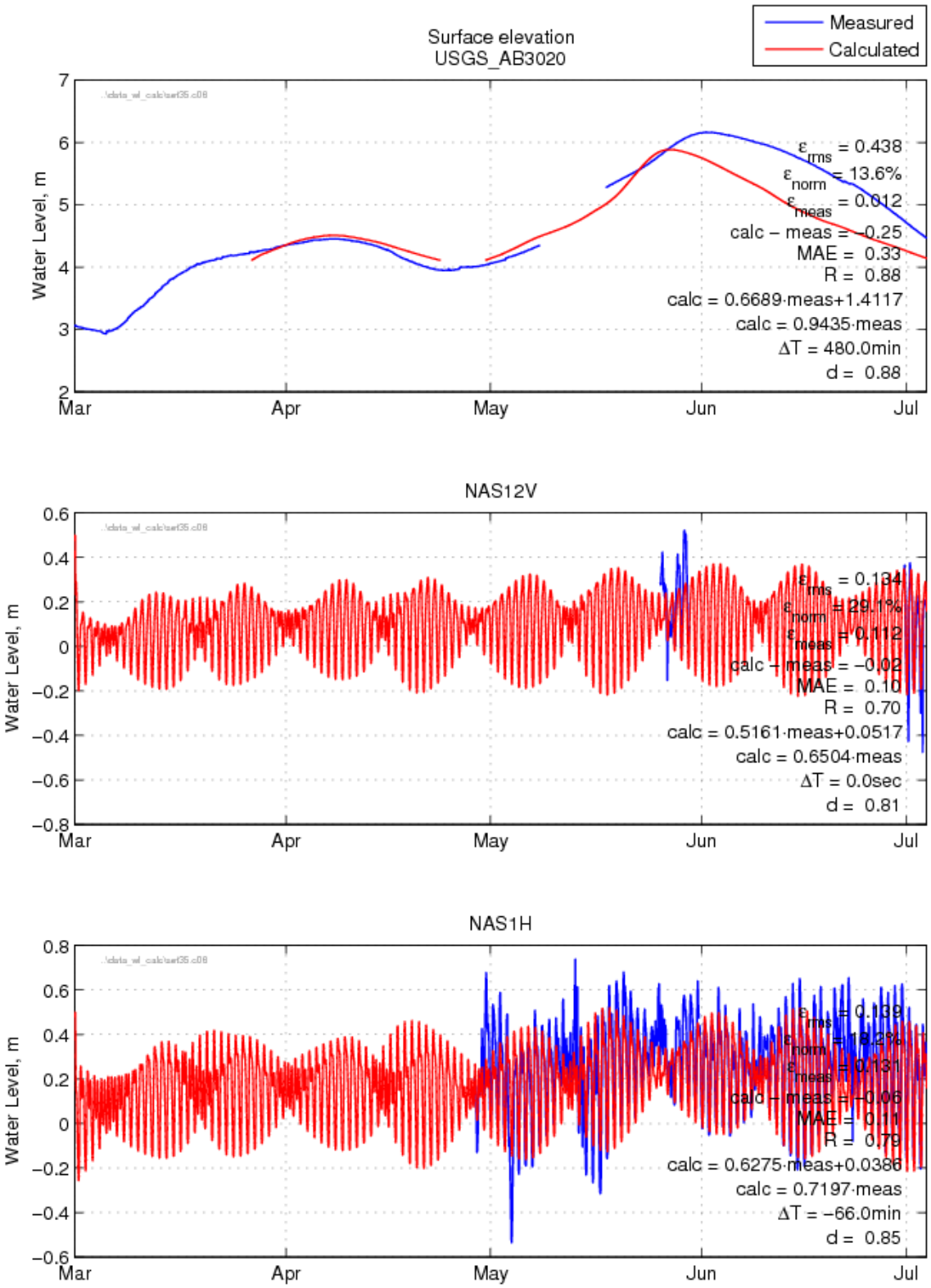

Figure 4-11: Model calibration results for 2011 flood water levels [m] for Lake Pelba (USGS_AB3020), Southwest Pass near Porpoise Pt. (NAS12V), and Eugene Island (NAS1H)

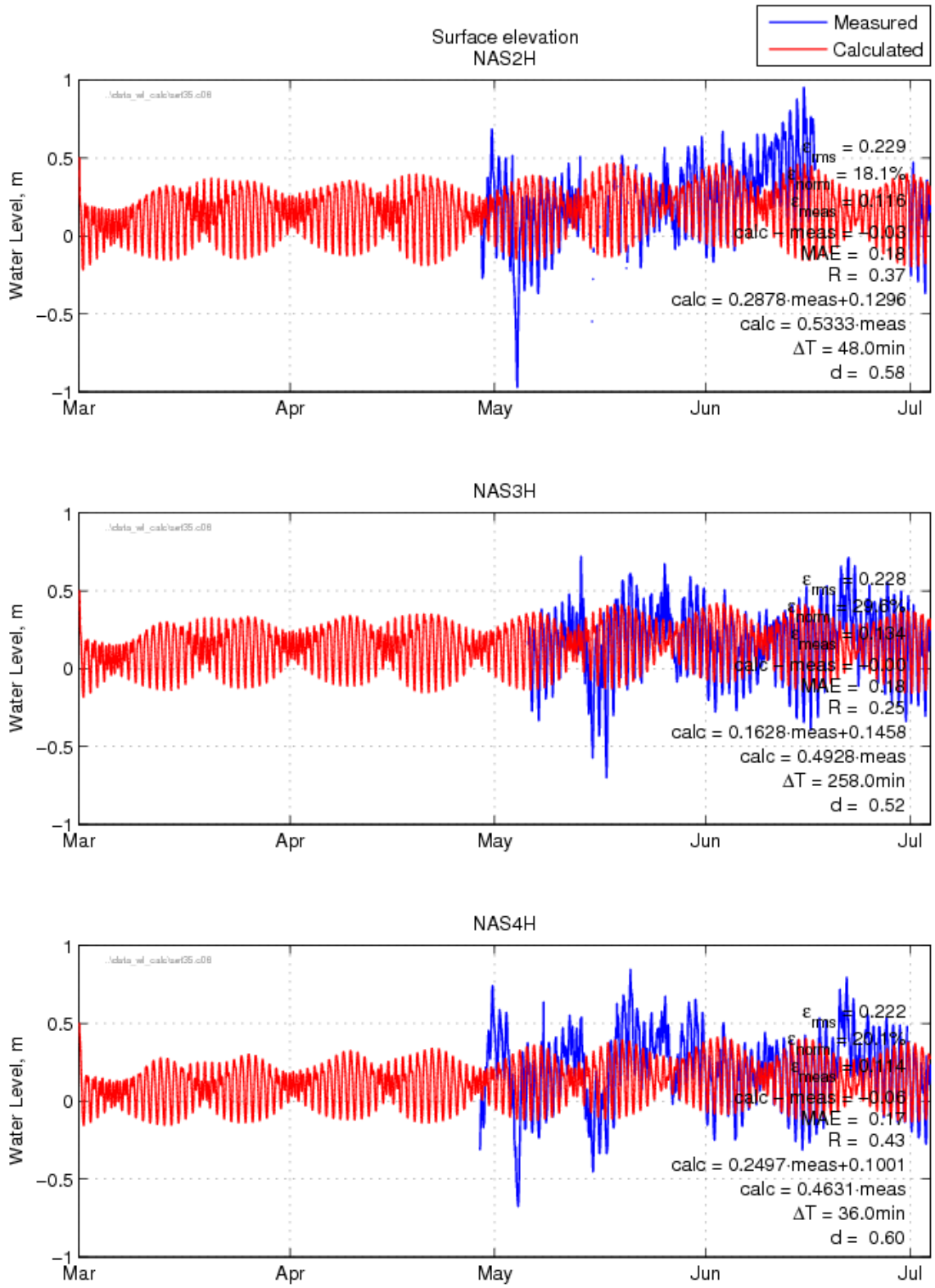

Figure 4-12: Model calibration results for 2011 flood water levels [m] for East Cote Blanche Bay (NAS2H), West Cote Blanche Bay (NAS3H), and Vermilion Bay (NAS4H)

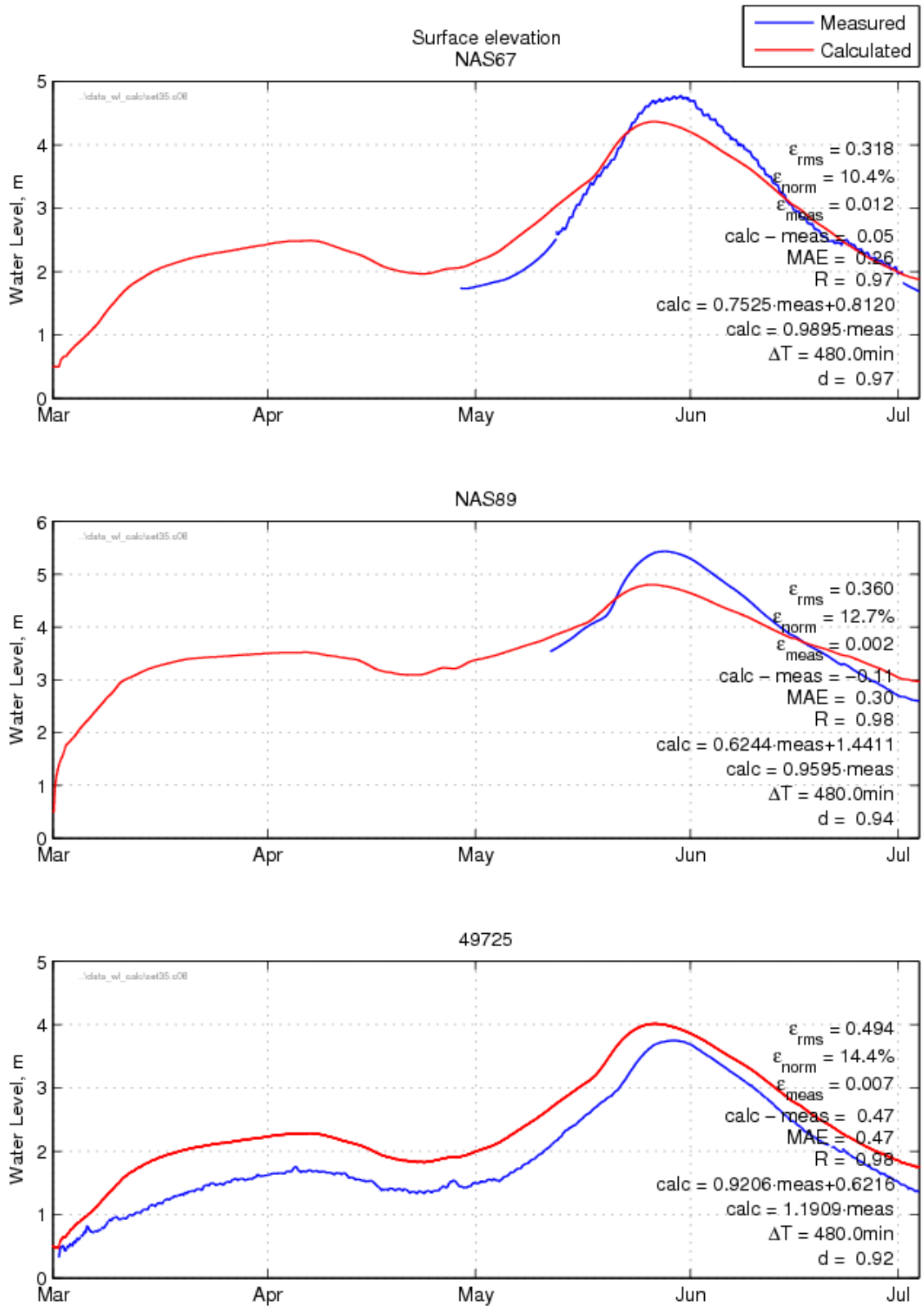

Figure 4-13: Model calibration results for 2011 flood water levels [m] for Old River (NAS67), Bayou Sorrell (NAS89), and Little Bayou Sorrell (49725)

Table 4-1: Summary of Water Level Calibration Results

Station	mean absolute error (m)	RMS error (m)	% RMS error	Location
03045	-0.09	0.31	3.3	Atchafalaya River at Simmesport
03060	0.17	0.33	4.1	Atchafalaya River at Melville
03075	0.27	0.32	4.4	Atchafalaya River at Krotz Springs
03120	-0.08	0.16	3.0	Atchafalaya River at Butte La Rose
03550	-0.15	0.19	4.8	Grand Lake At Charenton Floodgate
03615	0.19	0.38	11.7	Keelboat Pass below Lake Chicot
03645	0.56	0.56	16.4	Six Mile Lake NE of Verdunville
03820	0.06	0.11	7.6	Lower Atchafalaya River Below Sweet Bay Lake
43500	0.52	1.08	27.2	Bayou Latenache Below Pointe Coupe Drainage Structure
46375	0.06	0.28	18.2	WABPL Borrow Pit (FWS) Near Courtableau, LA
46750	0.14	0.29	11.8	Bayou Courtableau Outlet Channel Near Southwest Wing Wall
49195	-0.23	0.24	11.0	WABPL (FWS) At Lower Grand Bayou
49570	0.16	0.19	18.3	Upper Grand River (FWS) At Dike
49630	-0.06	0.23	5.6	EABPL Borrow Pit (FWS) At Bayou Sorrel Lock
49690	0.40	0.47	12.6	Intracoastal Waterway Near Pierre Pass, LA
76400	0.29	0.31	13.2	Bayou Boeuf Lock - West
07381590	-0.03	0.10	3.7	Wax Lake Outlet at Calumet, LA
07381600	0.13	0.17	6.9	Lower Atchafalaya River at Morgan City, LA
07381670	-0.11	0.14	10.8	GIWW at Bayou Sale Ridge near Franklin, LA
07387040	-0.42	0.47	31.3	Vermilion Bay near Cypremort Point, LA
073815450	-0.17	0.21	5.7	Chicot Pass near Myette Point near Charenton, LA
073815925	0.07	0.12	12.5	Crewboat Channel at Wax Lake Outlet nr Calumet, LA
USGS_AB2932	0.09	0.16	15.7	near Belle Isle
USGS_AB3016	-0.04	0.33	11.2	Pontoon Bridge Canal near Butte Larose, LA
USGS_AB3020	-0.25	0.44	13.6	Lake Pelba at I-10 near Henderson, LA
NAS12V	-0.02	0.13	29.1	Southwest Pass near Porpoise Pt.
NAS1H	-0.06	0.14	18.2	Eugene Island
NAS2H	-0.03	0.23	18.1	East Cote Blanche Bay
NAS3H	0.00	0.23	29.6	West Cote Blanche Bay
NAS4H	-0.06	0.22	20.1	Vermilion Bay near Intracoastal City, LA
NAS67	0.05	0.32	10.4	Old River
NAS89	-0.11	0.36	12.7	Bayou Sorrell
49725	0.47	0.49	14.4	Little Bayou Sorrel At Jct. With GIWW

Normalized RMS Error Statistics

Stations < 20%	28/33
% stations < 20%	85%

4.2.2 Spatial Distribution of Water Level Calibration Results

Figure 4-14 below presents the mean absolute error between calculated and measured water levels, derived from the time series presented earlier, at each gage location in the model domain to better indicate spatial variation in model performance.

The three upper-basin gages with the highest “c minus b” (mean absolute error between calculated and measured values) values are concentrated in the southern portion, upstream of the WLO at Calumet and the Atchafalaya River outlet at Morgan City. The gage 03645 located in Six Mile Lake has a high error value, but the difference in calculated and measured water levels is very consistent over the full simulation period. The nearly constant offset and the much better performance at gage locations both immediately upstream and downstream of this gage could indicate that a datum adjustment issue is responsible. Examination of the gages 49690 and 49725, both located in the GIWW along the eastern boundary of the upper basin, shows that the overprediction is more prominent during the earlier, lower-flow portion of the flood and less prominent during the peak and falling limb. The gages on primary conduits of flow into this area of the GIWW, NAS67 and NAS89, show an even greater discrepancy in the differences at lower and higher flows. The gage 03615, located in the upper East Grande Lake area, also shows the same pattern of overprediction during lower flows and upderprediction at the peak. This area of the basin, formed from the infilling of Grande Lake with lacustrine deltas, contains complex and shallow connecting channels that were difficult to reproduce in the model. It can be seen from Figure 3-6: that all of the channels in this area lacked detailed bathymetry sources, so the substantial assumptions required for defining channel bathymetries most likely resulted in some misrepresentation of the hydrodynamics. Additionally, measured water levels at gage 43500 located in the far northwest corner of the Morganza spillway were only recorded during a very short time period during the calibration simulation duration, so comparisons to calculated water levels were only calculated using a couple overlapping times, resulting in a poor mean absolute error.

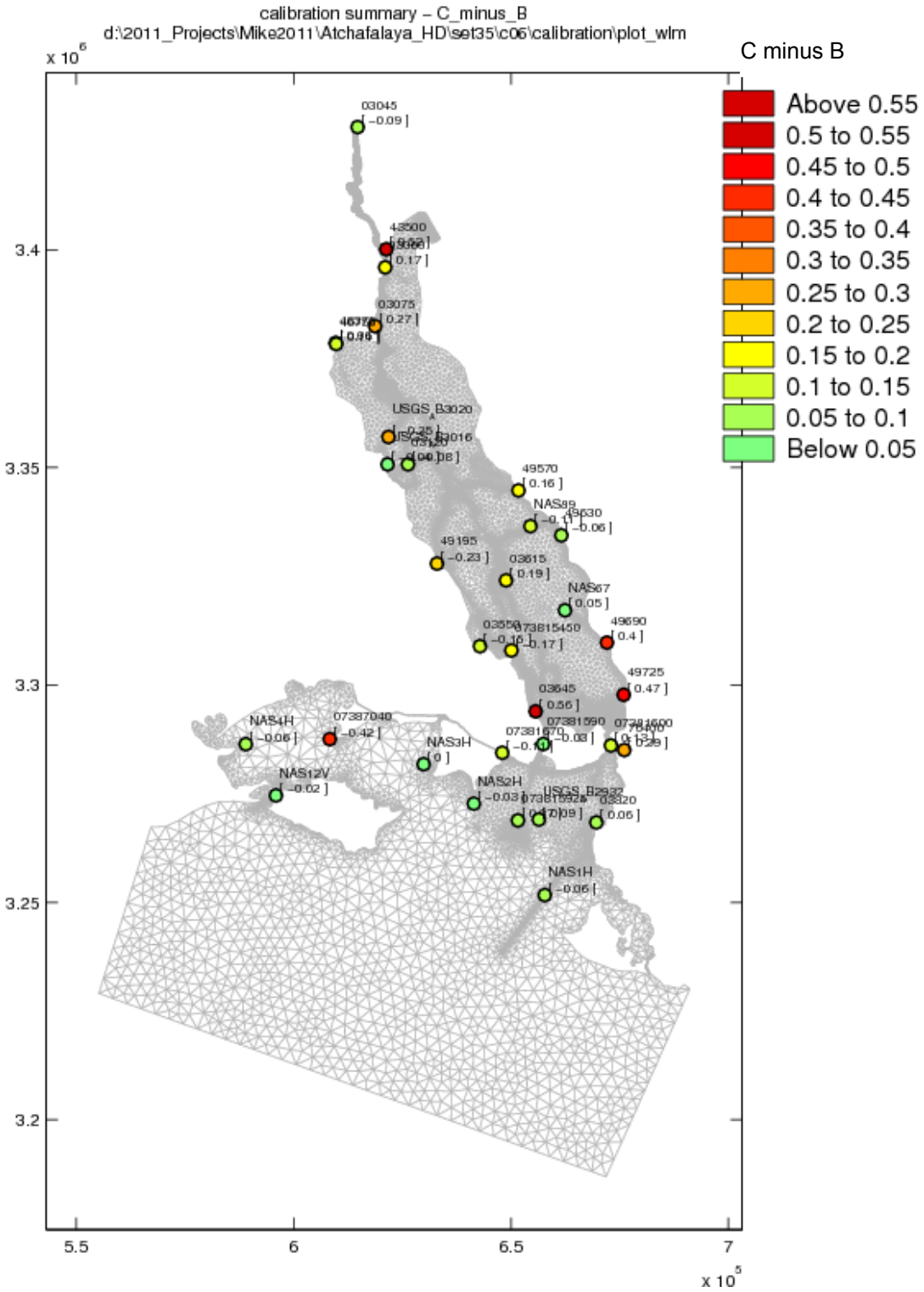

Figure 4-14: Mean absolute error between calculated and measured water levels at particular gage locations in the basin as a geographical representation of values presented in Table 5-1

4.2.3 Flood Arrival Timing

Figure 4-15 highlights the model's performance in simulating the phasing of the flood peak. The moderate flood stage for the Lower Atchafalaya River at Morgan City gage is defined as 7 ft. or approximately 2.1 m. The calculated water surface elevation reaches this stage approximately 3.5 days before the measured data water surface. Flood peak arrival time is a few days early as well, which is consistent across most of the basin. Various test runs preceded and improved model performance with respect to this aspect; Depending on future application of the model, further study could be recommended. Considering the length of the simulation and the spatial extent of the model domain, these final values were considered to indicate good performance in the routing of the flood downstream through the basin.

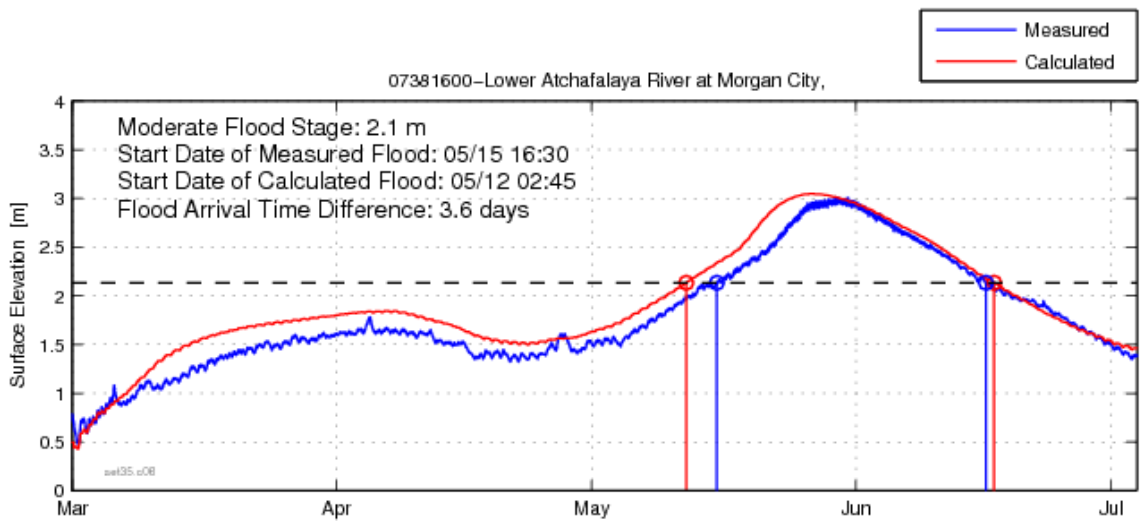

Figure 4-15: Difference between calculated and measured flood stage arrival times (time in GMT).

4.2.4 Tidal Constituent Analysis

Water level time series for coastal stations showed decreasing river influence with distance from the Atchafalaya and Wax Lake Deltas; instead, variations were mostly driven by tidal fluctuations. Measured water levels in these locations additionally show variations due to wind set-up and other meteorological forcings. Because the mean water levels remain roughly constant at many primarily-tidal stations, comparisons between the amplitude and phasing of the tidal oscillatory constituents presents an additional means to assess model performance.

Though calibration of the model based on tidal station water level performance was not a focus of this project phase, comparisons between the calculated and measured tidal constituent amplitudes are given below to show the already substantial agreement for the more important constituents and the potential for improvement. The figures below compare performance for the five most important constituents at several selected

coastal stations. Generally, the highest amplitude constituents K1 and O1 are correctly predicted, with normalized amplitude errors increasing for constituents with much smaller amplitudes. At these coastal stations where the tidal signal is not significantly deformed from the boundary values, the errors are in general very small. The inland tidal stations (comparison plots not shown) where the tide must propagate over marshes and through narrow, winding tidal channels generally show a dampened tidal signal from what was measured. This can be attributed to the fact that model resolution is currently not sufficient to capture these features accurately.

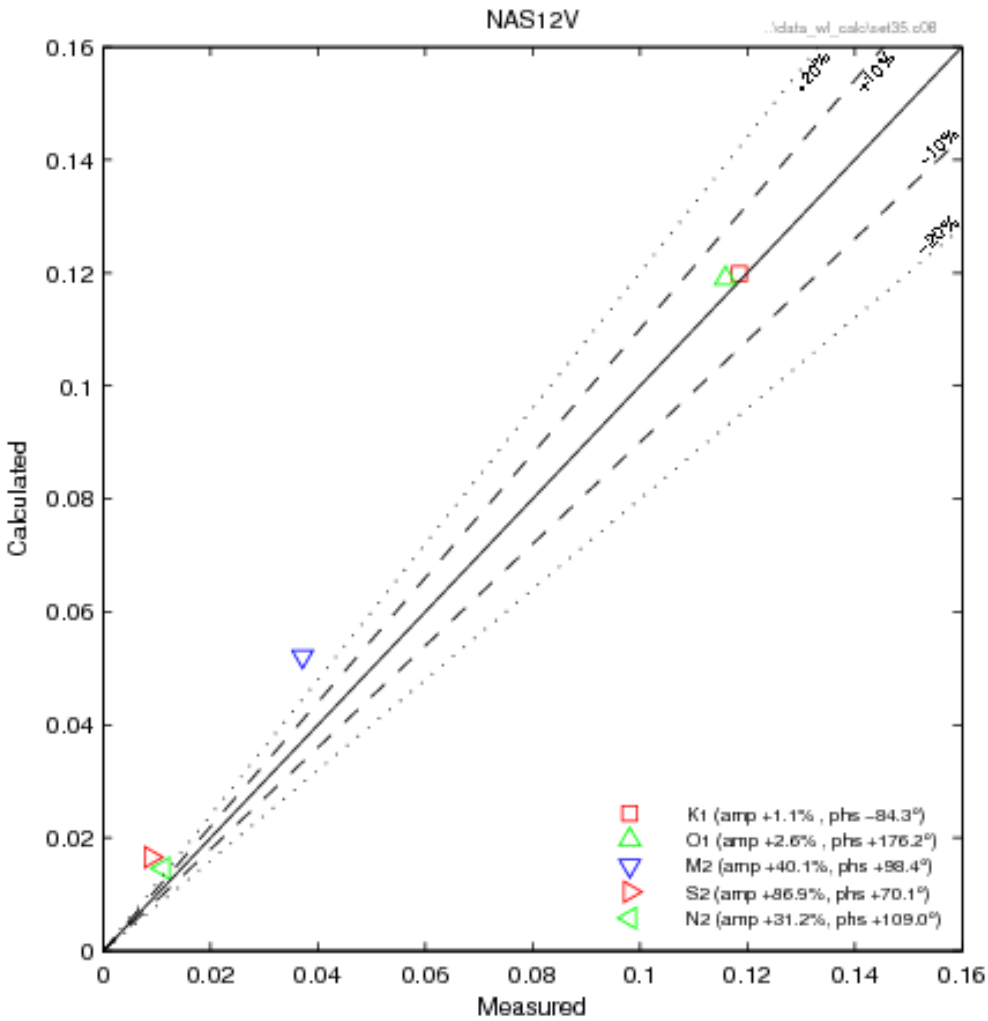

Figure 4-16: NAS12V (Southwest Pass near Porpoise Pt.) calculated and measured tidal constituent amplitude comparison

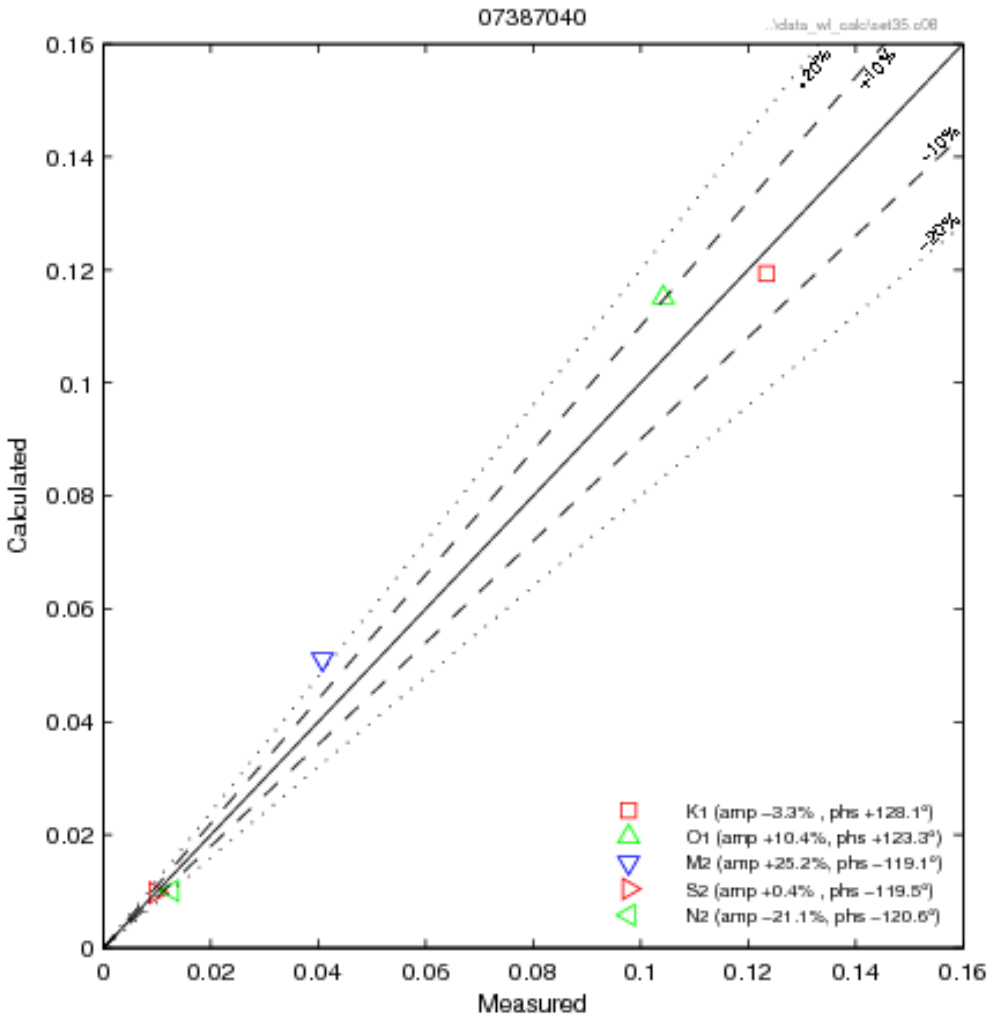

Figure 4-17: 07387040 (Cypremont Point) calculated and measured tidal constituent amplitude comparison

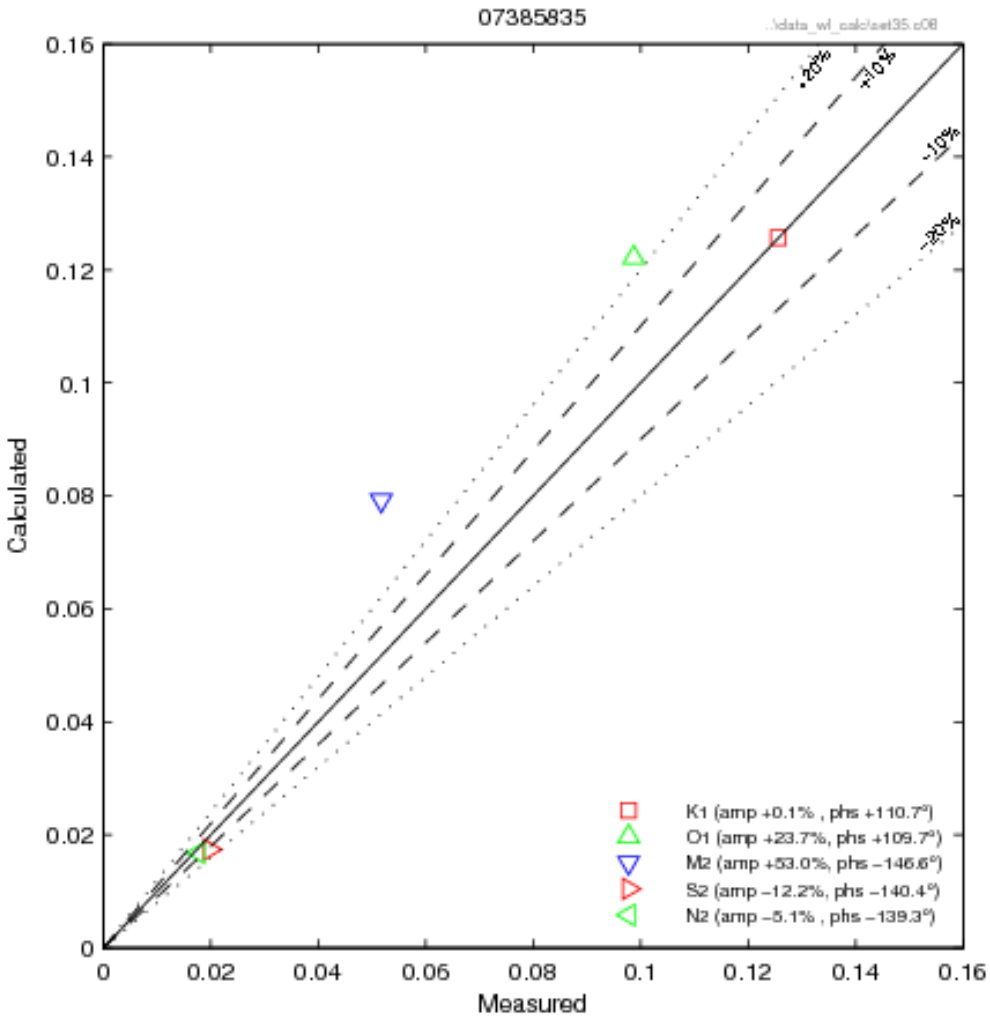

Figure 4-18: 07385835 (East Cote Blanche Bay) calculated and measured tidal constituent amplitude comparison

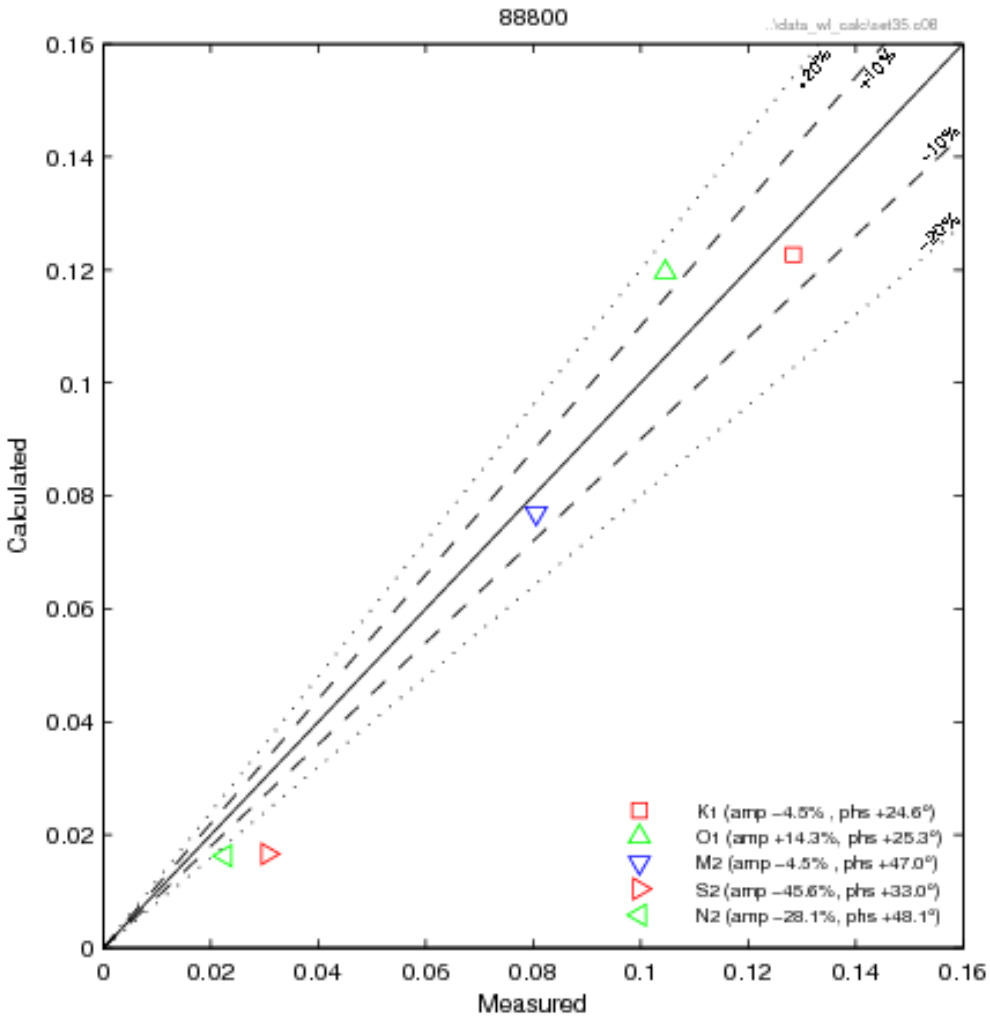

Figure 4-19: 88800 (East Cote Blanche Bay) calculated and measured tidal constituent amplitude comparison

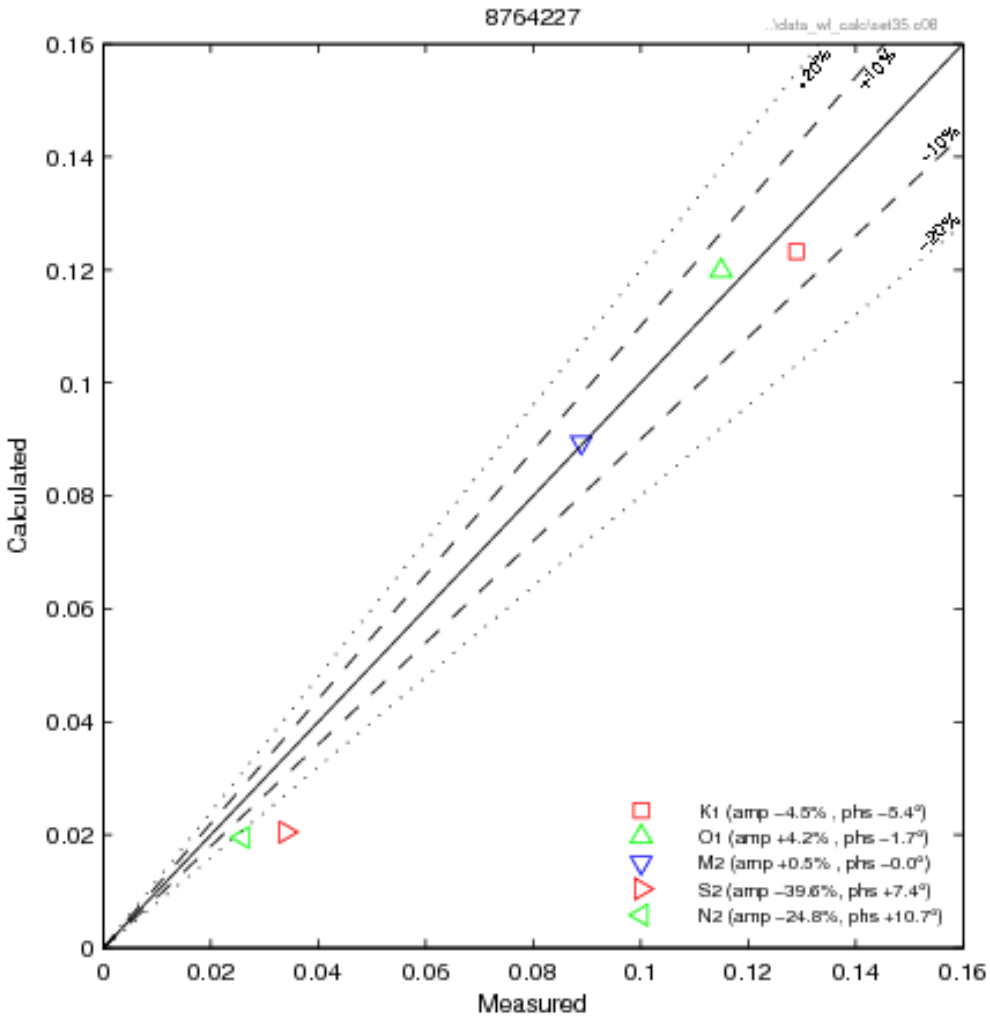

Figure 4-20: 8764227 (Amerada Pass) calculated and measured tidal constituent amplitude comparison

4.3 Discharge and Current Calibration

Discharge and channel-averaged current speed measurements were available for two of the NAS gages located in the Upper Bell River area and at the two outlets into the lower basin. The Wax Lake Outlet at Calumet and the Atchafalaya River at Morgan City are the only conduits for flow to exit the upper basin. Both have deep, channelized cross-sections where the flow is fully confined between the adjacent levees, offering ideal locations to evaluate the large-scale distribution of flow within the basin. The performance of the model in simulating the discharge through both outlets was very good, with normalized errors of approximately 5% for the Atchafalaya River and 9% for Wax Lake Outlet. Current speed was similarly well represented, though some overprediction of peak currents through the Wax Lake Outlet was present. Both discharge and channel-averaged current speed are much more dependent upon bathymetry than water level, so the degree of uncertainty in bathymetry and the corresponding flow area should be taken into account when analyzing the results. Fairly

recent, high-resolution surveys were used to define model bathymetry for the Wax Lake Outlet and the main Atchafalaya Channel; however, reliable bathymetry sources for Bayou Sorrell and Old River were not available. Additionally, high uncertainty in the measured data (see section Appendix A – A.2.3) for a description of the calculation procedure) exists which somewhat limits the usefulness of the gages for specific calibration to discharge. Despite these issues, simulated discharges, and to a lesser extent channel-averaged current speed, show fairly good agreement with measured values. A more detailed elaboration is included in the next section.

4.3.1 Measured and Calculated Discharge Comparison

Figure 4-21 and Table 4-2 give comparisons between the measured and calculated discharge time series at the upper basin outlets and the two NAS field campaign discharge gages in Bayou Sorrell and Old River. Based on the very accurate simulation of discharges through the Wax Lake Outlet (gage 07381590) and the Atchafalaya River at Morgan City (gage 07381600), the distribution of flow between the two outlets and the corresponding large scale flow patterns in the upper basin are adequately reproduced. Discharge through the WLO is slightly underpredicted during lower flows and slightly overpredicted at the flood peak, while discharge at Morgan City almost exactly follows the shape of the measured hydrograph. Mean absolute error is approximately +180 m3/s through the Morgan City outlet and -240 m3/s through the Calumet outlet, with both values representing a very small fraction of their respective peak discharges. The small tidal signal present in the measured discharges is not as pronounced in the model.

Calculated discharges through Bayou Sorrell (gage NAS89) and Old River (gage NAS67) in the Upper Bell River Region, as measured at the two NAS discharge stations, show fairly good agreement with measured time series though with high normalized RMS error percentages that reflect the low magnitudes of the measured flow. The measured flow at station NAS89 is fairly complex, a result of the high overland flow from the Morganza spillway, yet the model is able to approximate the hydrograph shape. Flow at station NAS67 more closely mirrors the shape of the inflow flood hydrograph, though the model overpredicts peak flows and spreads out the flood start and end times. Table 4-2 gives a summary of the model performance statistics at each discharge measurement station.

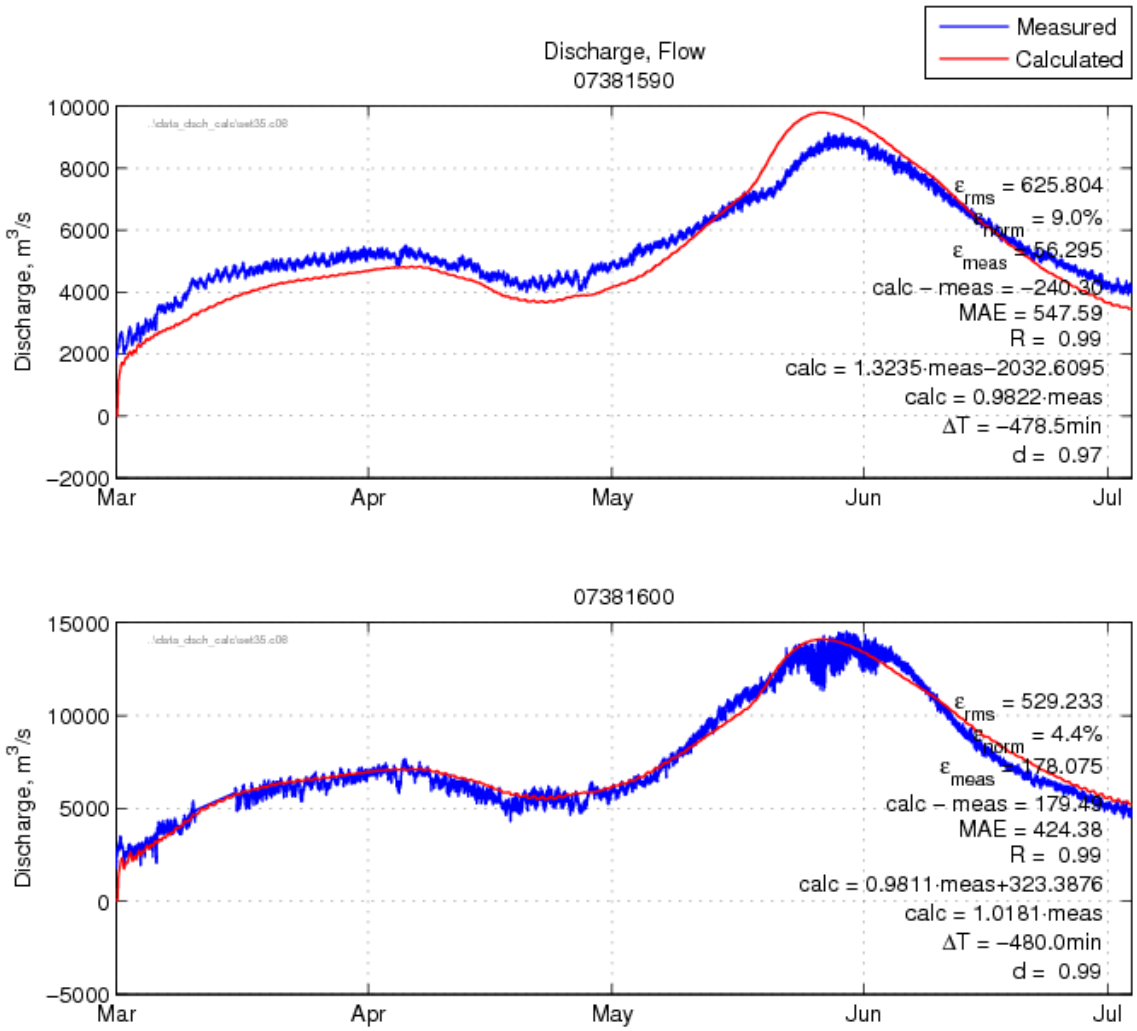

Figure 4-21: Model calibration results for 2011 flood with calculated and measured discharges - upper basin outlets [m3/s] at Wax Lake Outlet at Calumet (07381590) and Morgan City (07391600)

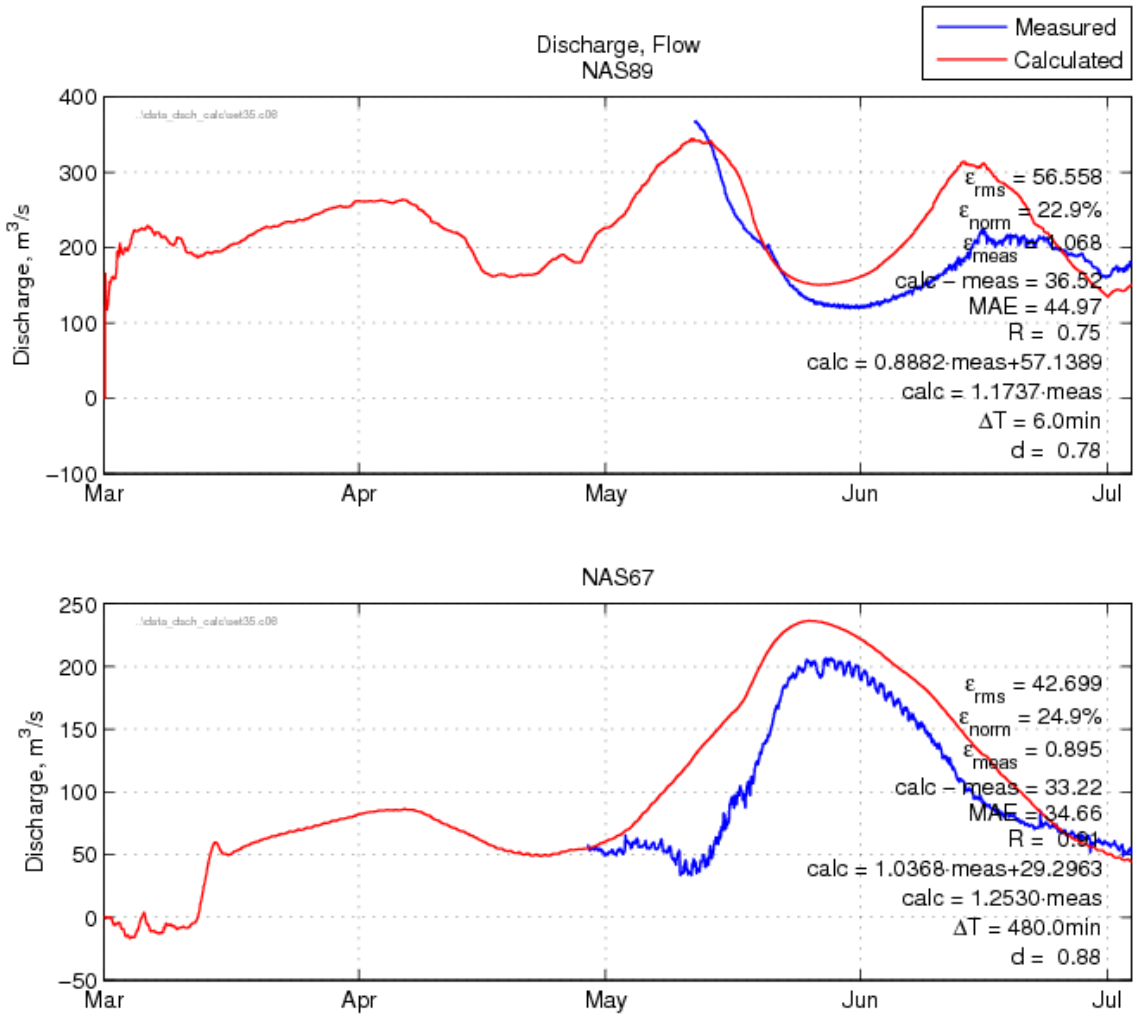

Figure 4-22: Model calibration results for 2011 flood with calculated and measured discharges [m3/s] - NAS gages at Bayou Sorrel (NAS89) and Old River (NAS67)

Table 4-2: Summary of Discharge Calibration Results

Station	**mean absolute error (m^3/s)**	**RMS error (m^3/s)**	**% RMS error**	**Location**
07381590	-240.3	625.80	9.0	Wax Lake Outlet at Calumet, LA
07381600	179.49	529.23	4.4	Lower Atchafalaya River at Morgan City, LA
NAS67	33.22	42.70	24.9	Old River
NAS89	36.52	56.56	22.9	Bayou Sorrell

Normalized RMS Error Statistics

Stations < 20%	2/4
% stations < 20%	50%

4.3.2 Measured and Calculated Current Comparison

Figure 4-23 and Figure 4-24 give comparisons between the measured and calculated channel-averaged current speed time series at the upper basin outlets and the two ENCOS discharge gages in Bayou Sorrell and Old River. Model performance for current simulation is similar to discharge simulation at the particular gages, though with increased errors where discharge was slightly misrepresented. Calculated current speed in the Atchafalaya River at Morgan City very closely matches the measured values. Additionally, the shape of the measured current speed time series at gage NAS89 is modeled fairly well. Modeled current speed through the Wax Lake Outlet at Calumet is very accurate during lower flows but increasingly overpredicts values by as much as 0.5 m/s as discharge reaches flood levels. Peak current speeds at the NAS67 gage in Old River are significantly underpredicted, possibly indicating an oversized channel. Table 4-3 gives a summary of the model performance statistics for channel-averaged current speed at each discharge measurement station.

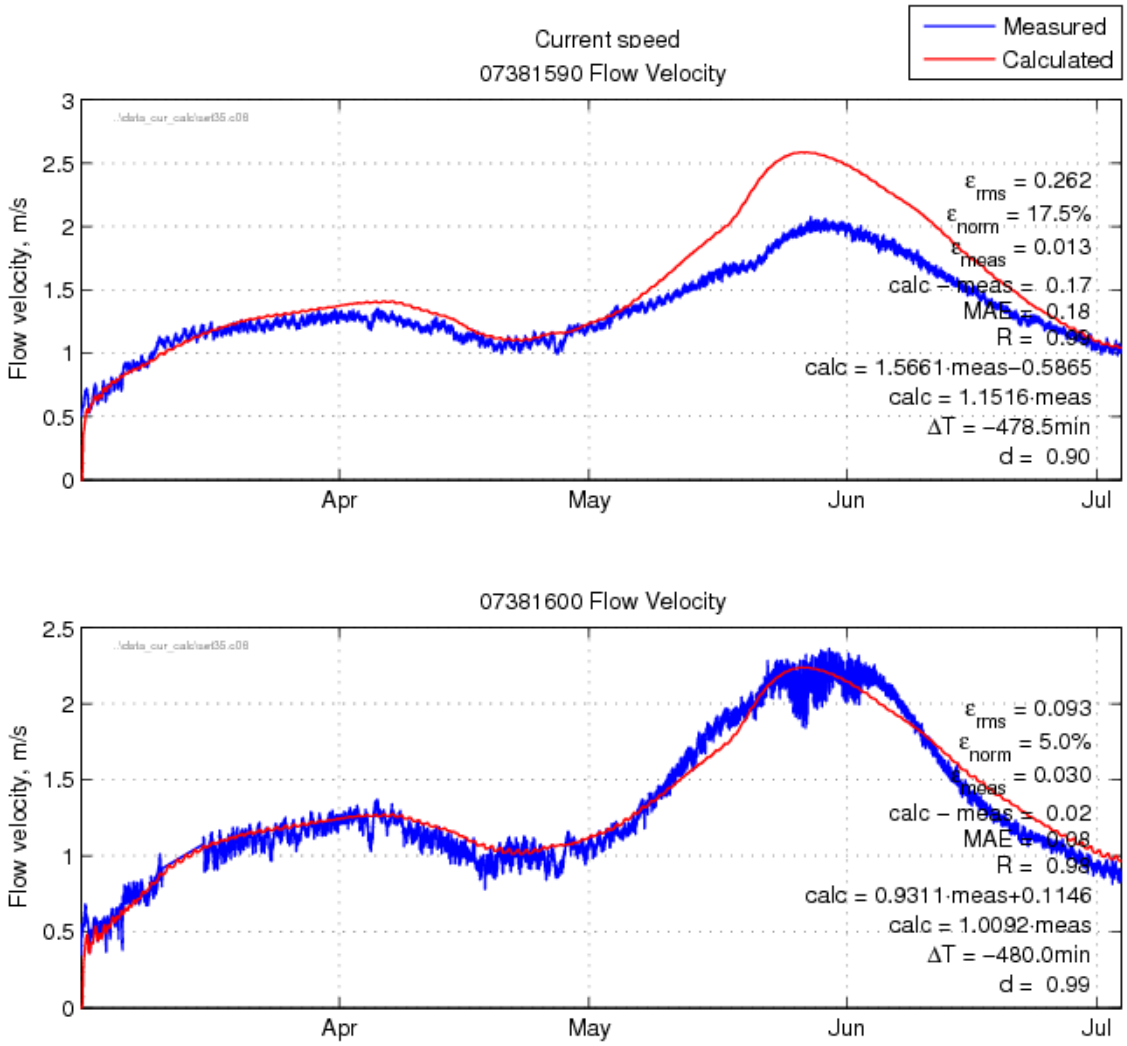

Figure 4-23: Model calibration results for 2011 flood with calculated and measured channel-averaged current speeds [m/s] - at Wax Lake Outlet at Calumet (07381590) and Morgan City (07391600)

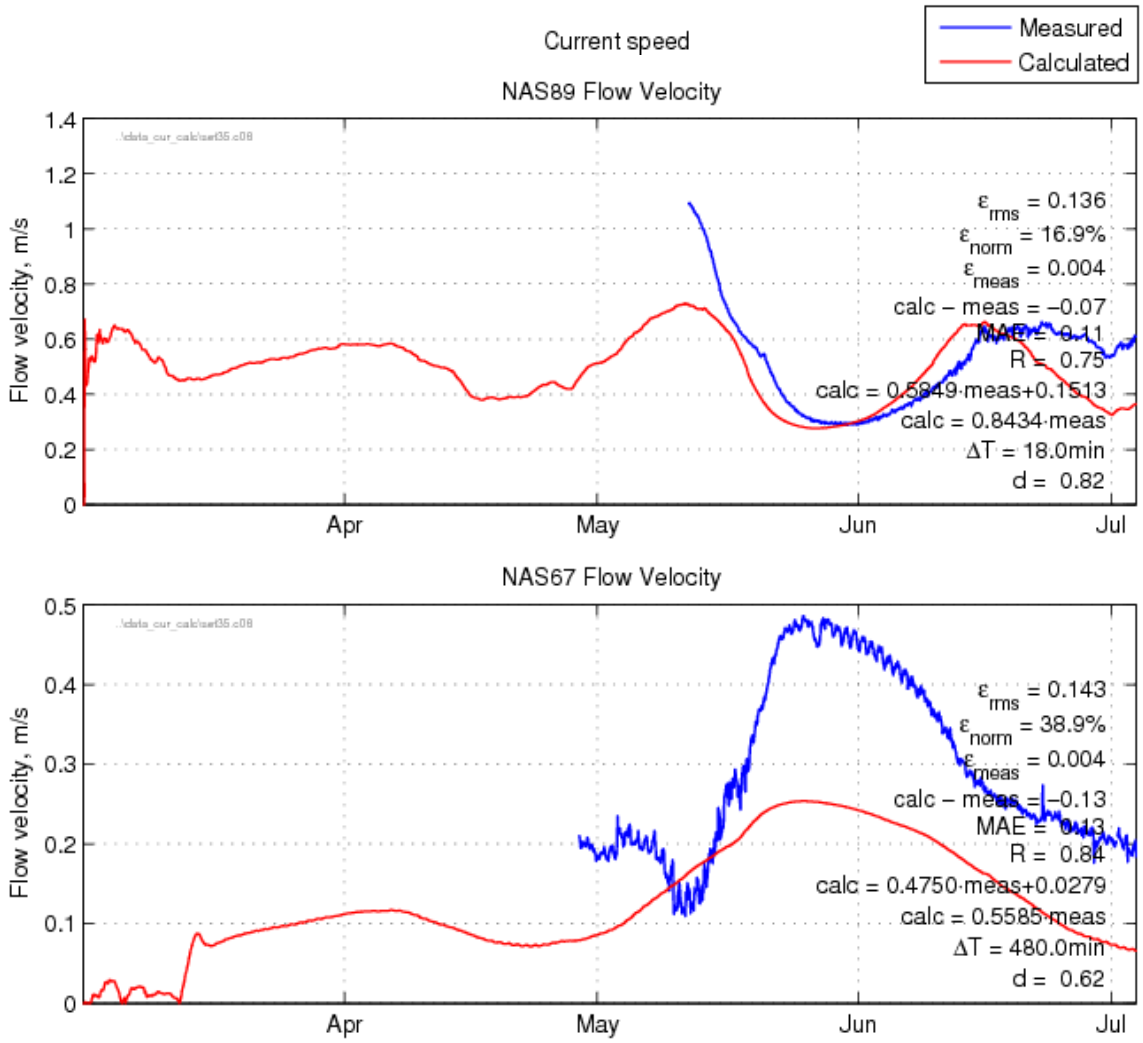

Figure 4-24: Model calibration results for 2011 flood with calculated and measured channel-averaged current speeds [m/s] –NAS gages at Bayou Sorrel (NAS89) and Old River (NAS67)

Table 4-3: Summary of Current Calibration Results

Station	mean absolute error (m/s)	RMS error (m/s)	% RMS error	Location
07381590	0.17	0.26	17.5	Wax Lake Outlet at Calumet, LA
07381600	0.02	0.09	5.0	Lower Atchafalaya River at Morgan City, LA
NAS67	-0.13	0.14	38.9	Old River
NAS89	-0.07	0.14	16.9	Bayou Sorrell

Normalized RMS Error Statistics

Stations < 20%	3/4
% stations < 20%	75%

4.3.3 Rating Curves and Discharge Distribution through Outlets

The discharge distribution through the two upper-basin outlets was further analyzed by comparing measured and calculated rating curves at the two stations. Figure 4-25 and Figure 4-26 present the rating curves calculated at Wax Lake Outlet and Morgan City (gages 07381590 and 07381600), respectively. The modeled rating curves for both gages match the calculated curves during low flow very well, though the meteorological influence on water levels during lower flows causes significant scatter that cannot be reproduced with only the model's astronomical boundary conditions. During lower flow periods, the tidal fluctuations will have a greater relative influence on water levels than during periods of high flow, causing substantial variation in water levels for the same discharges. This can be seen in the measured rating curves for both gages, where there is a much lower correlation between water levels and discharges for flows below a certain level. The Wax Lake Outlet modeled curve deviates from the measured curve at higher flows, reflecting the slight overprediction of peak discharges and underprediciton of peak stages. The Atchafalaya River rating curve still matches the general trend of the measured curve at higher flows; however, the model is not able to reproduce the hysteresis in the rising and falling limbs of the flood. The exact cause of the measured hysteresis at this location is uncertain; however, possible morphological causes will not be present in the current fixed-bed model configuration.

Figure 4-27 plots the fraction of total Wax Lake Outlet and Atchafalaya River discharge flowing through the Morgan City outlet as a function of the total discharge through both outlets. The measured data gives an indication of how the flow was split between the two outlets as the magnitude of discharge through the basin varied. At lower flows, there is significant variation in the proportion of flow discharging through Morgan City which is to be expected based on the increased influence of tides and meteorological events on discharge during low flows. As the combined flow rises above approximately 10000 m^3/s (353146 ft^3/s), there is significantly less variation. At this level of combined discharge and above, the split of flow between the outlets is nearly equal to a 50/50 split with a slight increase in discharge through Morgan City as combined discharge increases to a 60/40 ratio. At the highest discharges, the proportion of flow going through Morgan City instead of the Wax Lake Outlet is greater than at more moderate flows. The modeled discharge split approximates the measured data fairly well. During lower flows, but after a small spin-up period in the calculated data, the calculated proportion of discharge is near the centroid of the scatter measured data, of course showing less variation due to the neglected meteorological forcings in the model. The calculated proportion also begins to increase with increasing discharge, but instead peaks at approximately 10000 m^3/s of combined discharge. With further increasing discharge, the proportion through Morgan City slightly decreases, then stays constant at approximately 60%. The slight differences in the split of discharge through the outlets at higher flows, as presented in the below figure, is reflected in the discharge time series where flow through the Wax Lake Outlet is somewhat over predicted at the flood peak.

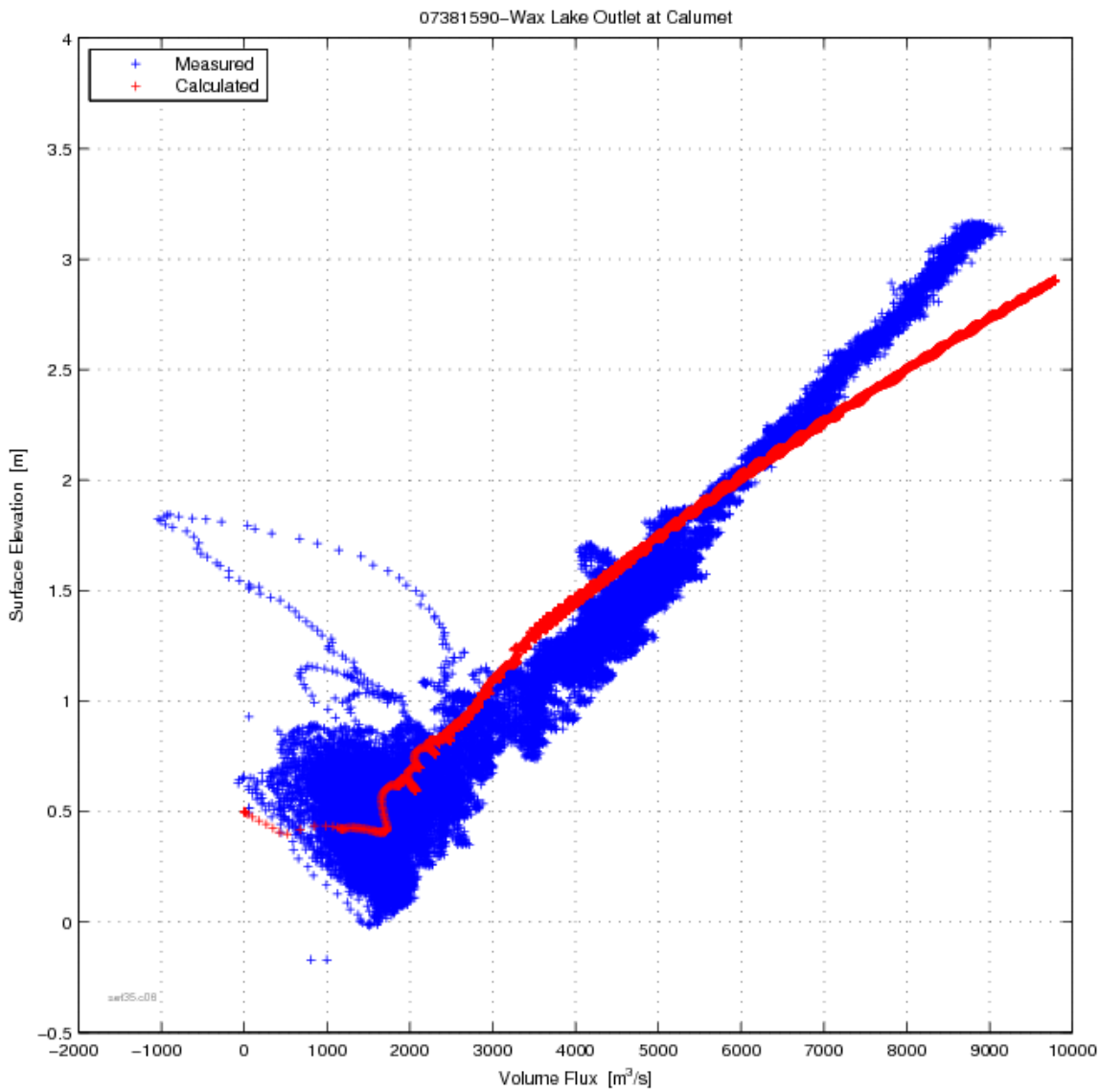

Figure 4-25: Measured and calculated rating curve at the Wax Lake Outlet at Calumet

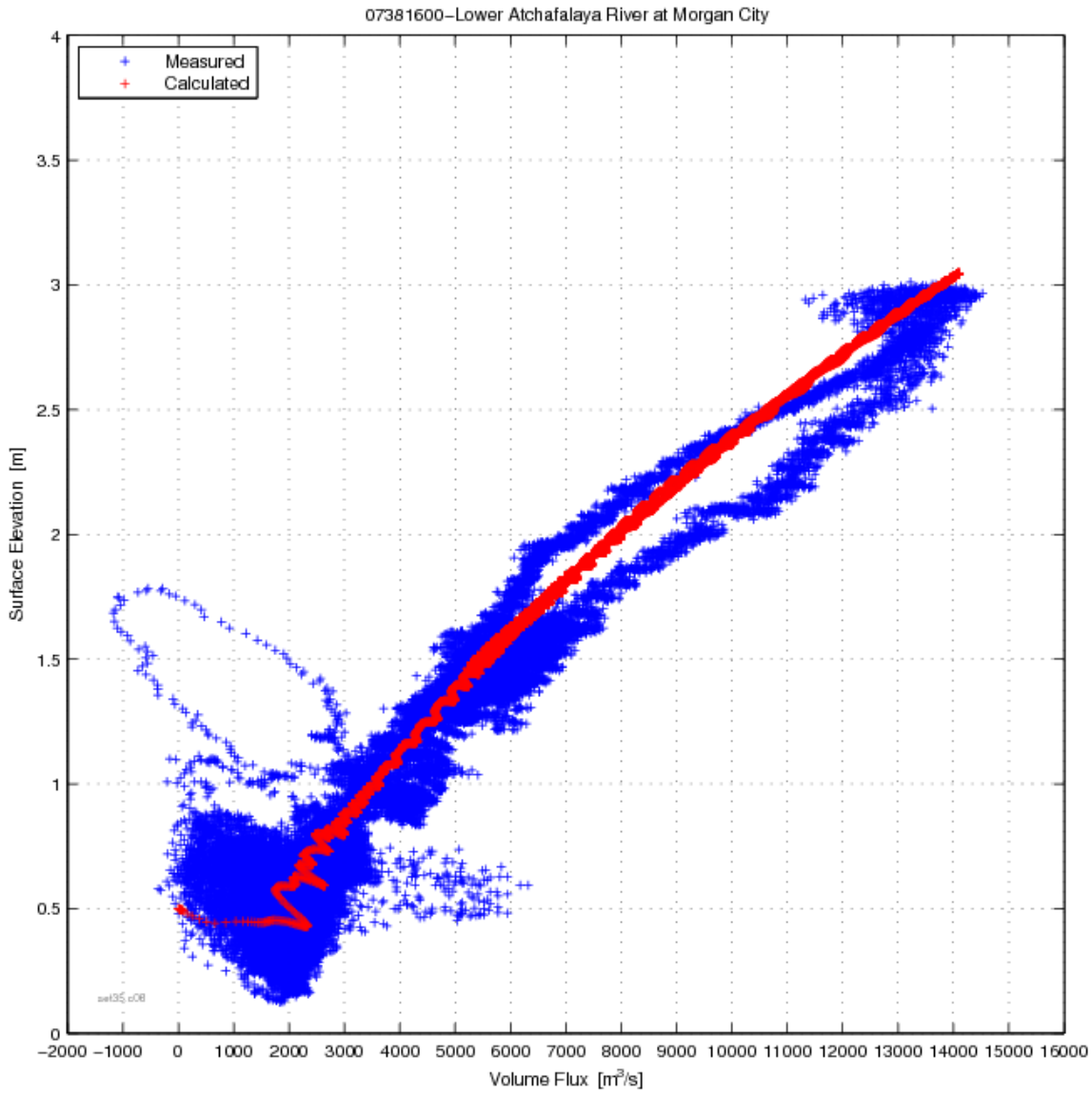

Figure 4-26: Measured and calculated rating curve at the Atchafalaya River at Morgan City

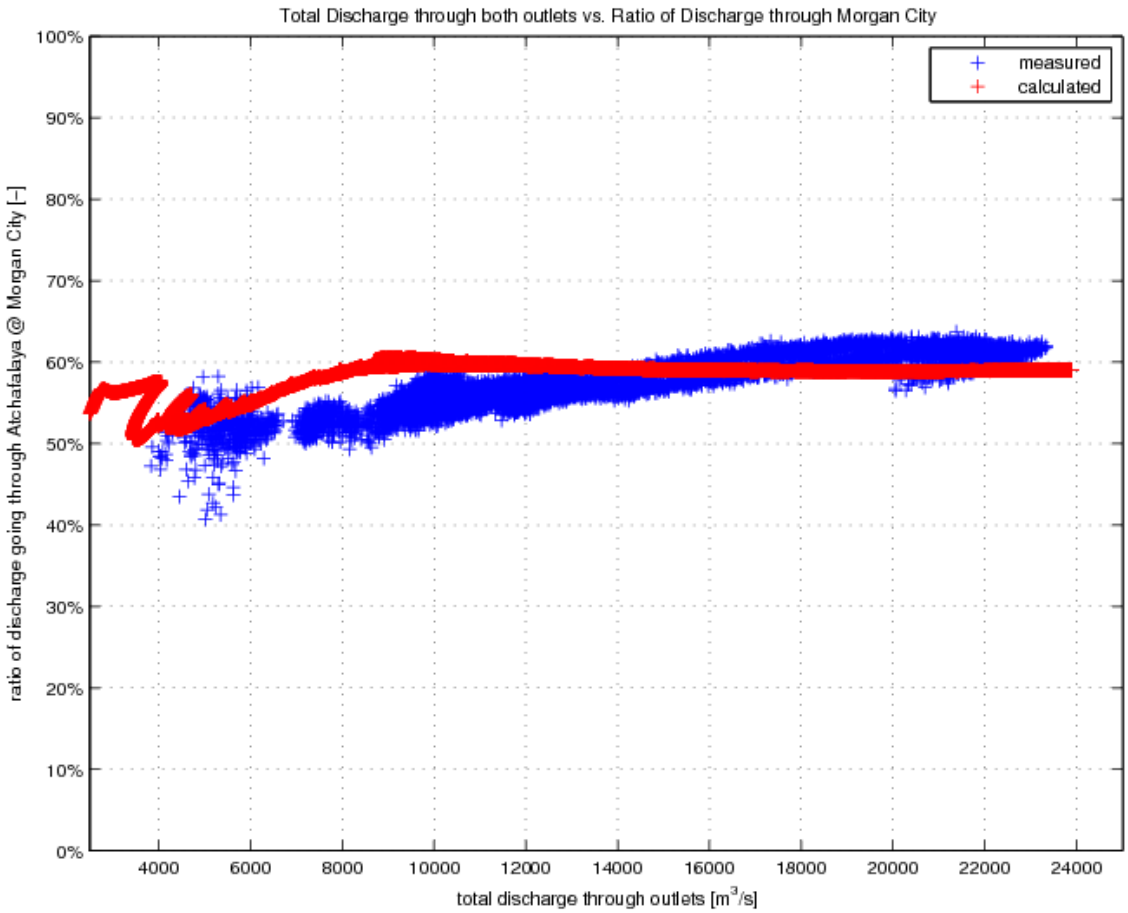

Figure 4-27: Measured and calculated proportion of discharge flowing through Morgan City vs. the total discharge through both outlets during calibration period

4.4 Synopsis of Model Calibration

The hydrodynamic model of the Atchafalaya Basin was calibrated using the wealth of measured data recorded during the historic 2011 flood period. This period encompassed some of the highest observed discharges in decades and included only the second diversion of Mississippi River flow into the basin through the Morganza Spillway in the structure's history. The focus of the calibration effort was on accurate simulation of water levels in the upper basin and accurate simulation of the discharge through the two outlets into the lower basin. Though comparisons were made for other model hydrodynamic parameters including channel averaged current speed, tidal constituents, and flood stage arrival time, their accurate simulation did not drive the model alterations through the calibration process.

The model simulates water levels very well at most gages, with average absolute differences typically on the order of 10 cm over a 4 month period. The small differences between measured and modeled water level time series at most of the measurement locations over such a large and complex domain indicate high performance in modeling

the flood hydrodynamics. Stations that had the largest differences between measured and modeled values were generally located in areas of the model domain for which bathymetry was synthesized based on ADCP bottom tracks or engineering judgment instead of reliable survey data.

A moderate flood stage at the Lower Atchafalaya River at Morgan City gage is defined as 7 ft. or approximately 2.1 m. The calculated water surface elevation reaches this stage approximately 3.5 days before the measured data water surface.

Performance for the five most important constituents at several selected coastal stations was evaluated. Generally, the highest amplitude constituents K1 and O1 are correctly predicted, with normalized amplitude errors increasing for constituents with much smaller amplitudes. The inland tidal stations where the tide must propagate over marshes and through narrow, winding tidal channels generally show a dampened tidal signal from what was measured

Discharge comparisons were made at only a few locations in the model domain; however, the distribution of discharge through the two upper-basin outlets was very accurately simulated with normalized RMS errors of less than 10% at both gages. The accurate division of flow between the Wax Lake Outlet and the Atchafalaya River indicates that the large scale distribution of flow in the basin is correctly simulated. Current speed was similarly well represented, though some overprediction of peak currents through the Wax Lake Outlet was present. Discharge comparisons were also made for the two 2011 field campaign NAS gages in the Upper Bell River region. Errors between measured and calculated discharges at these gages were greater, though the complex shapes of the flow hydrographs were well represented.

5.0 VALIDATION

5.1 Introduction

To validate the model performance in reproducing the hydrodynamics of the Atchafalaya Basin, a separate simulation encompassing a different time period with very different discharge boundary conditions was performed. The model was calibrated using a period of very high flows corresponding to the 2011 flood, so validation was performed for the period of September 6, 2011 through December 26, 2011 when flows where substantially lower and typical of non-flood conditions in the basin. The time period was chosen so that a sufficiently long period of low flow discharge boundary conditions could be applied while avoiding the substantial meteorological effects on measured hydrodynamics induced by Tropical Storm Lee in early September. Figure 5-1: gives the applied upstream discharge boundary condition at Simmesport. The operation of the Morganza Spillway had already ceased much earlier in the year, so a boundary condition at that location was not required. Furthermore, inflow from other structures (locks, sector gates and inflow structures) was neglected.

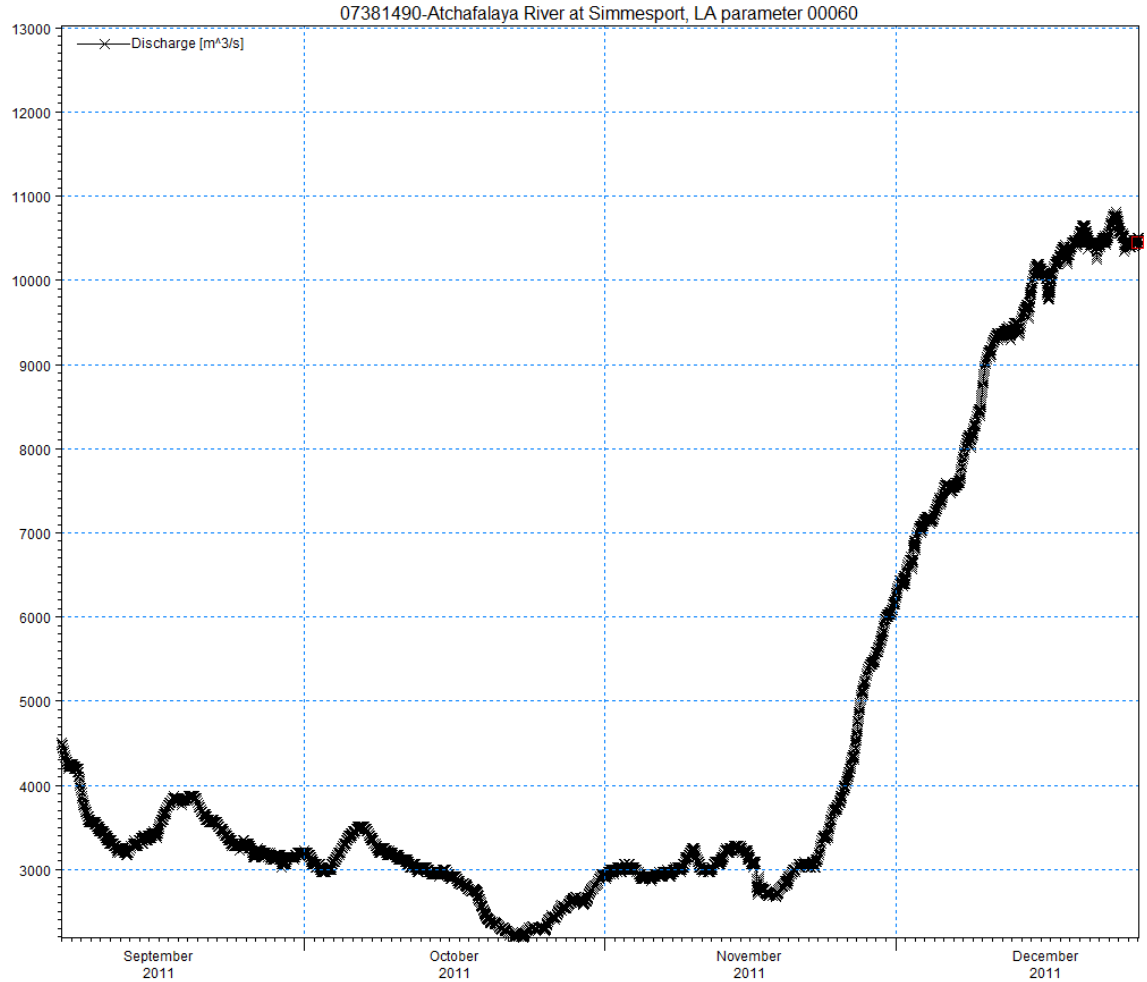

Figure 5-1: Simmesport discharge boundary condition for the validation period

5.2 Water Level Validation

5.2.1 Measured and Calculated Time Series Comparisons

Figures 6-2 to 6-9 below present comparisons between calculated and measured water levels at selected gage locations for the duration of the 2011 low-flow validation period. The validation comparison does not use every gage that was used in the calibration process because some gages were not inundated during this period of low stages or the quality of measurements for gages was much less than during the flood period. Model performance during the validation period is very similar to the performance during calibration, with many gages having very small mean absolute errors (10 cm or less) and corresponding small normalized RMS errors. There is further consistency with the calibration in that gages in areas where simulation of water levels was not as accurate in the calibration have the higher mean absolute errors among gages in the validation. Additionally, mean absolute errors in the most upstream portion of the Atchafalaya River (gage IDs 03045, 03060 and 03075) have somewhat increased over errors at the same stations during the calibration simulation, though normalized RMS errors remain at approximately 5% or less. The tidal oscillations are much more dominant during the low flow period and can be seen to propagate much further upstream in the model. Table 5-1: gives a summary of the model performance statistics for the validation run at each gage location.

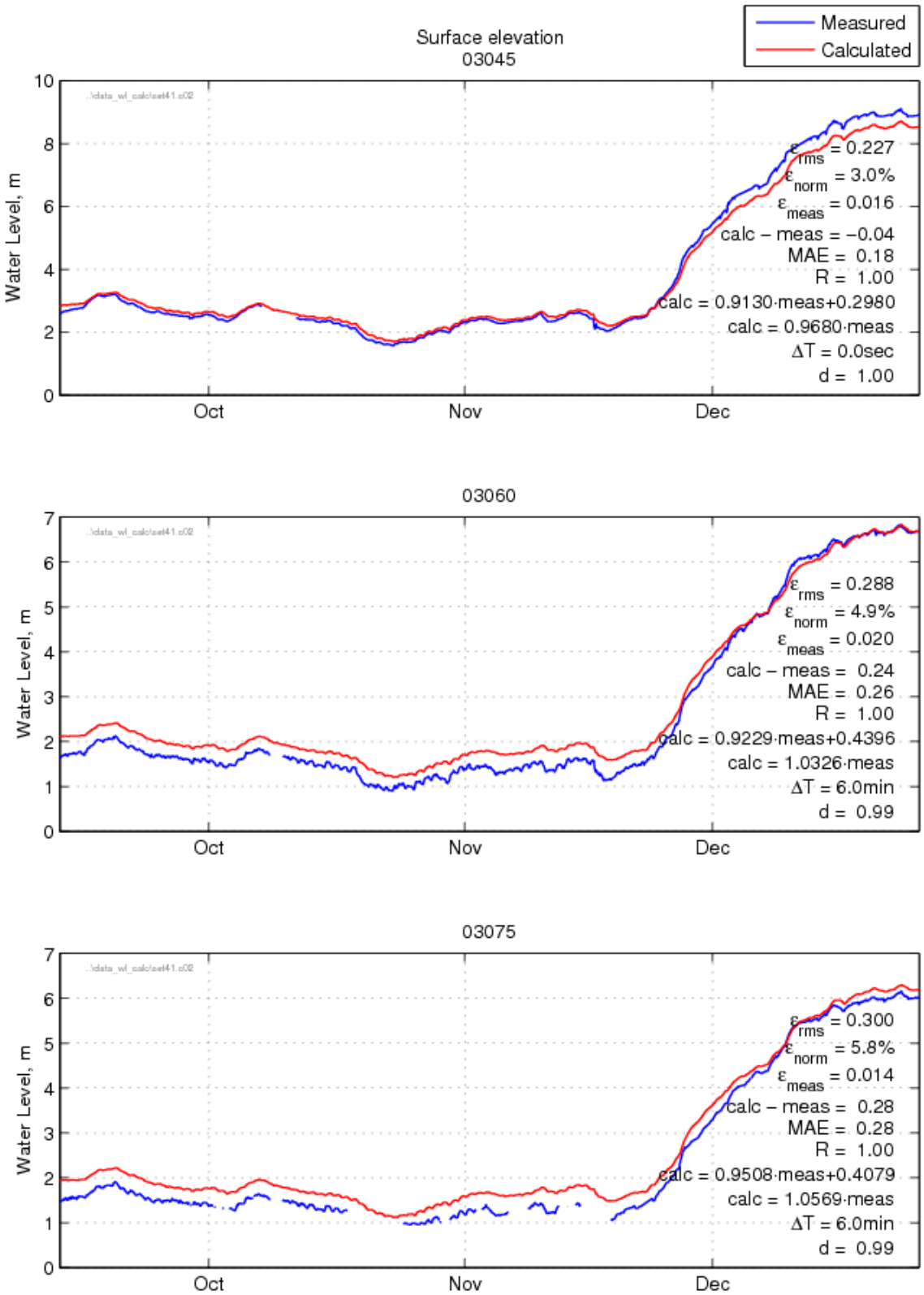

Figure 5-2: validation results for 2011 low-flow period with calculated and measured water levels[m] for Simmesport (03045), Melville (03060) and Krotz Springs (03075)

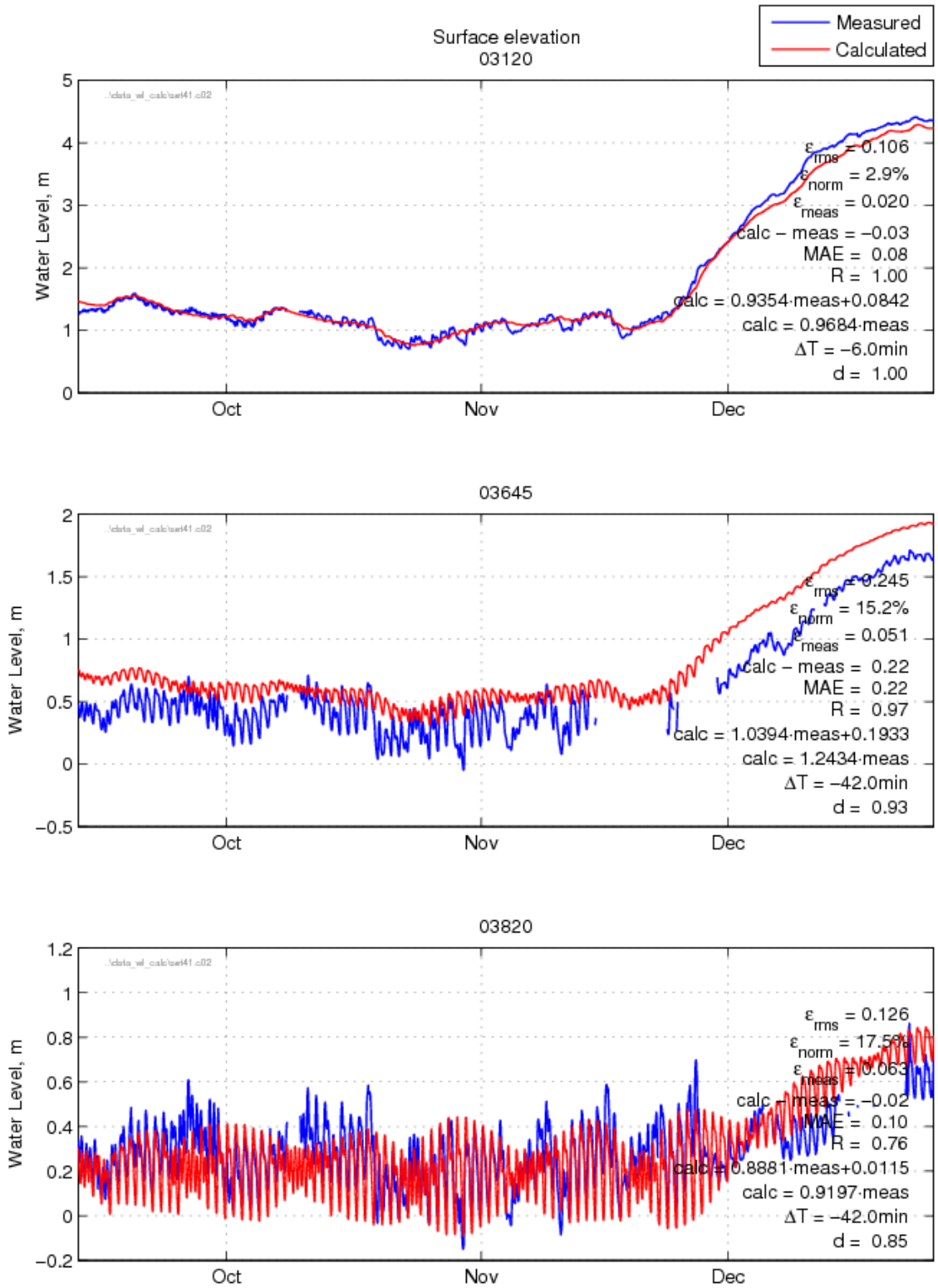

Figure 5-3: Model validation results for 2011 low-flow period with calculated and measured water levels [m] for Butte La Rose (03120), Six Mile Lake (03645), and Sweet Bay Lake (03820)

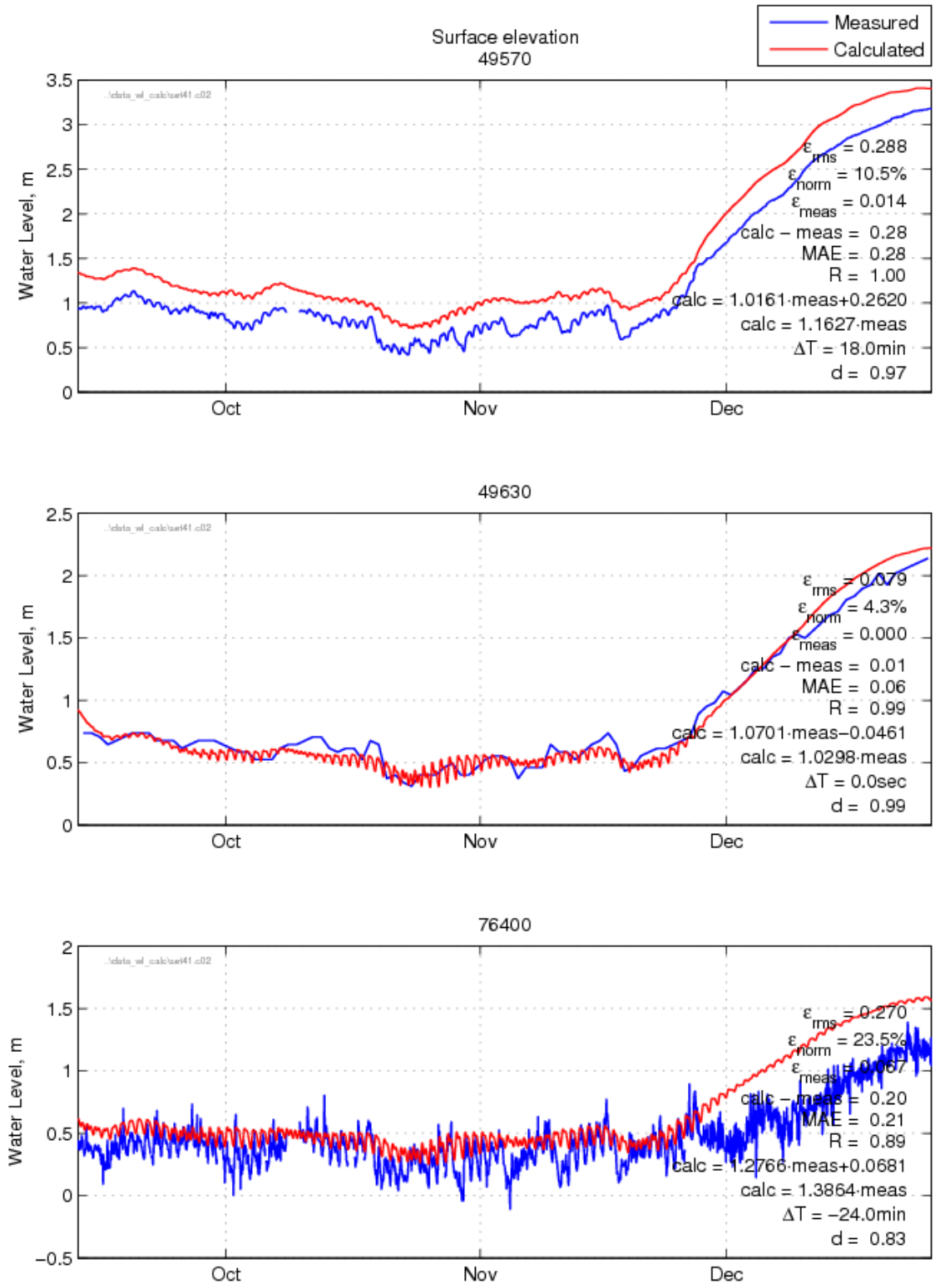

Figure 5-4: Model validation results for 2011 low-flow period with calculated and measured water levels [m] for Upper Grande River (49570), EABPL Borrow Pit (49630), and Bayou boeuf Lock (76400)

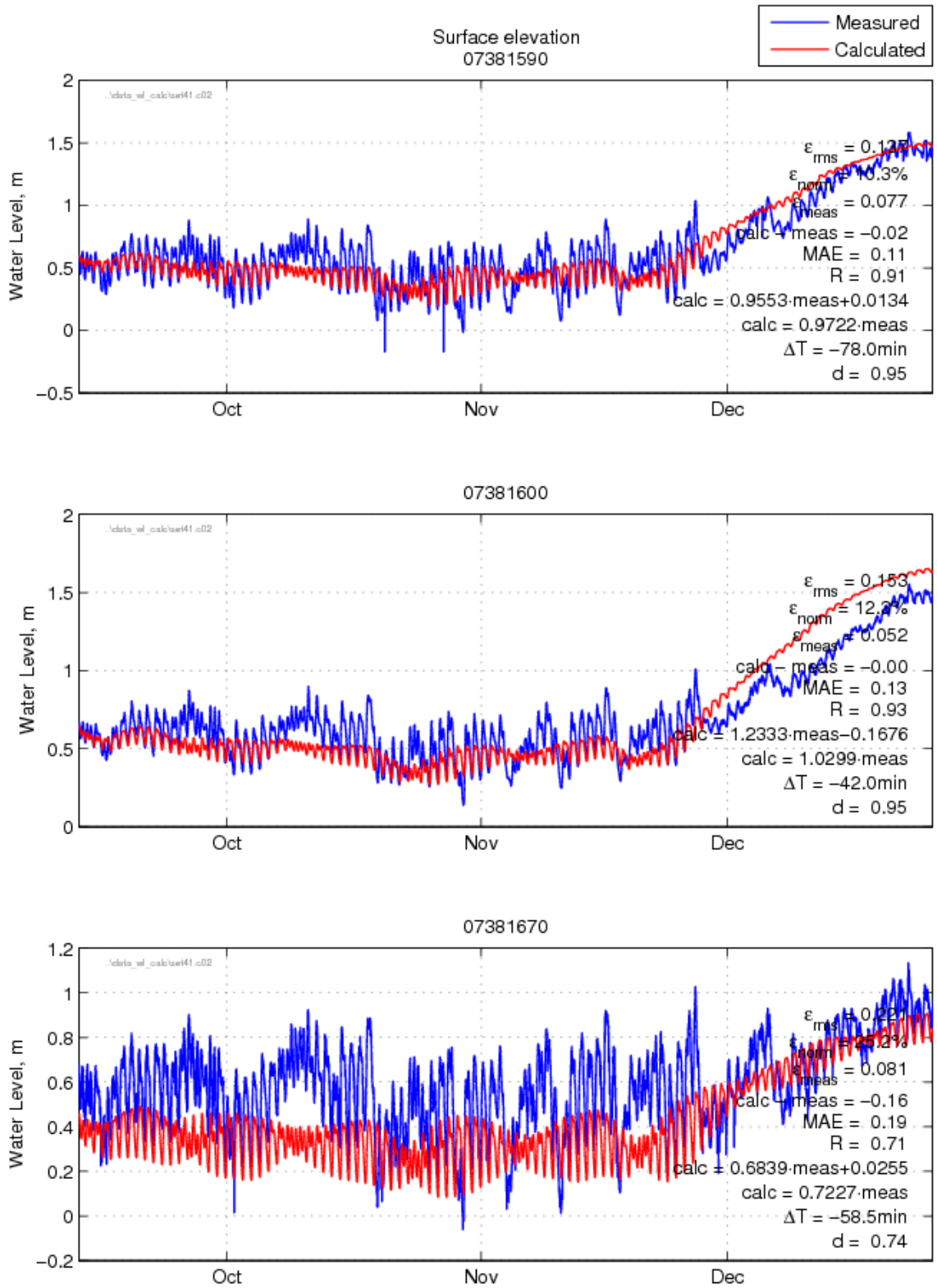

Figure 5-5: Model validation results for 2011 low-flow period with calculated and measured water levels [m] for Wax Lake Outlet at Calumet (07381590), Lower Atchafalaya River at Morgan City (07381600), and GIWW at Bayou Sale (07381670)

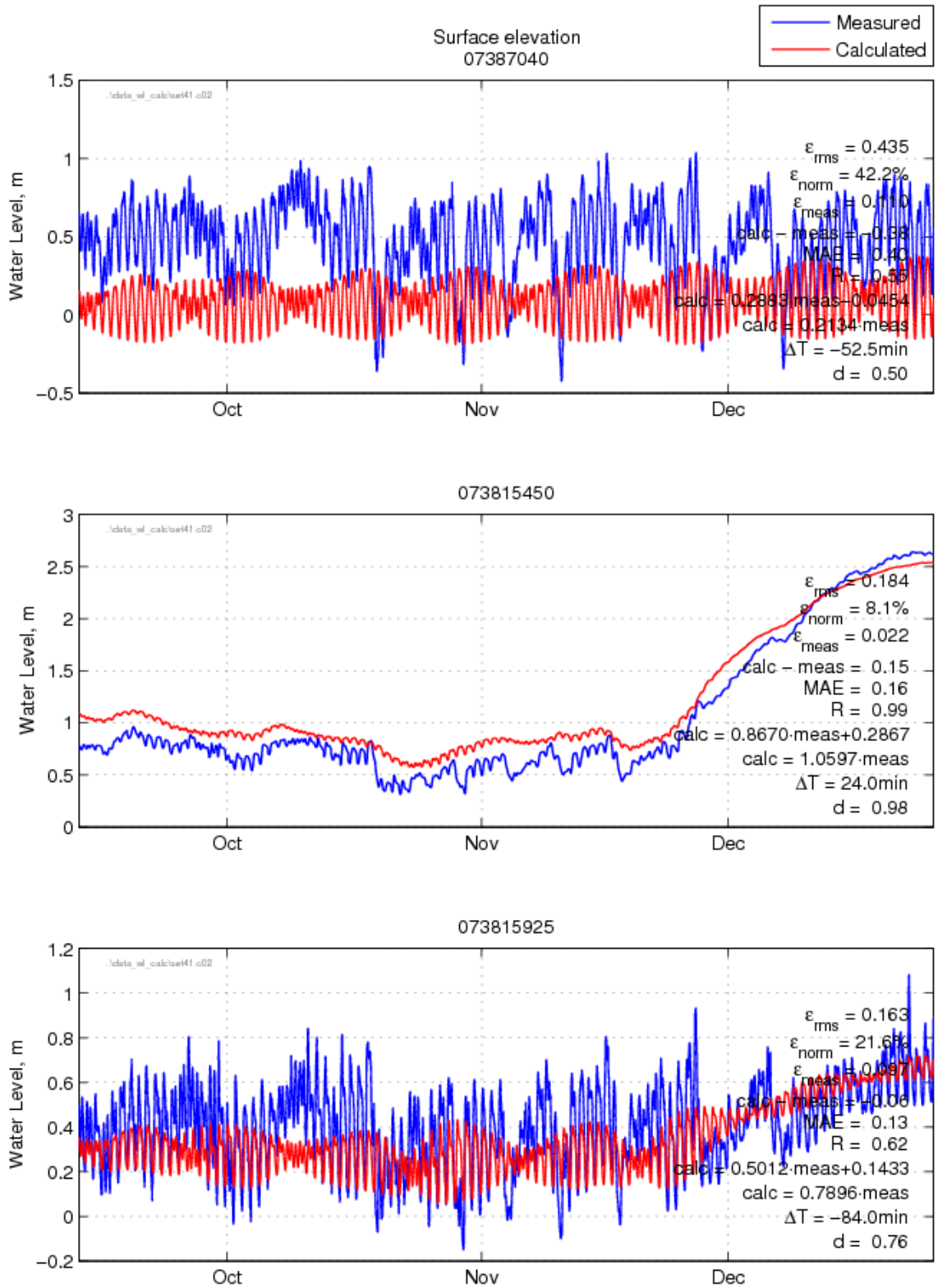

Figure 5-6: Model validation results for 2011 low-flow period with calculated and measured water levels [m] for Vermilion Bay (07387040), Chicot Pass (073815450), and Crewboat Channel (073815925)

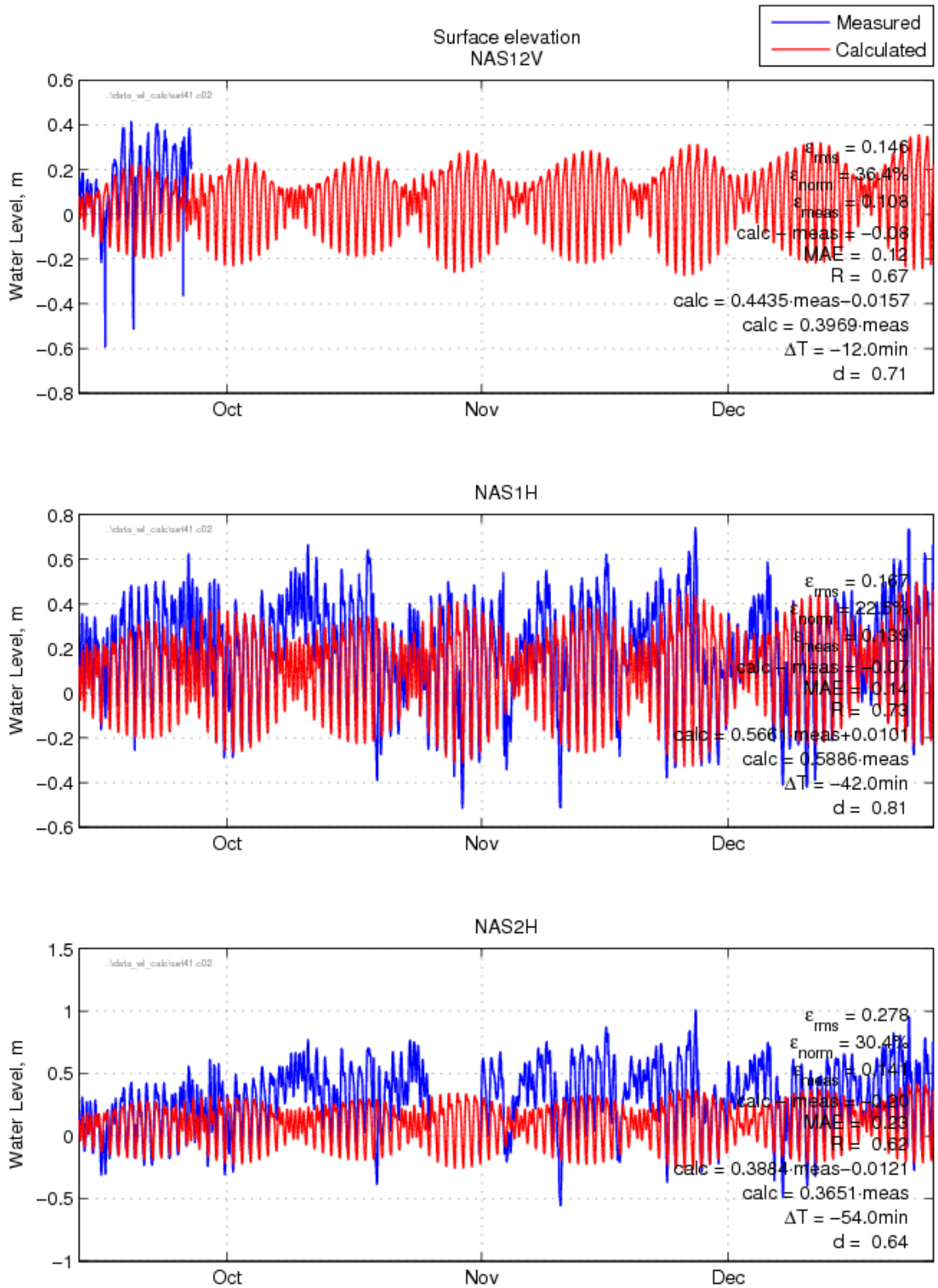

Figure 5-7: Model validation results for 2011 low-flow period with calculated and measured water levels [m] for Southwest Pass near Porpoise Pt. (NAS12V), Eugene Island (NAS1H) andEast Cote Blanche Bay (NAS2H)

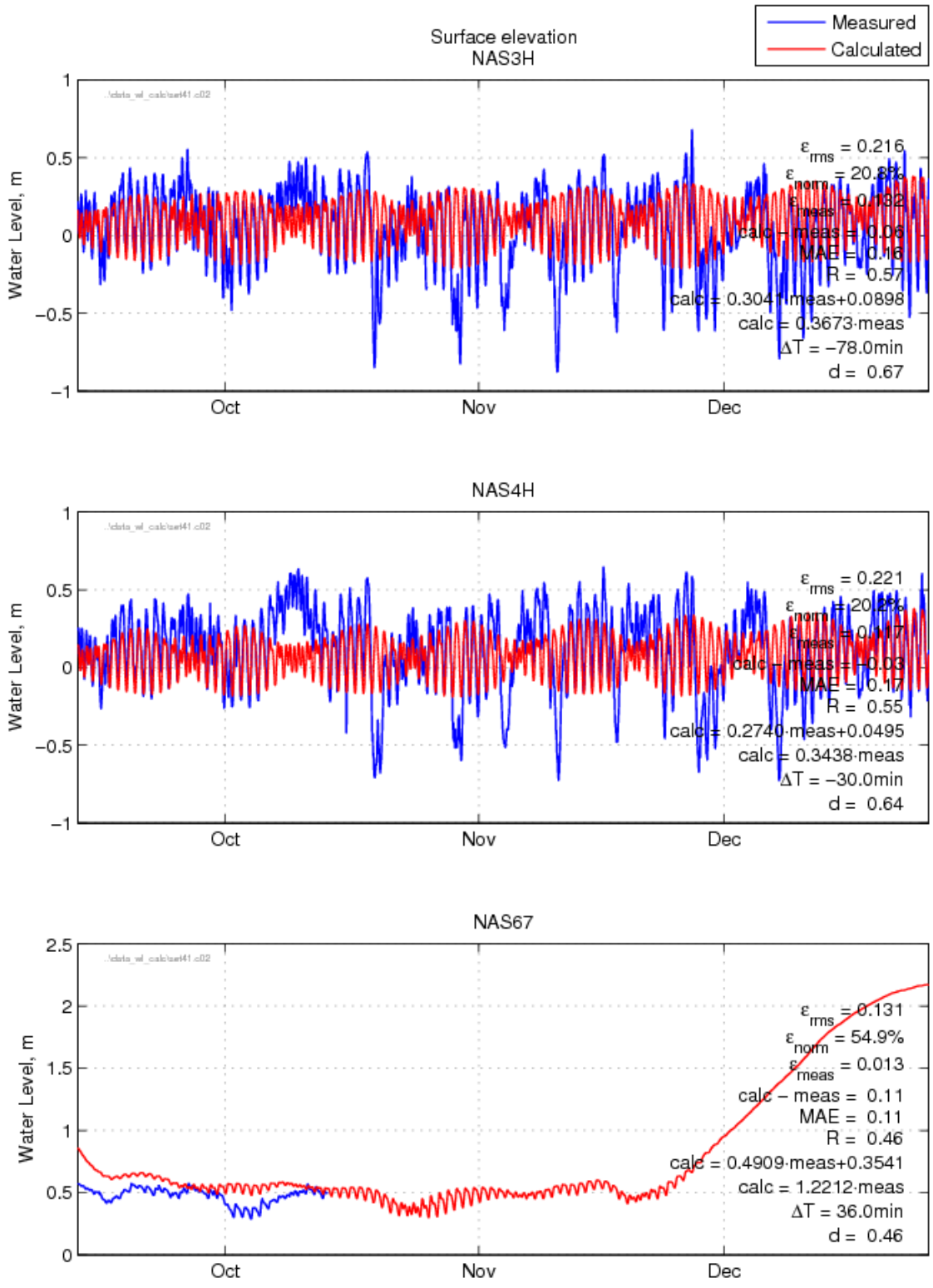

Figure 5-8: Model validation results for 2011 low-flow period with calculated and measured water levels [m] for West Cote Blanche Bay (NAS3H), Vermilion Bay (NAS4H), and Old River (NAS67)

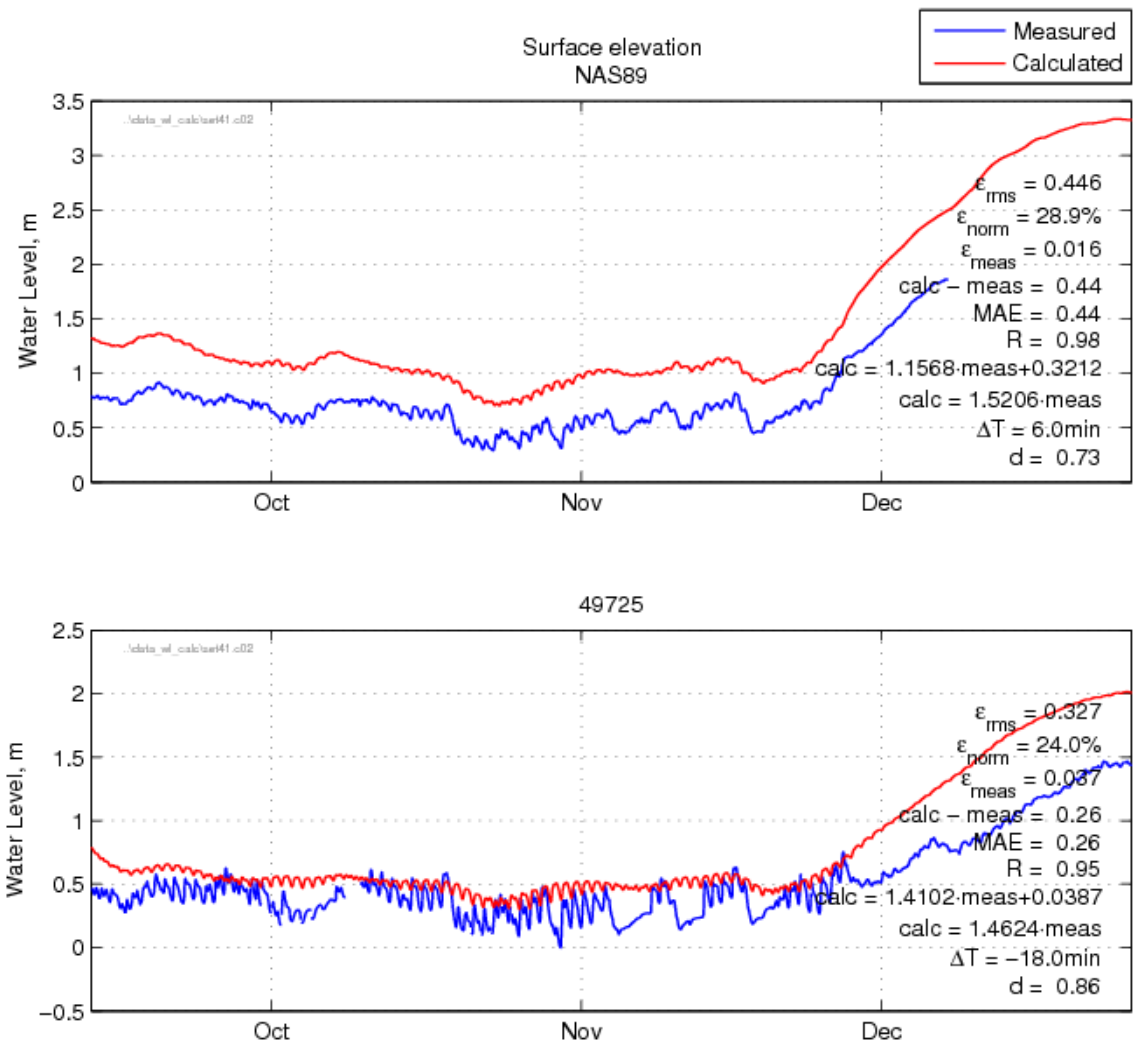

Figure 5-9: Model validation results for 2011 low-flow period with calculated and measured water levels [m] for Bayou Sorrell (NAS89), and Little Bayou Sorrell (49725)

Table 5-1:Summary of Water Level Validation Results

Station	mean absolute error (m)	RMS error (m)	% RMS error	Location
03045	-0.04	0.23	3.0	Atchafalaya River at Simmesport
03060	0.24	0.29	4.9	Atchafalaya River at Melville
03075	0.28	0.30	5.8	Atchafalaya River at Krotz Springs
03120	-0.03	0.11	2.9	Atchafalaya River at Butte La Rose
03645	0.22	0.24	15.2	Six Mile Lake NE of Verdunville
03820	-0.02	0.13	17.5	Lower Atchafalaya River Below Sweet Bay Lake
49570	0.28	0.29	10.5	Upper Grand River (FWS) At Dike
49630	0.01	0.08	4.3	EABPL Borrow Pit (FWS) At Bayou Sorrel Lock
76400	0.20	0.27	23.5	Bayou Boeuf Lock - West
07381590	-0.02	0.14	10.3	Wax Lake Outlet at Calumet, LA
07381600	0.00	0.15	12.3	Lower Atchafalaya River at Morgan City, LA
07381670	-0.16	0.22	25.2	GIWW at Bayou Sale Ridge near Franklin, LA
07387040	-0.38	0.44	42.2	Vermilion Bay near Cypremort Point, LA
073815450	0.15	0.18	8.1	Chicot Pass near Myette Point near Charenton, LA
073815925	-0.06	0.16	21.6	Crewboat Channel at Wax Lake Outlet nr Calumet, LA
NAS12V	-0.08	0.15	36.4	Southwest Pass near Porpoise Pt.
NAS1H	-0.07	0.17	22.5	Eugene Island
NAS2H	-0.20	0.28	30.4	East Cote Blanche Bay
NAS3H	0.06	0.22	20.8	West Cote Blanche Bay
NAS4H	-0.03	0.22	20.2	Vermilion Bay near Intracoastal City, LA
NAS67	0.11	0.13	54.9	Old River
NAS89	0.44	0.45	28.9	Bayou Sorrell
49725	0.26	0.33	24.0	Little Bayou Sorrel At Jct. With GIWW

Mean Absolute Error Statistics

Stations < 0.15 m	13/23
% stations < 0.15 m	57%

5.2.2 Spatial Distribution of Water Level Validation Results

Figure 5-10: below presents the mean absolute error between calculated and measured water levels, derived from the time series presented earlier, at each gage location in the model domain to better indicate spatial variation in model performance for the validation period.

Water levels in diverse areas of the model are very well represented, especially through the upper basin outlets, in the lower basin, and in the Butte La Rose area. The stations with the highest mean absolute error (c minus b) values are no longer concentrated in one area; however, reproduction with minimal error of measured water levels in the GIWW and Upper Bell River areas remains a challenge. The NAS89 gage has the highest mean absolute error of 44 cm; in this case the flow remains confined within Bayou Sorrell, aggravating the effects of any misrepresentation of channel bathymetry.

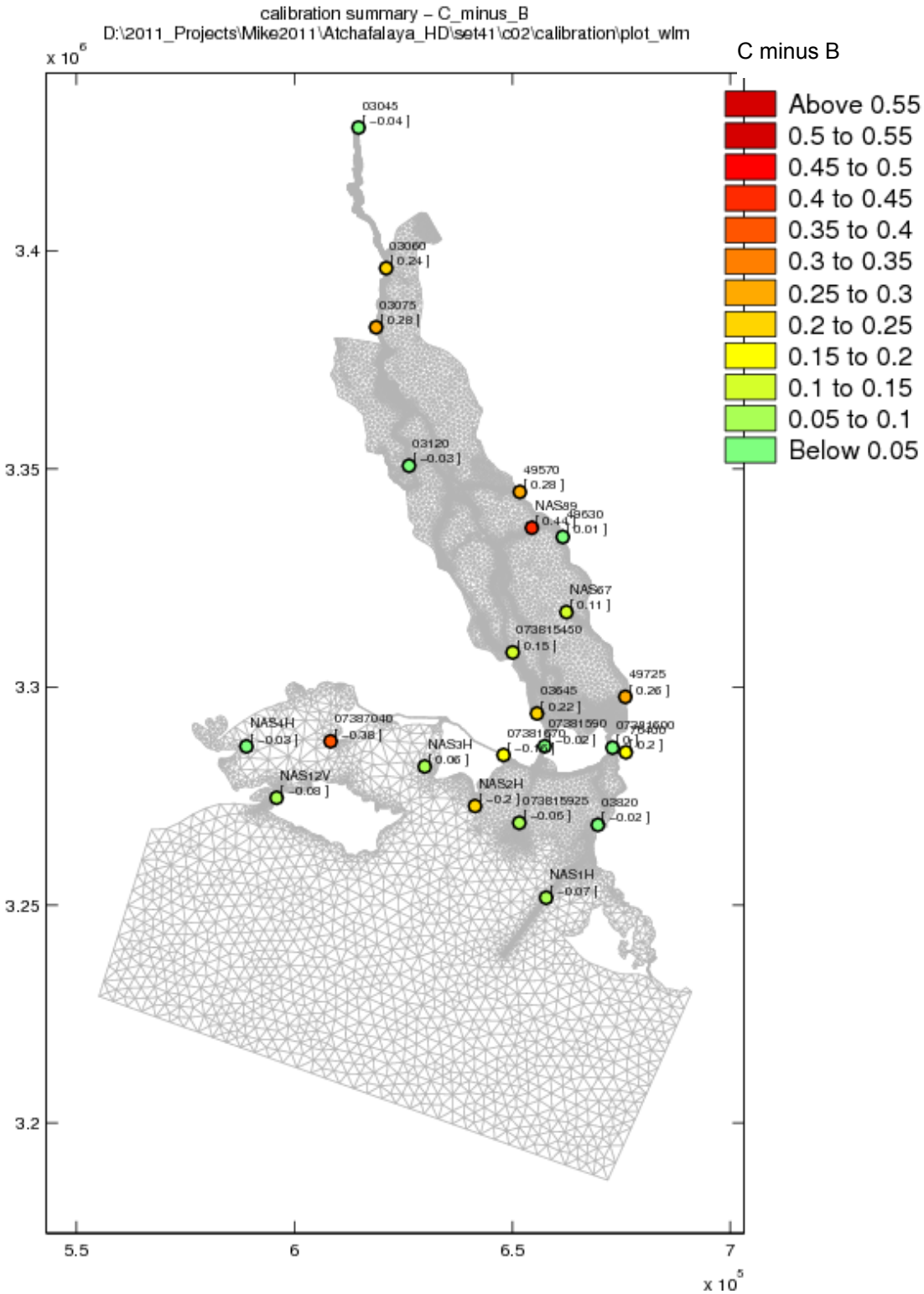

Figure 5-10: Mean absolute error between calculated and measured water levels over the entire validation period at particular gage locations in the basin [m]

5.3 Discharge and Current Validation

The following sections present the results of the validation run for discharge and channel-averaged current speed. The NAS gage located in Old River, NAS67, was in very shallow water for the first portion of the validation period and then went dry. During the period when it was still submerged, instrument depths were not great enough to produce reliable ADCP measurements, so only the NAS89 gage, in addition to the upper-basin outlet stations, was used for validation comparisons.

5.3.1 Measured and Calculated Discharge Comparisons

Figure 5-11: presents comparisons between calculated and measured discharge time series for the validation simulation period. Performance at each of the three discharge gages is very similar to that of the calibration run. The calculated discharges through the Wax Lake Outlet station and the Atchafalaya River station very closely follow the measured discharges for the lower flows until December, when flows increase and the errors slightly increase. The tidal signal is slightly damped in the modeled time series, though both stations still have normalized RMS errors of approximately 10% or less despite the low magnitudes of flow. The model again accurately simulates the discharge hydrograph shape through station NAS89 with a fairly constant, low-magnitude offset during the steady, lower-flow period of the simulation. Errors increase as flow magnitude increases in December, though the station still has an acceptable relative RMS error of less than 18% for the full simulation period. Table 5-2: gives a summary of the discharge performance statistics.

Table 5-2:Summary of Discharge Validation Results

Station	mean absolute error (m^3/s)	RMS error (m^3/s)	% RMS error	Location
07381590	-165.9	336.66	7.3	Wax Lake Outlet at Calumet, LA
07381600	134.14	594.72	10.2	Lower Atchafalaya River at Morgan City, LA
NAS89	20.54	24.85	17.6	Bayou Sorrell

Normalized RMS Error Statistics

Stations < 20%	3/3
% stations < 20%	100%

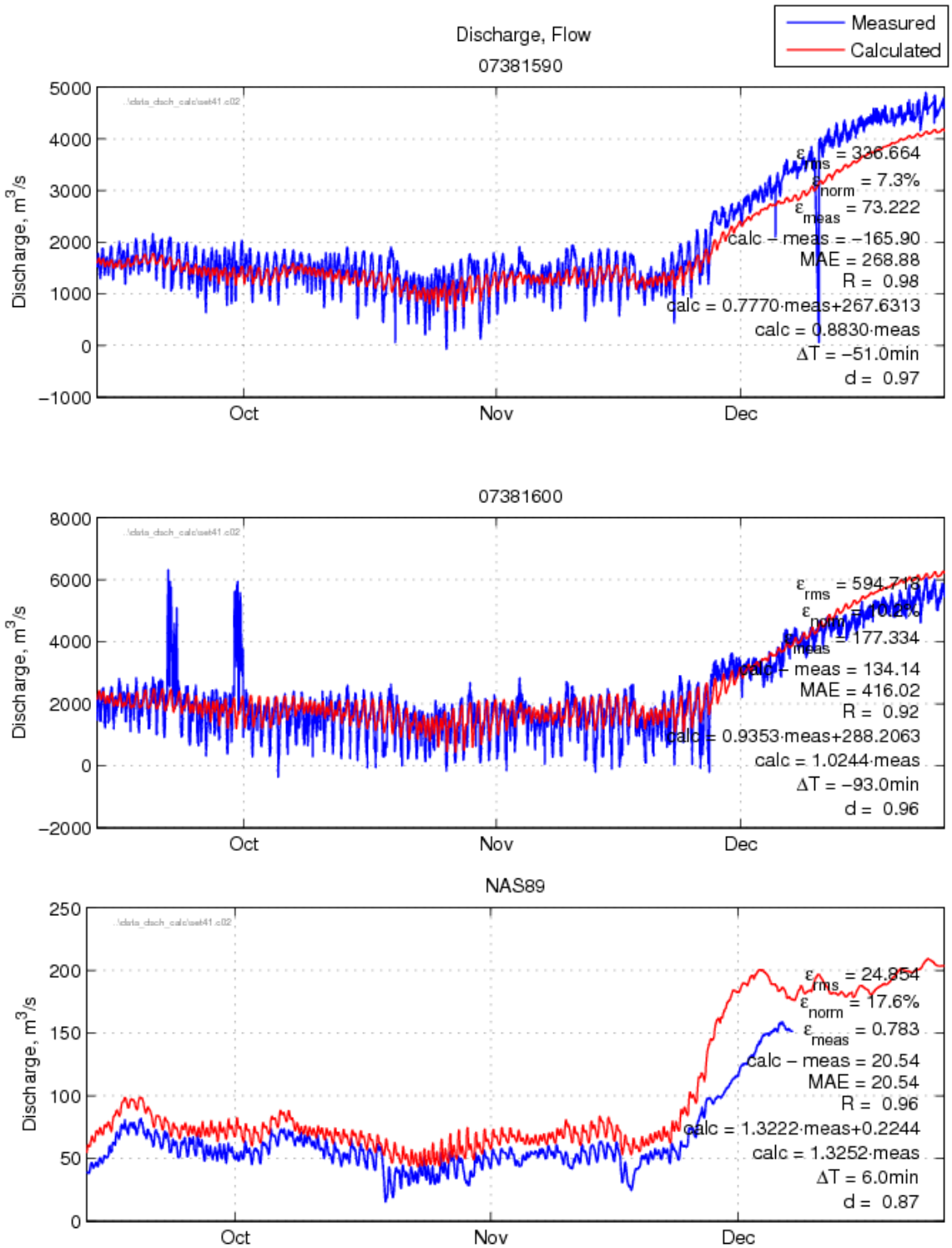

Figure 5-11: Model validation results for 2011 flood with calculated and measured discharges [m^3/s] for Wax Lake Outlet at Calumet (07381590), Lower Atchafalaya River at Morgan city (07381600), and Bayou Sorrel (NAS89)

5.3.2 Measured and Calculated Current Comparisons

Figure 5-12: gives the corresponding calculated and measured channel-averaged current time series for each of the three gages discussed in the previous section. Current speed through the two outlets is very accurately modeled, with normalized RMS error values of approximately 10% or less. Channel-averaged current speed through Bayou Sorrell is even more representative of measured values than discharge or water level calculates at the station. A normalized RMS error of approximately 7% indicates very good agreement with measured data, and examination of the time series indicates that even the smallest current speed fluctuations during the lowest flows are accurately simulated. Table 5-3: summarized the results of the current speed validation.

Table 5-3: Summary of Current Speed Calibration Results

Station	mean absolute error (m/s)	RMS error (m/s)	% RMS error	Location
07381590	0.06	0.09	7.9	Wax Lake Outlet at Calumet, LA
07381600	0.04	0.12	11.3	Lower Atchafalaya River at Morgan City, LA
NAS89	0.00	0.04	6.8	Bayou Sorrell

Normalized RMS Error Statistics

Stations < 20%	3/3
% stations < 20%	100%

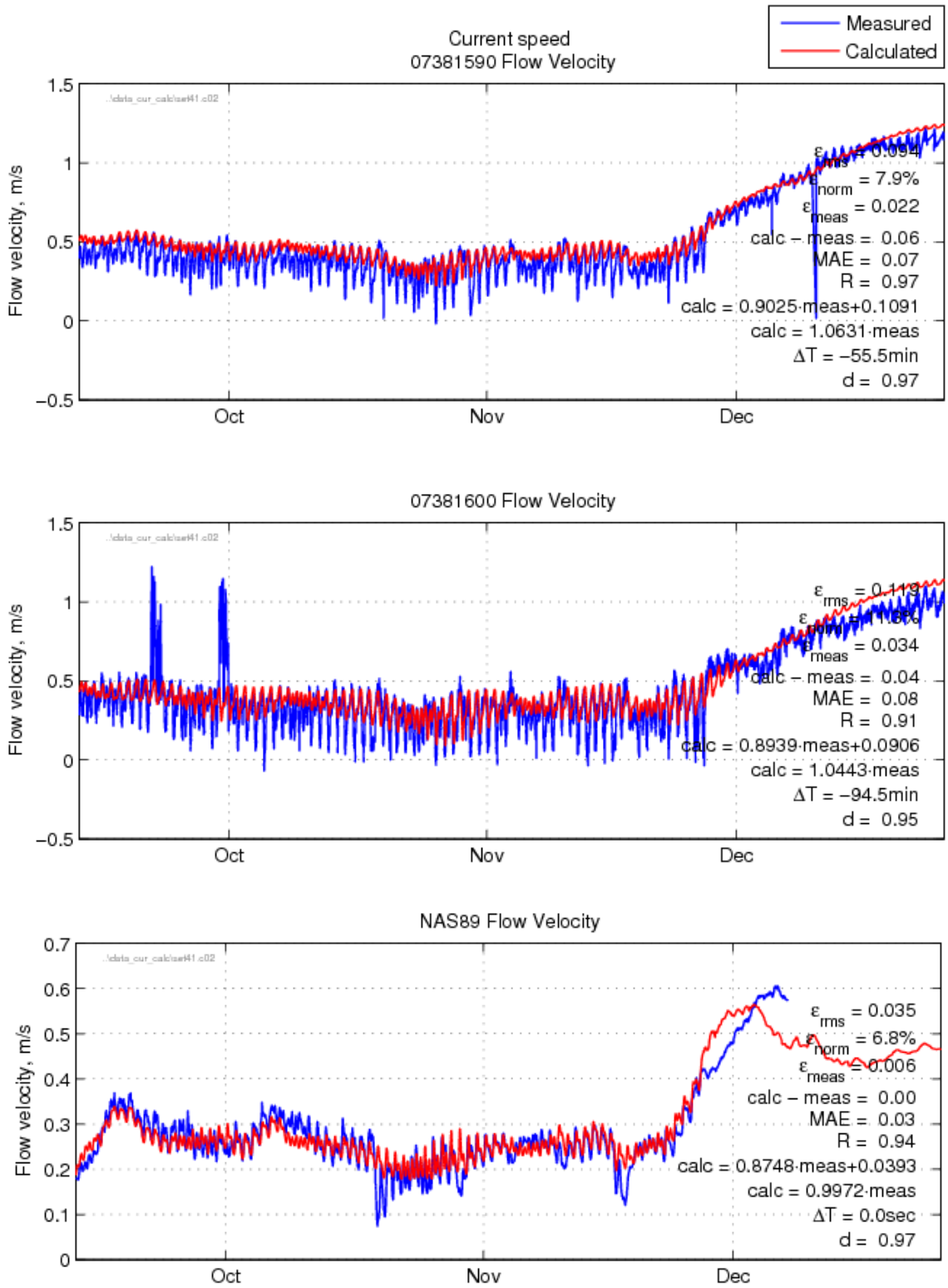

Figure 5-12: Model validation results for 2011 flood with calculated and measured channel-averaged velocities [m/s] for Wax Lake Outlet at Calumet (07381590), Lower Atchafalaya River at Morgan city (07381600), and Bayou Sorrel (NAS89)

5.3.3 Discharge Distribution through Outlets

Figure 5-13: plots the fraction of total Wax Lake Outlet and Atchafalaya River discharge flowing through the Morgan City outlet as a function of the total discharge through both outlets during the validation period. At these lower flows, the increased variation in the flow split due to tides is evident in the measured data. The additional scatter in the measured data set due to meteorological forcings is also visible. The calculated discharge split reproduces the measured data fairly well. Though showing slightly less variation due to the absence of meteorological forcings, the calculated data follows the the measured trend well, representing most of the inherent variability due to tides. After the combined discharge reaches approximately 5000 m^3/s, the measured and calculated data both show substantially less variation. At this point and at greater discharges, the calculated percent of discharge flowing through the Atchafalaya, staying nearly constant at 60%, is slightly elevated over the measured percent of flow.

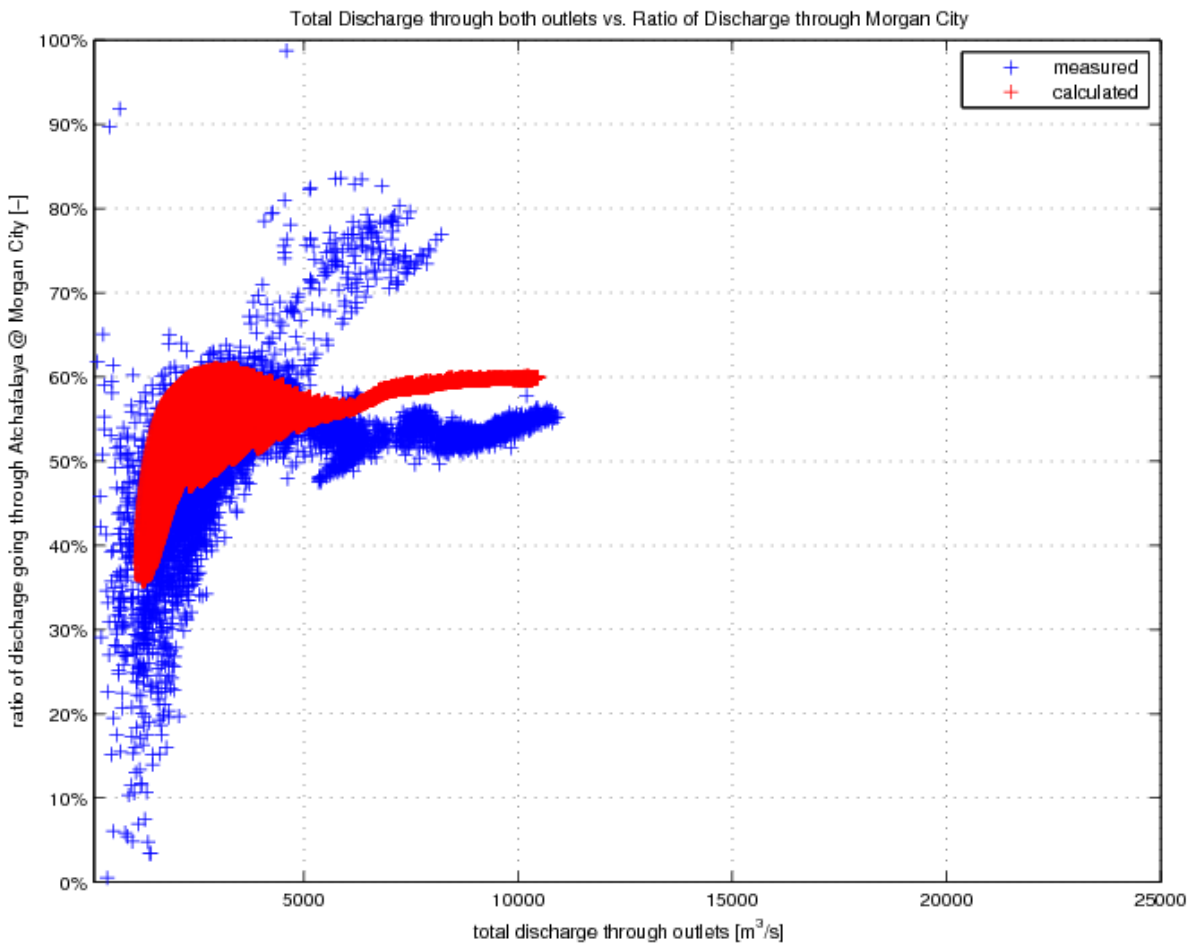

Figure 5-13: Measured and calculated proportion of discharge flowing through Morgan City vs. the total discharge through both outlets during validation period

5.4 Synopsis of Model Validation

The model was validated for a period from early September to late December 2011. This simulation period was chosen because of its low flows that are typical of the basin in non-flood conditions. Comparisons with measured data confirmed the model's ability to accurately simulate real basin behavior over the full range of possible flow magnitudes. Despite the increased influence of tidal fluctuations during the lower flows, measured water levels throughout the domain were still very well represented in the calculations. The normalized RMS errors for most gages still remain very low even with the much lower water levels. Water level validation results were consistent with the calibration results in that the few gages where results did not agree as well have the higher error values in both simulations. Again, it should be noted that gages with the highest errors are in areas without reliable bathymetry, and the confinement of the low flow in channels could compound the effects of unrepresentative bathymetry.

Again, the discharge distribution through the two outlets was very accurately simulated. Normalized RMS errors did increase slightly over values from the calibration but still are

approximately 10% or less. The more simplified flow patterns through Bayou Sorrell during this period are able to be better simulated, resulting in increased performance over the calibration run. Channel-averaged currents are very well represented at the three discharge stations as well. Overall, the validation results for both water levels and discharges are very good and confirm the model's ability to accurately simulate the hydrodynamics of the basin even during low-flow conditions.

6.0 HYDRODYNAMIC PRE-SCREENING SCENARIO RUNS

6.1 Introduction

After the model was calibrated and validated to measured data from the 2011 flood period and low-flow period, a preliminary set of model application scenarios were run to preliminary demonstrate the model capabilities. Developed in concert with the National Audubon Society, these preliminary scenarios reflect the intended application of the model: to evaluate large scale alterations in basin water management for hydrologic restoration. At present, the results of scenario runs are intended to be demonstrative; however, they indicate the degree to which both basin-wide and local hydrodynamic effects of proposed projects and management strategies can be evaluated.

The two tested scenarios are preliminary explorations of possible management strategies that alter the prescribed 30%/70% split of discharge at the Old River Control Structure between the Mississippi River and the Atchafalaya Distributary. The first proposes to stimulate circulation in the basin during the low-flow period by routing a pulse of much greater discharge from the Mississippi into the basin for a short period of time. The second proposes to reduce the flow on the falling limb of the typical spring flood hydrograph to 50% of what it would usually be. For comparison, runs without the altered conditions were also performed. These include a period of constant, low-flow discharge for the first scenario and a typical symmetric spring flood hydrograph for the second scenario. To more effectively evaluate changes in basin hydrodynamics only due to the changes in discharge, a constant water level was imposed at the offshore boundaries instead of the tidal fluctuations imposed during calibration and validation. The following sections present the boundary conditions and results of the preliminary model application runs in greater detail.

6.2 Pulse Flood

6.2.1 Scenario Description

During low flow conditions, circulation of water is reduced in the lower basin. It is possible that circulation could be stimulated with a short pulse of increased discharge released into the basin from the Old River Control Structure boundary. The magnitude and duration of such a pulse necessary to substantially improve circulation is unknown; however, the developed model could be used to test several scenarios to optimize the pulse and quantify the specific effects on improved circulation. An additional scenario was developed to demonstrate this model application, where a pulse of high discharge during a low-flow period was routed through the basin. The pulse parameters used in the scenario and steady-state low-flow comparison scenario are discussed below.

A preliminary objective of the pulse flood would be to elevate water levels in the upper basin above levels that are still heavily influenced by tidal fluctuations, which would presumably be enough to substantially increase circulation. At low flows, tidally-induced fluctuations are observed at the Calumet gage, as well as more upstream gages. This tidal influence decreases with increasing River discharge; at discharges of 4000 m^3/s at Calumet, tidal influence is already significantly reduced and with increasing discharge

becomes even less. In order to establish a pulse flood and elevate water levels out of the tidal influence zone, it is estimated that a discharge of approximately 4000 m^3/s at Calumet is needed. This outlet discharge corresponds to a discharge of approximately 8500 m^3/s at Simmesport. To preliminarily investigate the pulse flood concept and its influence on circulation, an approximately two-week long pulse with a peak discharge of 8000 m^3/s was applied during a period of steady low discharge. For comparison, an additional scenario comprising only the steady-state low flow was developed.

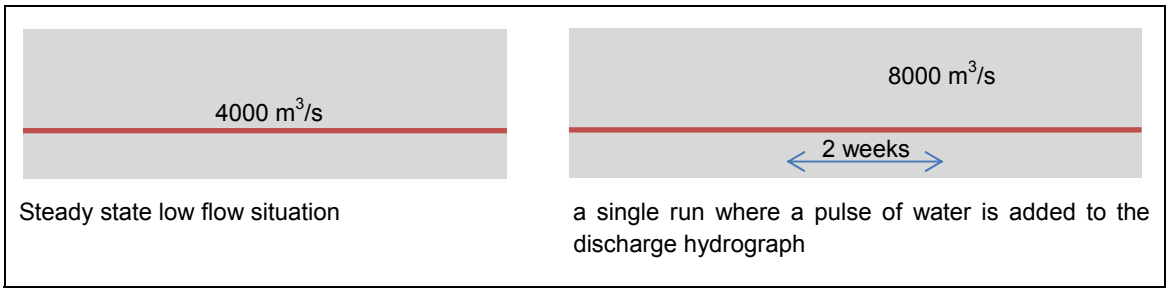

Figure 6-1: Schematic of preliminary model application to a high discharge pulse during a period of low flow (scenario A)

6.2.2 Boundary Conditions

Figure 7-2 below presents the applied upstream Simmesport discharge for the pulse scenario (scenario A1) and the comparison case of a steady-state low flow discharge (scenario A0). Both discharge boundary conditions are steady at 4000 m^3/s for the first few weeks of the simulation. The pulse scenario discharge then linearly increases over the course of a week to a peak of 8000 m^3/s, then decreases back to the initial steady value. The comparison scenario applies a constant discharge for the full simulation.

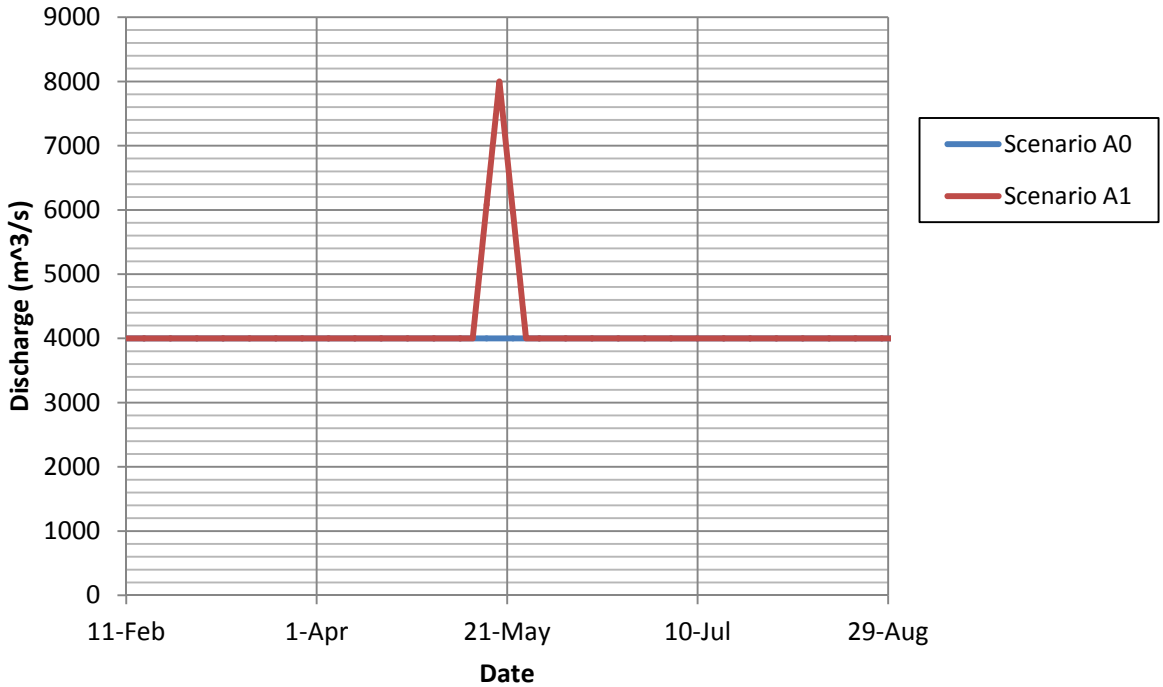

Figure 6-2: Simmesport discharge boundary conditions for scenario A0 (steady state low flow discharge) and scenario A1 (high discharge pulse)

6.2.3 Scenario Results and Analysis

Figure 7-3below presents a comparison of time series of calculated water levels for the steady discharge scenario (labeled Scenario A0 in the figure) and the pulse scenario (labeled Scenario A1). The time series were extracted at three separate station locations in the upstream, mid-basin, and coastal portions of the model domain (stations 03075, 03645, and 073815925, respectively) to demonstrate variation as the flood propagates downstream. The originally triangular-shaped pulse hydrograph is smoothed and modulated as it propagates downstream through the basin. At the tail end of the pulse, the water levels remain elevated above that of the steady state conditions for some time as the excess volume of water continues to drain. The peak water level in the upstream portion of the model is elevated over 2.5 m above that of the steady state condition, with the amplitude of elevation decreasing downstream to approximately 0.2 m in the Wax Lake Delta.

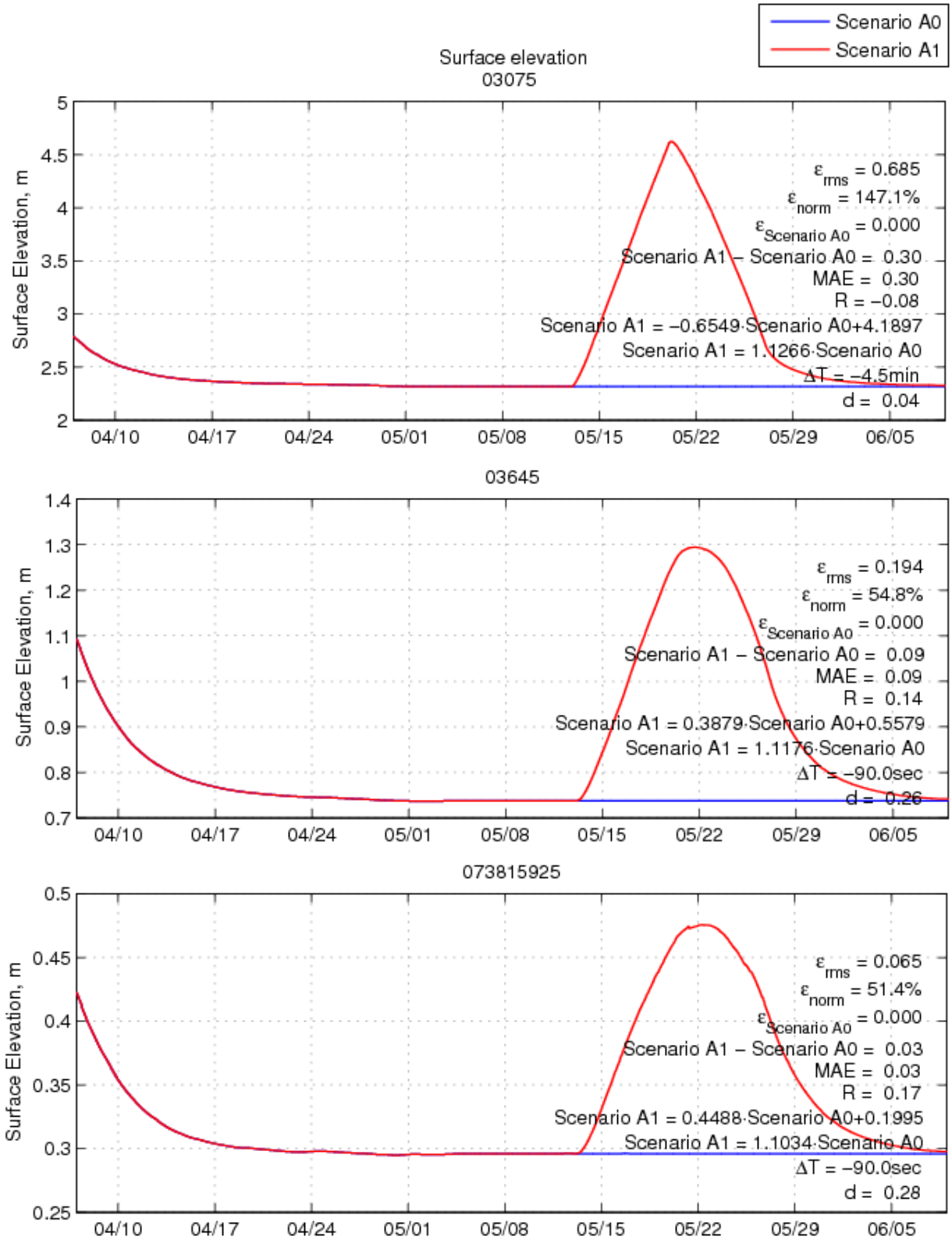

Figure 6-3: Comparison between scenario A0 and scenario A1 water level time series at selected upstream, mid-basin, and coastal stations

Figure 6-4 gives the difference between the peak water levels of the pulse scenario and the steady state levels of the comparison simulation at the submerged elements in the model domain. Similar to the results from the first model application scenario discussed earlier, the difference in water levels is greatest in the most upstream reach of the model and decreases downstream through the channels. Measureable differences are largely only present in the channels; however, differences of 0.5 to 1m are present in the floodplains of the southern Upper Bell River area and in Flat Lake.

Figure 6-5 gives the difference between the pulse peak current speeds over the steady sate values. The difference in current speeds is greatest in the main Atchafalaya Channel over most of its length before the Six Mile Lake/ Wax Lake Outlet bifurcation. Measurable differences in floodplain and swamp locations are only present in small areas of the Cocodrie Swamp, the Henderson Swamp, near Bayou Sorrell, and in large portions of the Upper Bell River and East Grande Lake areas. While current speeds in this last region only increase by less than 10 cm/s, the increase in water volume draining from the area has a greater effect on current speeds through Flat Lake and the Lower Atchafalaya River. The increased velocity in the shallow swamps of Upper Bell River during the pulse simulation indicates that this does have the potential to increase circulation in the lower basin during the periods of low flow. Under the current model bathymetry and configuration, circulation is only increased in limited areas of the other low-lying swamps and floodplains. Changes in the pulse magnitude and duration could increase the circulation in these regions to a greater extent.

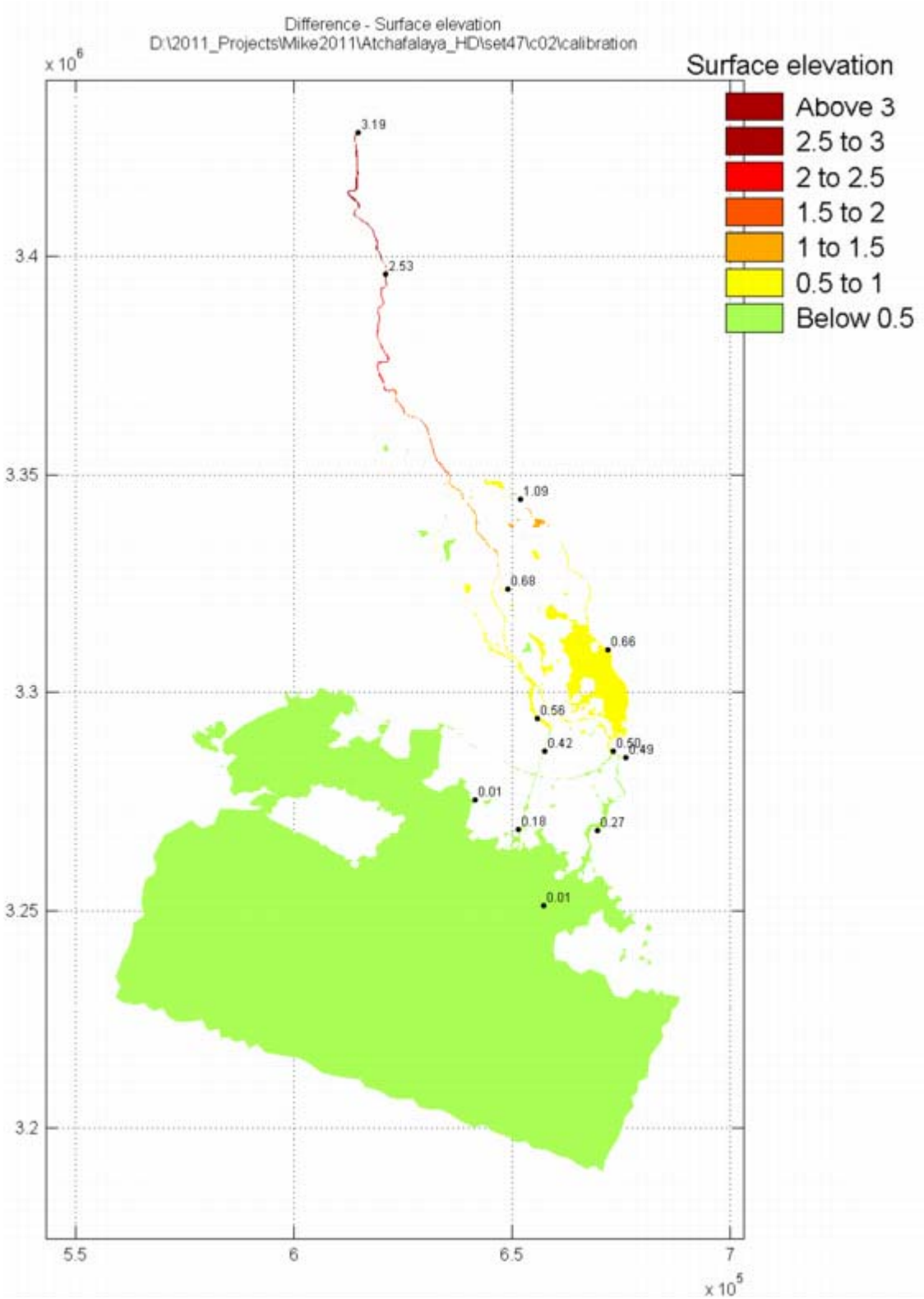

Figure 6-4: Spatial variation of differences between calculated peak water levels [m] for scenarios A0 and A1. Text in the figure gives values at indicated points.

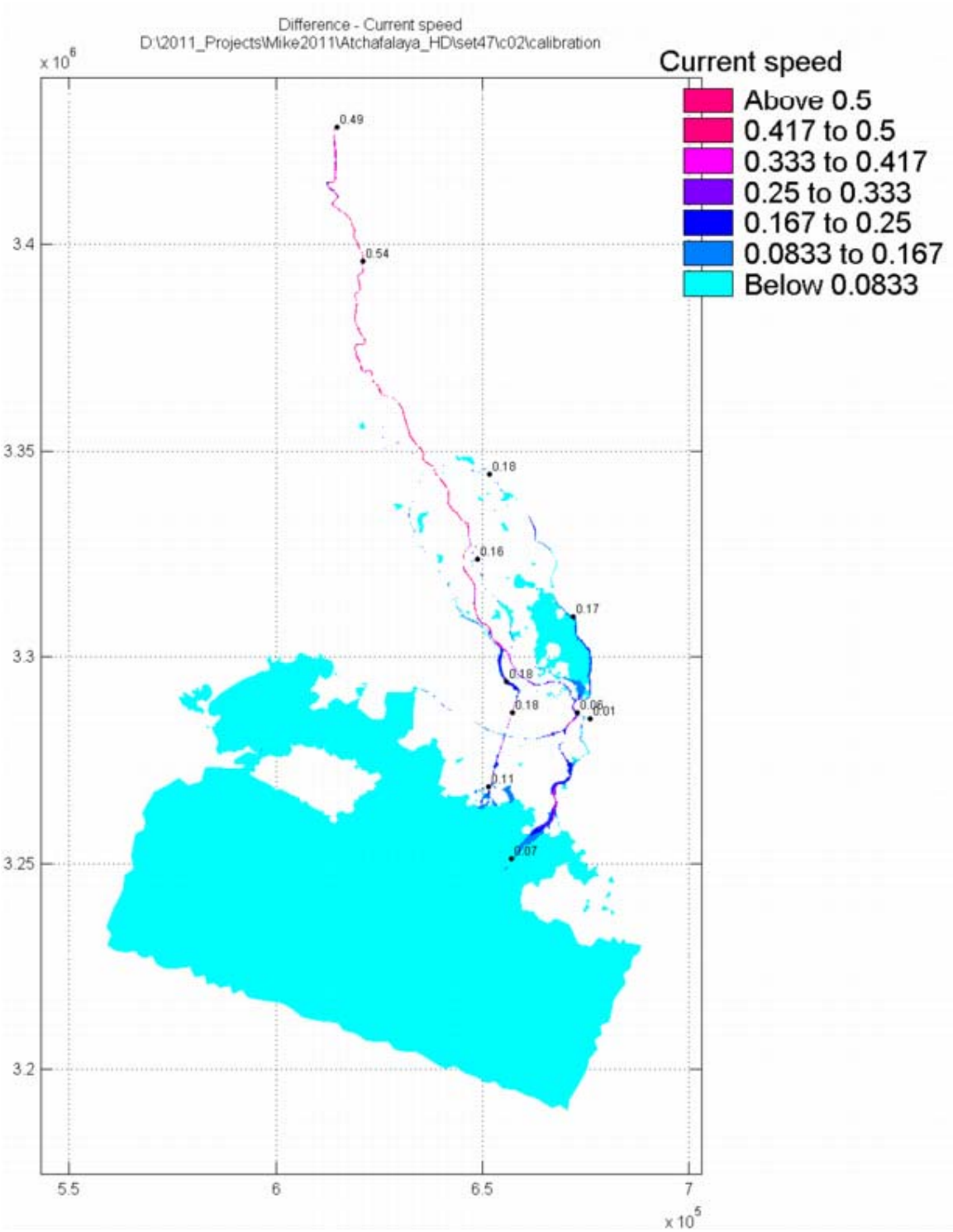

Figure 6-5: Spatial variation of differences between calculated peak current speeds [m/s] for scenarios A0 and A1. Text in the figure gives values at indicated points.

6.3 Atchafalaya River at 15% Latitude Discharge

6.3.1 Scenario Description

To demonstrate the model's ability to aid in evaluating possible alterations, a model scenario was developed where the upstream boundary discharge during the falling limb of a hypothetical hydrograph, typical of the annual spring floods, is reduced by 50%. This change would effectively change the flow distribution at the Old River Control Structure during the decreasing flow period to 15%/85%. A schematic of this scenario's discharge hydrograph and the typical flow distribution is given below in Figure 6-6: For comparison and to aid in evaluation of the effects, a companion run was performed where the 50% reduction was not applied, with upstream boundary discharge representing the unaltered typical hydrographs. This scenario is referred to as scenario B.

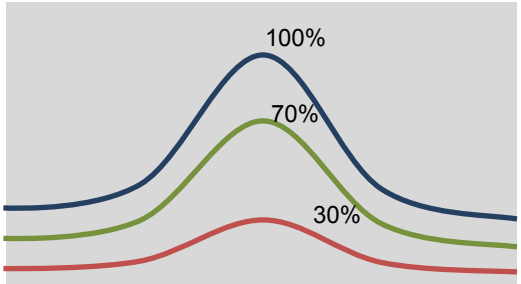

Schematic representation of Mississippi River latitude flow and 30%/70% split. Atchafalaya River discharge in Red.

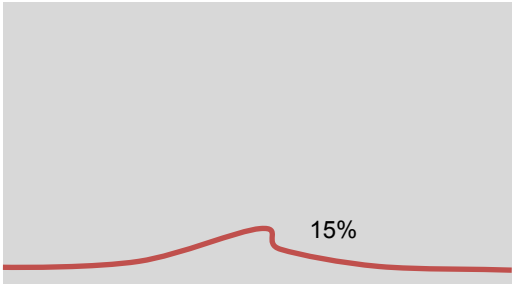

Suggested change to Atchafalaya River Discharge; 50% reduction of flow on the "fall" of the hydrograph.

Figure 6-6: Schematic of preliminary model application scenario B

6.3.2 Boundary Conditions

Figure 6-7: below presents the applied upstream Simmesport discharge for the first trial scenario (scenario B1) and the comparison case of an unaltered typical hydrograph (scenario B0). For both, the flood discharge peaks at approximately 19000 m^3/s, only slightly less than the 2011 peak discharge of over 19700 m^3/s. Discharge for scenario B1 then immediately drops to just over 9500 m^3/s, an approximation of the reduction that would most likely proceed over the course of a few days. Discharge continues to drop and then converges with the unaltered hydrograph at low flow conditions of around 3500 m^3/s.

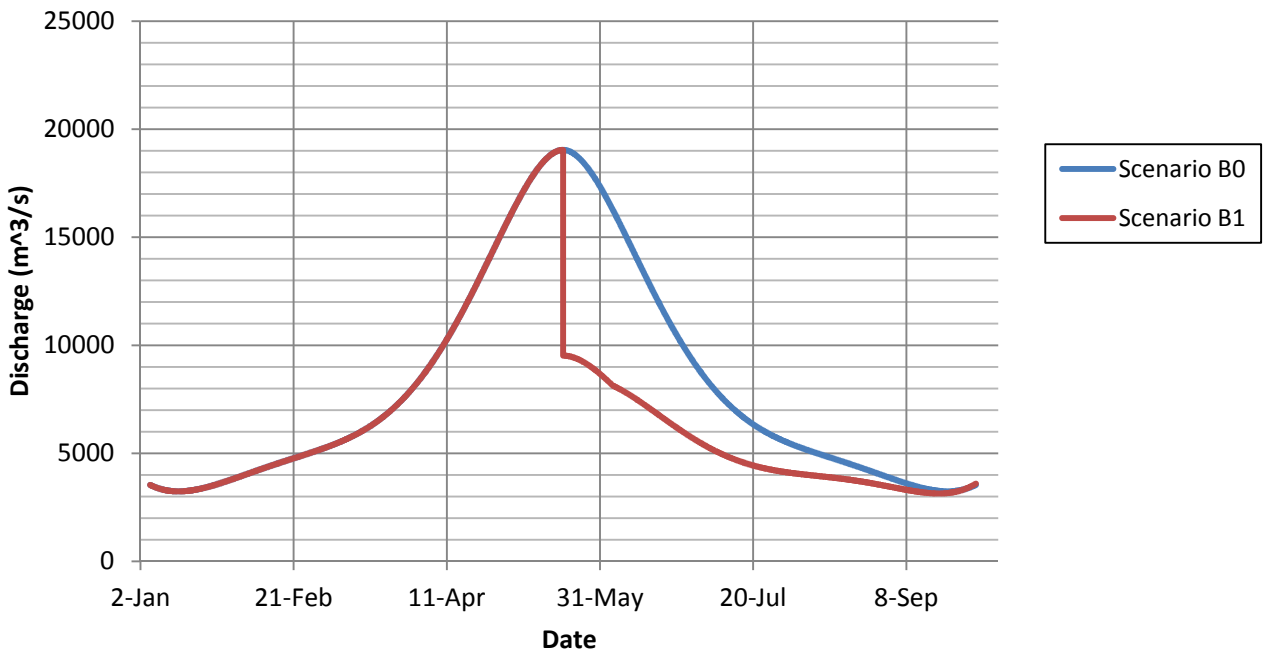

Figure 6-7: Simmesport discharge boundary conditions for scenario B0 (symmetric typical flood hydrograph) and scenario B1 (50% reduction in flow during falling limb)

6.3.3 Scenario Results and Analysis

Figure 7-8 below presents a comparison of time series of calculated water levels for scenario B0 and scenario B1. The time series were extracted at three separate station locations in the upstream, mid-basin, and coastal portions of the model domain (stations 03075, 03645, and 073815925, respectively) to demonstrate variation as the flood propagates downstream.

Figure 6-9: gives the mean difference between scenario water levels during the falling limb of the flood for areas of the model domain that were flooded during the simulations. As expected, the difference is the greatest in the most upstream portions of the model where flood wave amplitude is the greatest. As the flood propagates downstream, it is deformed and modulated with the increasing complexity of the channel networks, so mean differences in water levels decrease. Figure 6-10: gives the mean difference between scenario current speeds at locations in the model domain during the falling limb of the flow hydrograph. In this case, locations of the greatest mean difference are concentrated in the main flow channels regardless of location along the length of the basin. Flow velocities over floodplains for both scenarios are very low to begin with, so the corresponding differences are also very low. Mean differences in current speed in some of the secondary channels, especially in the Upper Bell River area are typically less than in the main Atchafalaya River and outlet channels. This comparison of flow velocities illustrates the spatial extent over which the measure is “felt” throughout the Basin.

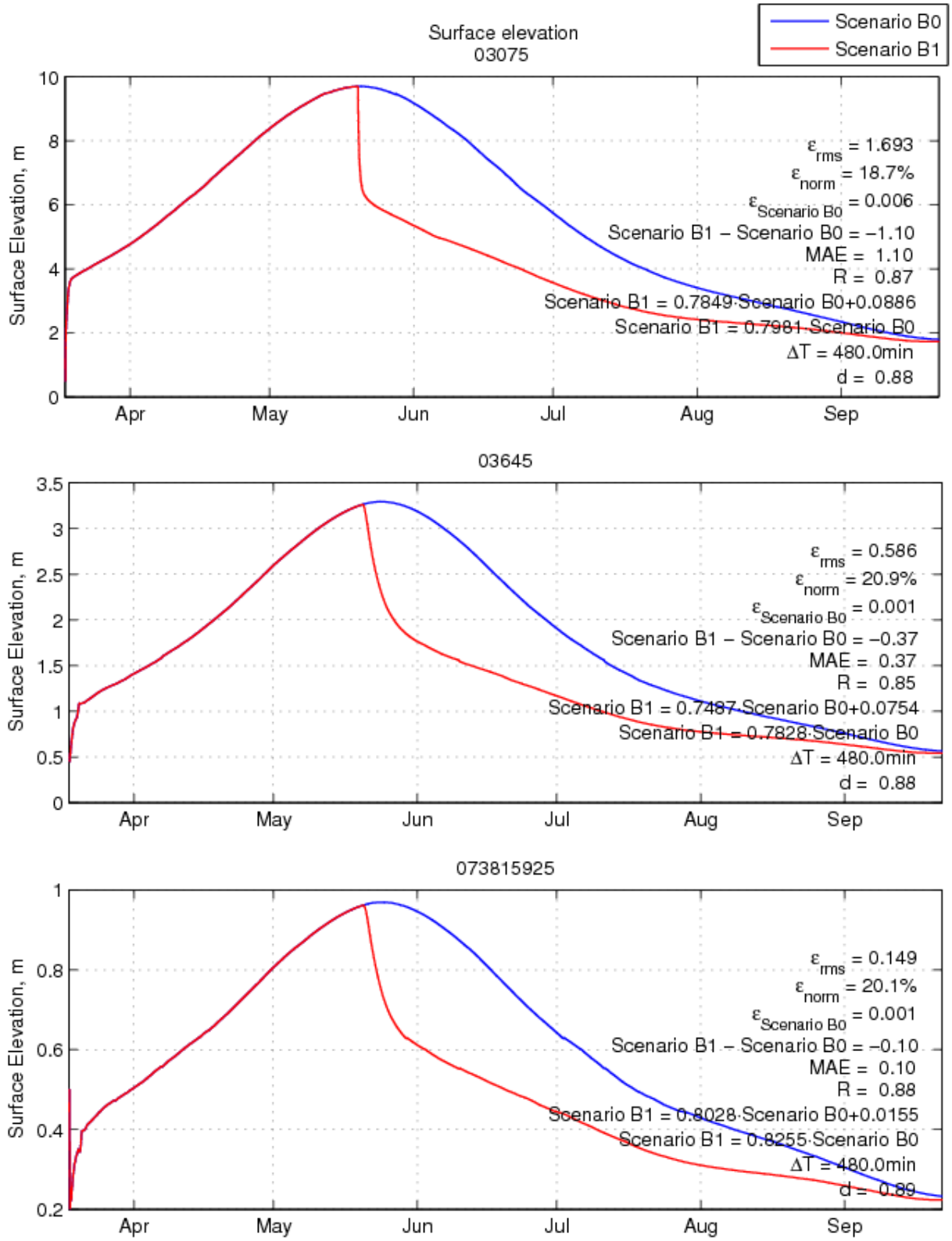

Figure 6-8: Comparison between scenario B0 and scenario B1 water level time series [m] at selected upstream, mid-basin, and coastal stations

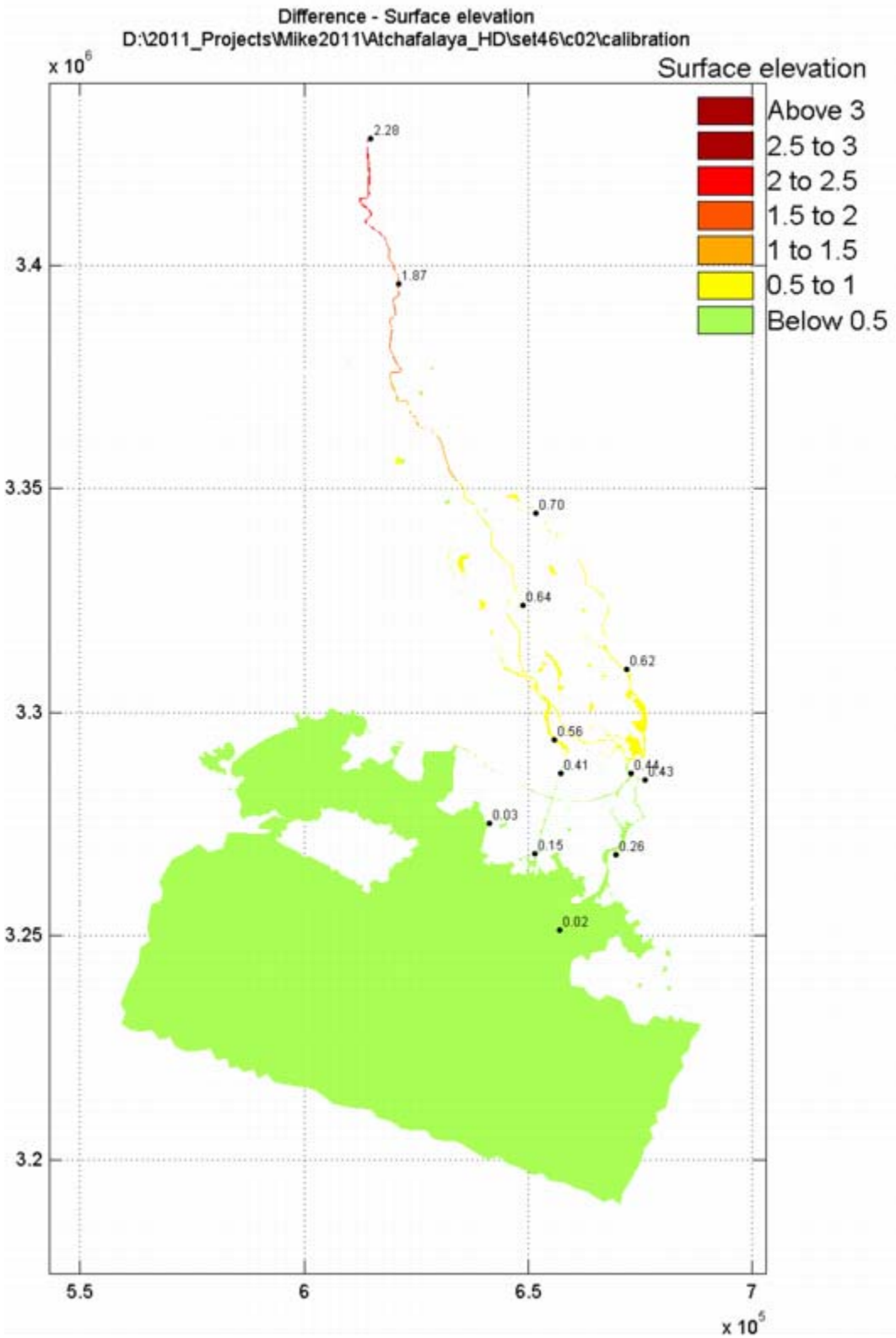

Figure 6-9: Spatial variation of differences between mean water levels [m] during the falling limb of scenarios B0 and B1 hydrographs. Text in the figure gives values at indicated points.

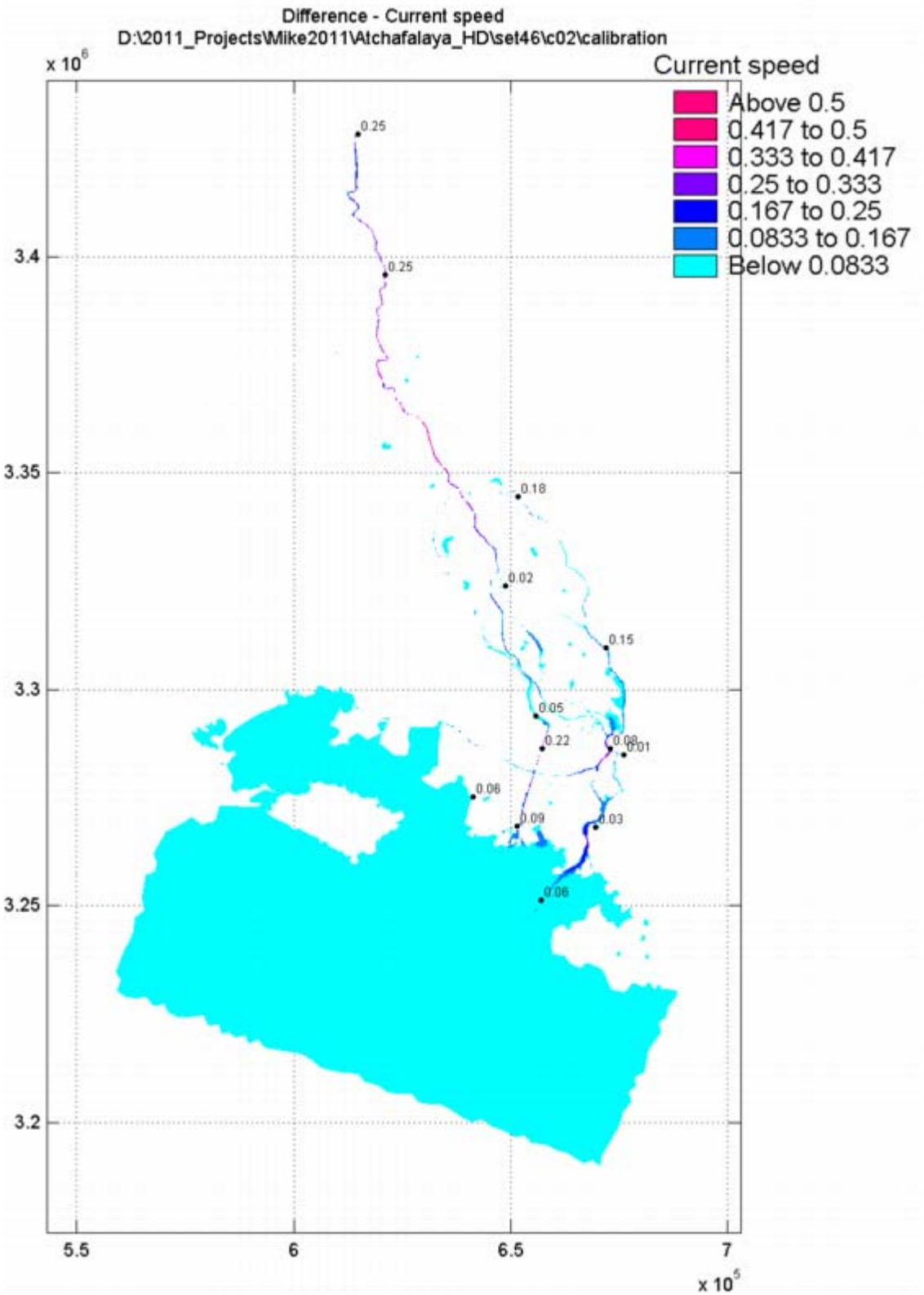

Figure 6-10: Spatial variation of differences between mean current speeds [m/s] during the falling limb of scenarios B0 and B1 hydrographs. Text in the figure gives values at indicated points.

6.4 Synopsis of pre-screening runs

The two model application scenarios presented above, along with the accompanying comparison scenarios, demonstrate the calibrated and validated model's capability to evaluate the various management scenarios. Basin-wide effects are easily evaluated from rather simple water level and current speed comparisons, and the model platform supports the development of more in-depth evaluation tools (use of tracers, etc.). These preliminary scenarios and results can support the development of more specific management alternatives for which the model can then aid in optimization and evaluation.

7.0 CONCLUSIONS AND RECOMMENDATIONS

7.1 Introduction

The objective of this study was to develop a 2D hydrodynamic model of the full Atchafalaya Basin and the Atchafalaya Bay and Coastal Zone for the potential future use of predicting water flow rates, velocities, circulation patterns, depths, and stages resulting from various water management and restoration alternatives. The DHI MIKE21-FM modeling suite was used to develop the model, and substantial data sources from the historic 2011 flood and subsequent low-flow period were then used in the calibration and validation process.

The hydrodynamic modeling was performed using DHI's MIKE21-FM modeling system, a cell-centered, finite volume, 2D, hydrostatic, shallow water hydrodynamic model with possibilities for coupled baroclinic salinity and temperature transport modeling. The flexible mesh option allowed for effective discretization of the very complex system of deep river channels, shallow bayous, swamps, lakes, and bays that form the basin and coastal zone. Both triangular and quadrilateral elements were employed to more efficiently represent the varying flows in coastal areas, floodplains, and channels. The model domain encompasses the full Upper and Lower Atchafalaya Basins, the shallow bay system into which the Wax Lake Outlet and Atchafalaya River discharge, and a portion of the Gulf of Mexico offshore of the coastal bay limits. The domain land boundaries were located to coincide with the extensive levee systems that bound the upstream Atchafalaya channel, the Morganza floodway, the upper basin, and the urbanized areas of St. Mary parish that separate the upper and lower portions of the basin. It was assumed that these boundary levees hydraulically isolate the model domain from the areas to the east and west.

This final chapter reiterates the main conclusions drawn from the study and presents recommendations for further work to improve the model.

7.2 Conclusions

The model bathymetry was compiled from a number of sources and drew from the most recent, highest resolution data available. Though the main channels and floodplain areas were derived from high-quality data, many minor channels that were still important to the basin-wide hydrodynamics lacked sufficient bathymetry information. For these cases, bathymetry was synthesized based on channel orientation, ADCP bottom tracks where available, and engineering judgment.

The model domain was specified to extend into the Gulf of Mexico, encompassing the full Atchafalaya Bay system and extending a sufficient distance both offshore and along the coast to free the open boundaries from influence from the river discharges and upstream water level variation. Here the model was forced with an astronomical tidal signal composed of both water level and velocity fluctuations derived from the most important tidal constituents. At present, residual tidal water levels and any meteorological forcings were not included at the model offshore boundaries. Inflow

discharge boundary conditions were imposed at the upstream Simmesport and Morganza Spillway boundaries. An additional simple source representing outflow from the model domain was imposed downstream of the Avoca Island Cutoff levee.

The model was calibrated using the wealth of measured hydrodynamic data recorded during the 2011 flood, with a primary focus on accurate simulation of upper-basin water levels and the discharge distribution through the Wax Lake Outlet and Atchafalaya River at Morgan City. From the model calibration effort the following is concluded:

- The model simulates water levels very well at most gages, with average absolute differences typically at or below 15 cm.
- The small differences between measured and modeled water level time series at most of the measurement locations over such a large and complex domain indicate high performance in modeling the flood hydrodynamics.
- Stations that had the largest differences between measured and modeled values were generally located in areas of the model domain for which reliable bathymetry sources did not exist and had to be synthesized.
- The discharge distribution through the outlets was very well reproduced with normalized RMS errors of less than 10% at both stations.
- The accurate division of flow between the Wax Lake Outlet and the Atchafalaya River indicates that the large scale distribution of flow in the basin is correctly simulated.
- Errors between measured and calculated discharges through channels in the Upper Bell River region were greater, though the complex shapes of the flow hydrographs were well represented.

To ensure the accurate simulation of hydrodynamics over the full range of possible hydraulic regimes, the model was validated using a low-flow period from early September to late December 2011. From the model validation effort the following is concluded:

- Despite the increased influence of tidal fluctuations during the lower flows, measured water levels throughout the domain were still very well represented in the calculations.
- The normalized RMS errors for most gages still remain very low even with the much lower water levels.
- Water level validation results were consistent with the calibration results in that the few gages where results did not agree as well have the higher error values in both simulations. Again, gages with the highest errors are in areas without reliable bathymetry, and the confinement of the low flow in channels could compound the effects of unrepresentative bathymetry.

- Again, the discharge distribution through the two outlets was very accurately simulated. Normalized RMS errors did increase slightly over values from the calibration but were still approximately 10% or less.

- Channel-averaged currents are very well represented at the three discharge stations as well.

- Overall, the validation results for both water levels and discharges were very good and confirm the model's ability to accurately simulate the hydrodynamics of the basin even during low-flow conditions.

Finally, two example model application scenarios were presented. The two simulations, representing a 50% drawdown in flow after a flood peak and a discharge pulse during a low flow period, demonstrate the calibrated and validated model's capability to evaluate various potential management scenarios. These preliminary scenarios and results can support the development of more specific management alternatives for which the model can then aid in optimization and evaluation.

7.3 Recommendations

Although the model accurately reproduced hydrodynamics over such a large and complex domain for both the model calibration and validation, opportunities for further work in several areas exist that could potentially improve model behavior. From the conclusions presented above and other observations made throughout this report, the following recommendations are made:

- As previously discussed, bathymetry for most of the channels in the Upper Bell River region, including Upper Grande River, Bayou Sorrell, Old River, and the GIWW, lacked reliable sources so was synthesized. During the calibration and validation, it was found that errors between measured and calculated water surface elevations were highest in this region. Hydrographic surveys of the channels in question would most likely enable much improved performance at these gages, bringing errors in line with the very small values observed in the rest of the model domain.

- Though present in the measured water level time series for the coastal stations, meteorological forcings were not included in the offshore model water level boundary conditions which were solely derived from tidal constituents. Incorporating the measured differences between predicted and observed tides into the boundary conditions would enable better comparisons to measured data for model results in the coastal region.

- The Avoca Island Cutoff is an import hydraulic connection between the Atchafalaya River and the coastal marshes of Terrebonne Parish and the GIWW. The connection is currently artificially included in the model. Expansion of the model domain into Terrebonne Parish would aid in understanding the distribution and exchange of flow and zone of influence of the Atchafalaya River

- During the latter part of the 2011 field campaign, the water level and ADCP current meter for the NAS67 station were relocated when water levels fell below

the instrument sensors. Measurements from the new location in the GIWW south of Flat Lake could aid in better representing the flow in the GIWW; however, the station was not vertically referenced so measurements at present are unusable. A survey to relate the gage datum to the NAVD88 vertical datum would provide more measured data for an important region of the model which could be used to improve performance.

- A preliminary vegetation and hydrologic site type map for a large portion of the upper basin was provided by the USGS. Model runs using roughness values derived from this map showed promising results, with errors on the order of those observed in the final calibrated model. More investigation into the use of observed vegetation/site types for roughness derivation is recommended.

8.0 REFERENCES

Allison, M.A., Demas, C.R., Ebersole, B.A., Kleiss, B.A., Little, C.D., Meselhe, E.A., Powell, N.J., Pratt, T.C., and Vosburg, B.M., A water and sediment budget for the lower Mississippi–Atchafalaya River in flood years 2008–2010: Implications for sediment discharge to the oceans and coastal restoration in Louisiana, Journal of Hydrology, Volumes 432–433, 11 April 2012, Pages 84-97, ISSN 0022-1694, 10.1016/j.jhydrol.2012.02.020.

Chow, V.T.,1959, Open Channel Hydraulics, McGraw-Hill, New York, NY

Egbert & Erofeeva, 2010, OTIS Regional Tidal Solutions: Gulf of Mexico 1/45°, retrieved November 1, 2011, from http://volkov.oce.orst.edu/tides/region.html.

ENCOS, 2012. Decommissioning Report for the Atchafalaya Basin Hydrologic Model Project, report submitted to Moffatt & Nichol Engineers, Baton Rouge, LA

John Chance Land Surveys, 2012. Survey Report: National Audubon Society Water Level Stations, submitted to the National Audubon Society, Baton Rouge, LA.

Julien, Pierre Y., 1998. Erosion and Sedimentation. Cambridge University Press, Cambridge, United Kingdom.

Lake Pontchartrain Basin Foundation and Coalition to Restore Coastal Louisiana. 2007. Comprehensive Recommendations Supporting the Use of Multiple Lines of Defense Strategy to Sustain Coastal Louisiana, draft report, http://www.mlods.com/2007draftreport.html.

Moffatt & Nichol. 2000. Barataria Basin, Existing Data and Numerical Model Review and Analysis, submitted to the State of Louisiana Department of Natural Resources. Raleigh, NC.

Moffatt & Nichol, 2009a. Work Plan for Development of Hydrodynamic and Salinity Models of the Atchafalaya basin for Evaluating Restoration Alternatives, report submitted to the Audubon Society, Baton Rouge, LA.

Moffatt & Nichol, 2009b. Review of Requirements to Develop a Two-Dimensional Hydrodynamic Model of the Atchafalaya Basin, report submitted to the Audubon Society, Baton Rouge, LA.

Moffatt & Nichol, 2010. Preliminary Data Gaps Analysis for Development of a Hydrodynamic and Salinity Model of the Atchafalaya Basin for Evaluating Restoration Alternatives, report submitted to the Audubon Society, Baton Rouge, LA.

Willmott, C.J. "Some comments on the evaluation of model performance." Bulletin American Meteorological Society 63.11 (1982): 1309-1313.

APPENDIX A

DATA SOURCES PROCESSED

A.1 Water Level Data

A.1.1 USACE Hourly Data

Hourly real time gages the following gages are located within the Atchafalaya Basin (Table A-1). Hourly data has been retrieved for these gages from www.rivergages.com. The used vertical datum for these gages differ, so the table below gives a summary of the source datum and the conversion applied to convert the elevation data to NAVD88 is listed in the last column (source: pers. Communication with G. Brown USACE MVN). All elevation records have been converted to NAVD88 in meters. Subsequently the data time series have been converted to GMT time (day light savings adjustments have been removed).

Table A-1: USACE Hourly Gages

'03045'	'Atchafalaya River at Simmesport (03045)'	'NGVD'	NaN
'03060'	'Atchafalaya River at Melville (03060)'	'Gage'	
'03075'	'Atchafalaya River at Krotz Springs (03075)'	'Gage'	
'40900'	'Bayou Latenache Above Pointe Coupee Drainage Str (40900)'	'NGVD'	
'43500'	'Bayou Latenache Below Pointe Coupee Drainage Str (43500)'	'NGVD'	
'58400'	'Bayou Courtableau above Drainage Structure (58400)'	'NGVD29'	
'03240'	'Whiskey Bay Pilot Channel Below Head (03240)'	'NGVD29'	
'03120'	'Atchafalaya River at Butte La Rose (03120)'	'NGVD29'	-0.04
'03210'	'Bayou La Rompe at Lake Long (03210)'	'NGVD29'	
'03615'	'Keelboat Pass below Lake Chicot (03615)'	'Gage'	
'03645'	'Six Mile Lake NE of Verdunville (03645)'	'NGVD'	
'03830'	'Crewboat Channel at Wax Lake Outlet nr Calumet (03830)'	'Gage'	
'03720'	'Wax Lake Outlet at Calumet (03720)'	'NGVD'	
'64650'	'Bayou Teche at West Calumet Floodgate (64650)'	'Gage'	-1.18
'64700'	'Bayou Teche at East Calumet Floodgate (64700)'	'Gage'	
'76360'	'Bayou Boeuf Lock - East (76360)'	'NGVD'	
'76400'	'Bayou Boeuf Lock - West (76400)'	'NGVD'	
'76480'	'Wax Lake East Drainage Area at Control Structure (76480)'	'NGVD'	
'03780'	'Lower Atchafalaya River at Morgan City (03780)'	'NGVD'	
'52750'	'Lake Palourde near Morgan City (52750)'	'Gage'	
'03820'	'Avoca Island Cutoff south of Morgan City (03820)'	'Gage'	-1.93
'88600'	'Atchafalaya Bay at Eugene Island (88600)'	'Gage'	
'49415'	'Workman Canal near I-10 (49415)'	'NGVD'	
'49570'	'Upper Grand River (Flood Water Side)(49570)'	'NGVD29'	-1.49
'49725'	'Little Bayou Sorrel At Junction with GIWW (49725) '	'Gage'	
'88800'	'East Cote Blanche Bay at Luke''s Landing (88800)'	'NGVD'	
'76305'	'Bayou Petit Caillou at Cocodrie (76305) '	'Gage'	

After a thorough inspection of the data available at the listed stations, the following were omitted for inclusion in the model since no or very limited data was available for the period of interest; “03240’, “03210”. Other stations were omitted since they did not lie within the Atchafalaya Basin, but just outside the basin behind control structures such as floodgates and locks: “40900”, ‘58400”, “64650”, “64700”, “76360”, “76480”.

The following table list the stations used in the model and designated as model output save locations (USACE_stations.xyz). The USACE hourly Water level stations are depicted in Figure A-1:.

Table A-2: USACE water level stations

ID	X [UTM15 in meter]	Y [UTM15 in meter]
3045	614743.3	3428282
3060	621051.1	3395990
3075	618767.8	3382472
40900	621274.1	3400228
43500	621308.3	3400171
58400	609413.5	3378537
3240	625927.7	3362204
3120	626314.6	3350696
3210	635711.1	3345467
3615	648882.9	3324051
3645	655686.7	3293934
3830	651587.9	3268836
3720	657424	3286397
64650	657179.3	3287091
64700	657855	3286891
76360	676967	3285063
76400	676051.1	3285015
76480	662554.7	3280320
3780	673098.3	3286483
52750	675342.9	3289074
3820	669635	3268354
88600	657044.4	3251077
49415	638616.8	3362546
49570	651740.2	3344695
49725	677114.5	3297521
88800	641383.7	3275473
76305	727084.9	3237424

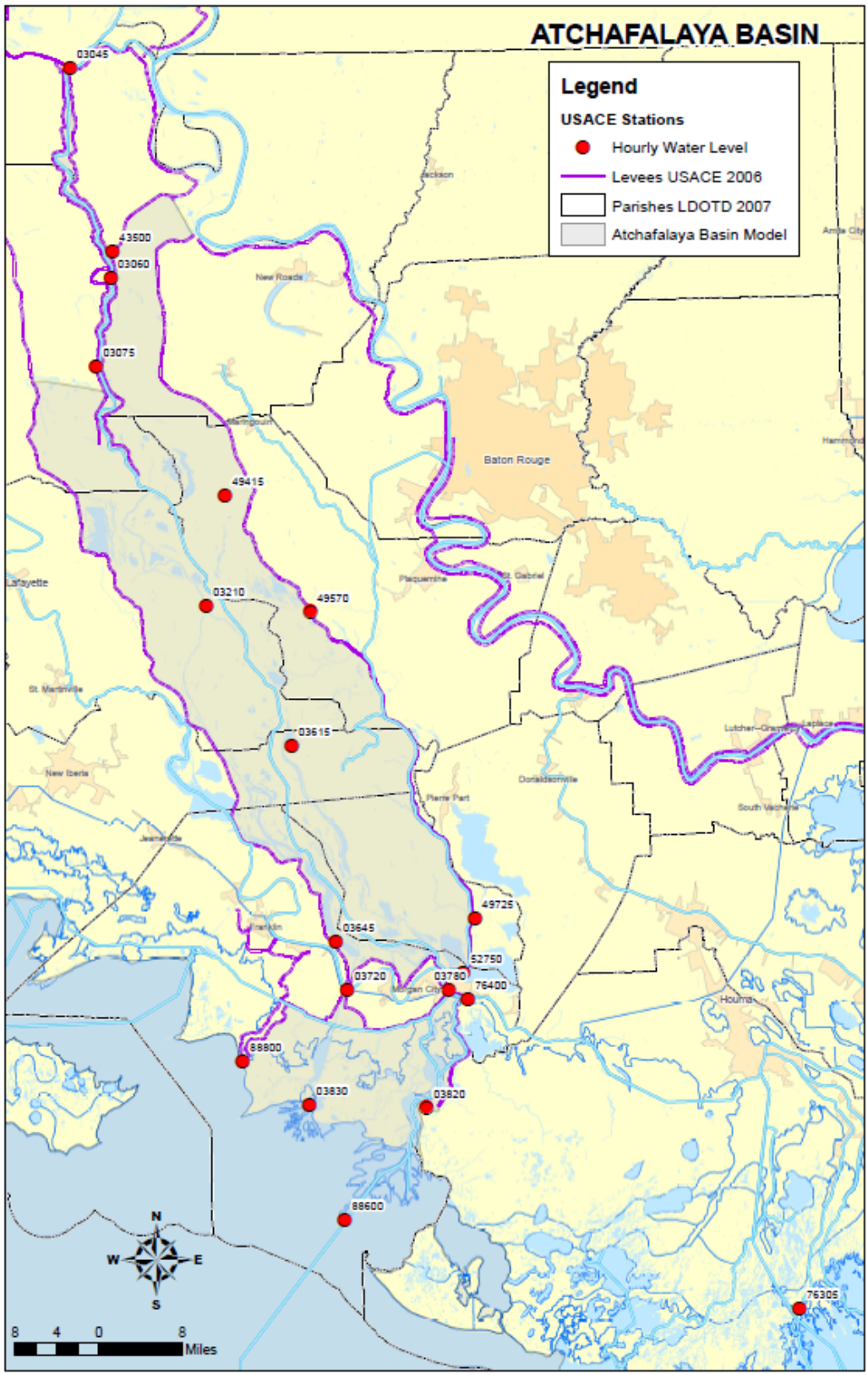

Figure A-1: USACE hourly gages

A.1.2 USACE Daily Data

Several more gages operated by the USACE record water level measurements on a daily basis. The ids and coordinates for the USACE daily gages that were used in the model are given below in Table A-3: . The measured data for these gages was retrieved from http://www.mvn.usace.army.mil/eng/edhd/wcontrol/atch.asp. Similar to the hourly gages discussed above, gage vertical datums were not consistent. Table A-4: gives the adjustments used to convert elevations to NAVD88 for several of the gages (source: personal communication with O. Orwick, USACE MVN). All adjusted elevations were then converted to meters and measurement times converted to GMT.

Table A-3: USACE daily gages

Gage ID	east_UTM15	north_UTM15
03315	641889.01160	3346361.06500
03550	642890.35200	3308871.00900
46375	609705.45210	3378657.19400
46750	609788.20980	3378380.93500
49195	632977.28330	3327898.46600
49630	661591.23950	3334378.17000
49690	672066.36250	3309747.10000
03830D	655614.48980	3267751.61800

Table A-4: USACE daily gage datum adjustments

Gage ID	NAVD88 adjustment (ft)
03550	-1.12
03555	-0.71
46375	-0.46
46750	-0.45
49195	-0.52
49630	-0.88
49690	-1.12

A.1.3 USGS Data

Measured water level data from gages in the basin operated by the USGS were available from the USGS National Water Information System site (http://water.usgs.gov/data.html). The most recent recorded data that had not yet been posted to the website was obtained directly from the USGS. The data was downloaded, adjusted to NAVD88 if needed, converted to meters, and shifted to GMT time reference. Table A-5: below gives the datum information for each gage in the second column and, if

available, an adjustment value to NAVD88 (source: personal communication with D. Walters, USGS, Baton Rouge, LA). The locations of the USGS water level gages are given in Figure A-2: below.

Table A-5:USGS water level gage datum information

ID	vertical gage Datum
07381450	3.81 ft. below NAVD88
07381490	NGVD29
07381515	NGVD29
073815450	NAVD88
07381567	NGVD29
07381590	0.56 below NAVD88
073815963	Not Determined
07381600	0.45 below NAVD88
073816501	Not Determined
07381654	Not Determined
07381670	NAVD88
07385820	Not Determined
07385835	Not Determined
07387040	NAVD88
07387050	Not Determined
293229091230800	Not Determined
294736091164200	Not Determined
295011091184300	Not Determined
295447091191500	Not Determined
300312091320000	NGVD29
301002091344100	Not Determined
302020091435700	NAVD88
303314091414900	Set to COE staff gage, datum = ?

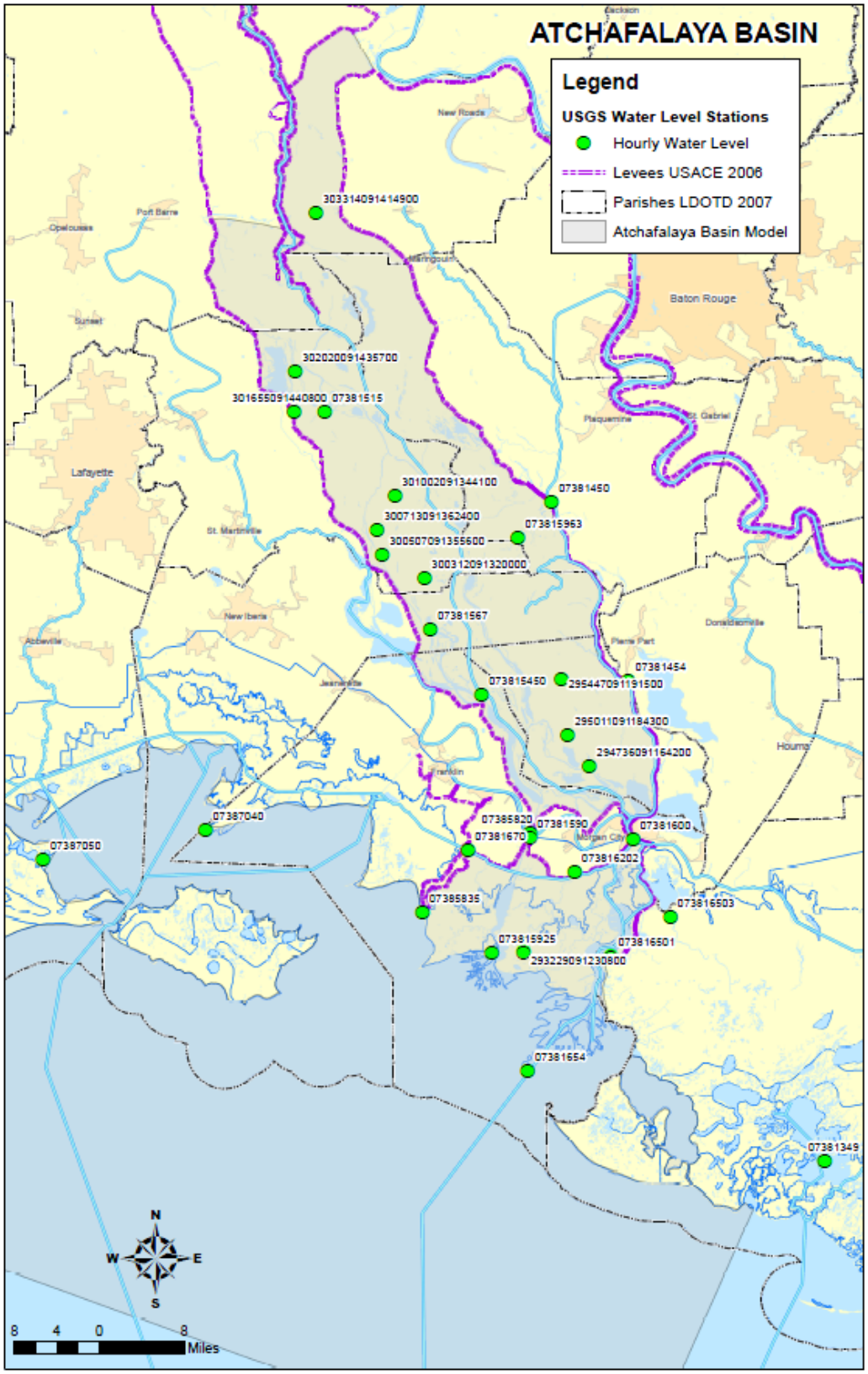

Figure A-2: USGS water level gages

A.1.4 CRMS data

The Louisiana Office of Coastal Protection and Restoration operates a system of gages, the Coastwide Reference Monitoring System (CRMS), along the Louisiana Coast for the purpose of measuring the performance of CWPPRA projects by recording various hydrographic, geologic, and biological parameters. For the present study, the two parameters of interest were the water surface elevation above the NAVD88 datum and the salinity measured in PPT. Of the many CRMS gages along the coast, a total of 16 were selected to use for model comparisons based on their location within the model domain and the quality and availability of the needed parameters during the period of interest. The selected CRMS gages and their locations are presented in Figure A-3:. All available data for the full period of record for each gage was obtained through the LADNR OCPR SONRIS data system. The water surface elevation data, already referenced to the NAVD88 datum, only needed to be converted from English to metric units. The measurement times were referenced to the local time zone including adjustments for daylight savings time, so the full record was shifted to reference GMT without daylight savings time adjustments. Finally, only water level measurements during the period of interest for this study (later than approximately 1 Jan. 2011) were written to time series for comparison with model results.

Table A-6:Selected CRMS gages

gage_ID	shortid	type	east_UTM15	north_UTM15
CRMS0305-H01	CRMS0305	CRMS	674860.30340	3252497.24100
CRMS0463-H01	CRMS0463	CRMS	662543.04760	3263525.88300
CRMS0479-H01	CRMS0479	CRMS	650292.32310	3266994.03800
CRMS0489-H01	CRMS0489	CRMS	641203.13920	3275496.95800
CRMS0493-H01	CRMS0493	CRMS	620055.29890	3292364.28400
CRMS0517-H01	CRMS0517	CRMS	638183.37680	3280048.75400
CRMS0527-H01	CRMS0527	CRMS	610595.69400	3287382.19500
CRMS0532-H01	CRMS0532	CRMS	601584.00560	3299868.62000
CRMS0549-H01	CRMS0549	CRMS	610690.55520	3300696.78000
CRMS4014-H01	CRMS4014	CRMS	662479.08000	3269939.65500
CRMS4782-H01	CRMS4782	CRMS	650740.89490	3282658.36200
CRMS4808-H01	CRMS4808	CRMS	653391.51170	3279436.34200
CRMS4809-W01	CRMS4809	CRMS	653059.98900	3280891.97200
CRMS4900-H01	CRMS4900	CRMS	668522.25530	3279597.07900
CRMS6038-H01	CRMS6038	CRMS	659527.99730	3276125.80100
CRMS6304-H01	CRMS6304	CRMS	666985.72480	3255800.54000

Figure A-3: Selected CRMS gages

A.2 Current Velocity and Discharge Data

A.2.1 USGS Data

Current velocity and discharge measurements were also available at several USGS stations within the basin. Again, the bulk of the data was downloaded from the USGS National Water Information System, with the most recent measurement values obtained directly from the USGS. The measured current and discharge values were first converted from English to metric units. Measurement times were then shifted to GMT with any daylight savings time adjustments removed. The gage id's and transect start and end coordinates in meters, UTM15 for the USGS current velocity and discharge gages are given below in Table A-7:.

Table A-7:USGS current velocity and discharge gages

Gage ID	start_east	start_north	end_east	end_north
07381490	614097.00000	3428117.00000	614657.00000	3427622.00000
07381590	657077.00000	3286556.00000	657597.00000	3286304.00000
07381600	672566.00000	3286184.00000	673179.00000	3286341.00000
07381670	647980.30000	3284450.20000	647889.10000	3284308.90000

A.2.2 USGS Synoptic Data

Synoptic measurements of discharge during the 2011 flood at various locations within the Atchafalaya Basin were available from the USGS. The data was provided in the form of a summary spreadsheet containing id's, coordinates, measurement time, velocity, discharge, flow area, and other parameters for each measurement location as well as the raw output files from the survey instruments for each location. For comparison to model results, the measurements were first grouped by location then written as time series where each instantaneous synoptic measured value was assumed to be a constant value for the full day on which the measurement was taken. Measured values were also converted from English units to metric. Because of the large scale of the model domain and Atchafalaya Basin discharges, it was assumed that measured discharges of less than 100 m^3/s would be very difficult to reproduce and could be considered negligible to the modeling of the 2011 flood; thus, any synoptic locations where measured discharge did not exceed 100 m^3/s were omitted. The measurement locations and ids are given in Figure A-4:. The location ids were assigned sequential numbered prefixes to aid in comparison processing which are given in the table but not in the figure.

Table A-8: Selected USGS synoptic measurement locations

gage_ID	shortid	type	east_UTM15	north_UTM15
USGS102_Atchdistrib	USGS102	USGS	650752	3307028
USGS072_BA18Phillips_at_atch	USGS072	USGS	646481	3329443
USGS074_BA21lkfausseptcut	USGS074	USGS	634265	3329609
USGS066_BA23Atchafalaya	USGS066	USGS	641913	3338194
USGS036_BearByu	USGS036	USGS	673132	3295594
USGS106_Big_Bayou_Jessie_nr_Flat_Lake	USGS106	USGS	671620	3294049
USGS051_Bluepoint2	USGS051	USGS	658191	3303560
USGS050_Bluepointchute	USGS050	USGS	657115	3300741
USGS031_ByuLong	USGS031	USGS	675832	3293403
USGS056_Byupigeon	USGS056	USGS	662883	3328562
USGS091_centerlowerlklong	USGS091	USGS	642950	3315441
USGS006_Coon_Trap	USGS006	USGS	647338	3330644
USGS044_DogIslandPass	USGS044	USGS	670073	3293618
USGS035_DogIslandPass2	USGS035	USGS	671588	3294013
USGS101_Epassatch	USGS101	USGS	650279	3307672
USGS034_FlatLakeS	USGS034	USGS	673396	3289866
USGS110_FlatlakeXtotal	USGS110	USGS	673092	3293687
USGS001_GIWW_@_sorrel	USGS001	USGS	658860	3338185
USGS033_GIWW3	USGS033	USGS	673782	3289645
USGS115_giwwNofgrand	USGS115	USGS	650980	3345728
USGS010_GIWWN_of_Old_River	USGS010	USGS	667398	3315922
USGS095_grandlakeE	USGS095	USGS	645299	3310568
USGS096_grandlakeW	USGS096	USGS	645012	3310311
USGS098_grandlkC	USGS098	USGS	646693	3308962
USGS097_grandlkE	USGS097	USGS	646842	3309164
USGS100_grandlknrChicot	USGS100	USGS	649662	3307593
USGS003_Jakes_Byu	USGS003	USGS	649775	3334678
USGS014_Little_byu_long_@_EGL	USGS014	USGS	657787	3308307
USGS088_lkfausseptcut	USGS088	USGS	641627	3318098
USGS092_lowerlklong	USGS092	USGS	642640	3316550
USGS011_Old_River	USGS011	USGS	666966	3314319
USGS005_Sorrel_@_Atchafalaya	USGS005	USGS	647010	3332821
USGS024_Thibideaux_@Schwing	USGS024	USGS	656657	3306154
USGS004_Unnamed_Byu	USGS004	USGS	647592	3332822
USGS113_uppergrand@giww	USGS113	USGS	650924	3345575
USGS094_Wlowerlklong	USGS094	USGS	642558	3315198
USGS112_workcanal	USGS112	USGS	641222	3346828

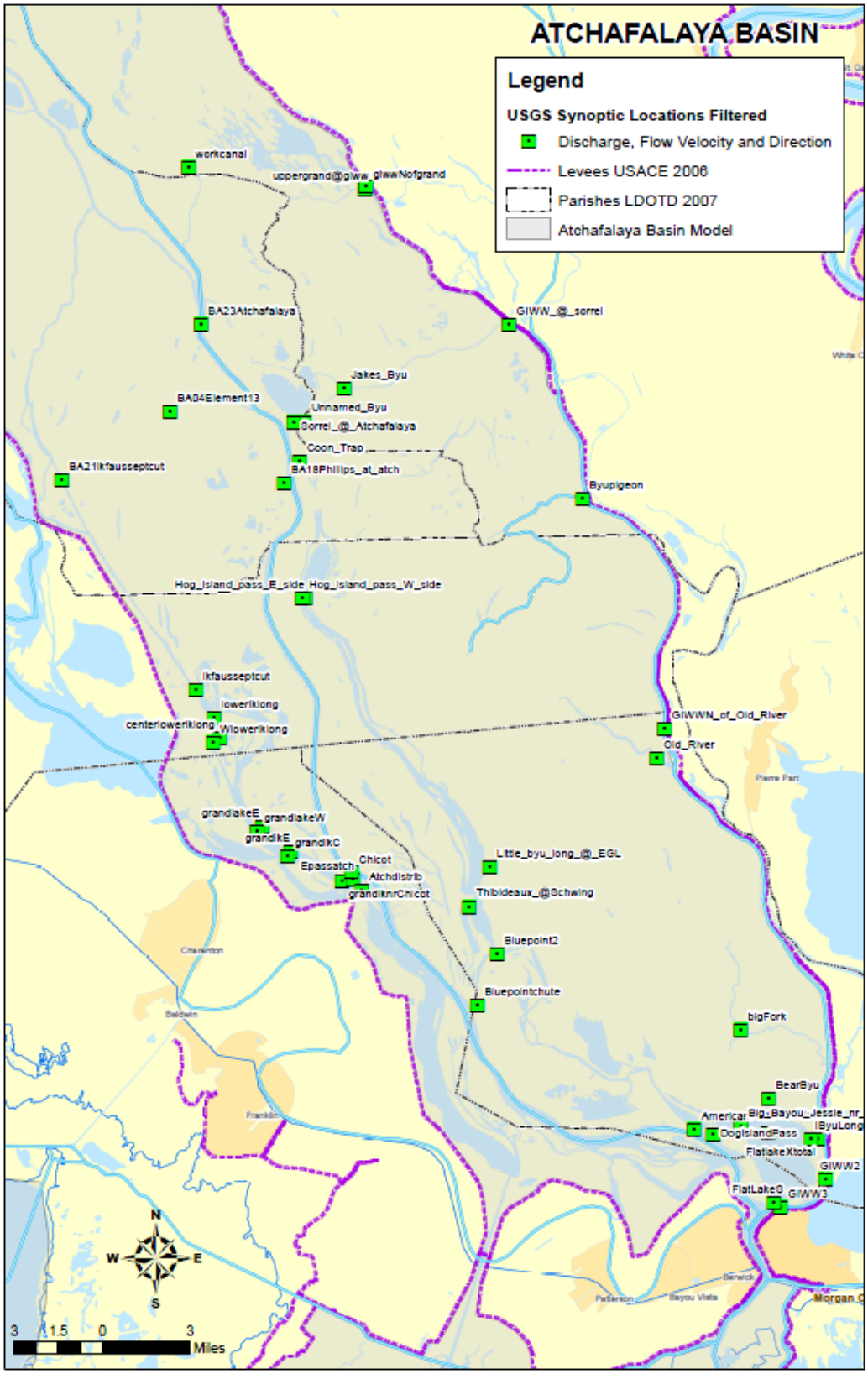

Figure A-4: Selected USGS synoptic measurement locations

A.2.3 NAS Data

The ADCP measurements at the two NAS discharge stations consisted of continuous current speed and direction values measured at the instrument depth and at regular intervals (referred to as bins) across the channel transect. The height of the instrument sensor above the transect bottom was also known. Additionally, a bottom depth profile was measured across the transect at a known time. The co-located water level gage allowed for conversion of depth values to vertically-referenced elevation values for all times based on the relationship derived from the single simultaneous depth/water surface elevation measurements. By the time of the bottom depth transect survey, water levels had dropped below the sensor elevation at the NAS67 stations while NAS89 continued to return valid measurements. To still be able to convert depths to bottom elevations at the NAS67 transect, the water level time series was extrapolated beyond the end of measurements by assuming a constant relationship between measured water levels at stations NAS89 and NAS67. The first task was to convert each instantaneous current speed measured at a single point over the channel depth into a representative depth-averaged value. The point current speed measurement was fit to an analytical expression for the logarithmic velocity profile over a hydraulically rough boundary which was then integrated over the calculated bin depth for depth-averaging (Julien, 1998). An instantaneous incremental discharge for each bin was then calculated using the depth-averaged current speed, the known bin width, and the calculated depth at the horizontal measurement point. At each time step, all the incremental discharges across the channel were summed to get the full discharge through the transect. This value was also divided by the calculated total flow area at each time step so that an accompanying channel-averaged velocity time series could be derived. The resulting measured discharge and current speed records spanned the flood and low flow periods so could be used for both calibration and validation comparisons.

A.2.4 NAS Synoptic Data

Synoptic measurements of discharge and velocity at alternate locations in the basin were also taken by ENCOS near the peak of the 2011 flood. Again, summary information including total discharge, channel-averaged velocity, flow area, and the precise time for each measurement transect location was provided in spreadsheets, and raw output files from the survey instruments were given, containing greater detail about the measurement transect location and individual measured values across the transect. The provided summary information was processed for each measurement location and written to both discharge and velocity time series for comparison to model results. The measurement locations and ids are given in Figure A-5:.

Table A-9: ENCOS synoptic transects

Gage ID	shortid	type	east_UTM15	north_UTM15
AlligatoBayouAtchRiver	alligator	ENCOS	641845.7	3336824
AtchRiverNorth	AtchN	ENCOS	625016.8	3365479
AtchRiverS	AtchS	ENCOS	667757.2	3266005
AvocaIslCutOff	Avoca	ENCOS	670225.7	3268552
BayouL'EmbarrasAtBayouLaRompe	B_Embarr	ENCOS	635716.7	3344344
BayouSchaffer	B_Schaffer	ENCOS	674160.6	3284438
ButteLaRose	Butte	ENCOS	626569.1	3350345
ButteLaRoseN	ButteN	ENCOS	626228.2	3351190
Delta1	Delta1	ENCOS	666814.3	3265582
Delta2	Delta2	ENCOS	665843.1	3262040
Delta3M	Delta3M	ENCOS	668193	3260803
Delta4M	Delta4M	ENCOS	666375.1	3258261
Delta5BM	Delta5BM	ENCOS	663051.5	3256791
HendersonLake(star)	Henderson	ENCOS	625409	3345339
LittleAtchRiverAtAtch	LAtch	ENCOS	626743.2	3362627
LittleDevil	Ldevil	ENCOS	636308.9	3344288
LittleWaxAtchRvrGIWWM	LittleWaX	ENCOS	669315.4	3282005
UnknownAtcha	AtchUnk	ENCOS	644421.4	3333616
WLODelta1M	WLODelta1	ENCOS	652448.6	3272459
WLODelta2M	WLODelta2	ENCOS	653084.4	3270738
WLODelta3M	WLODelta3	ENCOS	651674.7	3268743
WLODelta4M	WLODelta4	ENCOS	649848.9	3266095
WLODelta5M	WLODelta5	ENCOS	649767.6	3264712
WLODelta6M	WLODelta6	ENCOS	650353.6	3264122
WLODelta7M	WLODelta7	ENCOS	651420.2	3264402
WLODelta8M	WLODelta8	ENCOS	652056	3264543
WLODelta9M	WLODelta9	ENCOS	652836	3265167
WLOEastGIWWM	WLO_GIWW_E	ENCOS	656177.2	3280776
WLONorthOfGIWWM	WLO_GIWW_N	ENCOS	656000.2	3282352
WLOSouthOfGIWWM	WLO_GIWW_S	ENCOS	655332	3280377
WLOWestOfGIWWM	WLO_GIWW_W	ENCOS	654351.8	3281244

Figure A-5: ENCOS synoptic transects

A.3 Salinity Data

A.3.1 CRMS Data

As was already mentioned, salinity measurements were also available at the 16 selected CRMS gages in addition to water surface elevation data. The gage locations are given in Table A-6: and Figure A-3: above. The salinity data, measured in PPT, was downloaded from the LaDNR SONRIS website. The measurement times were referenced to the local time zone including adjustments for daylight savings time, so the full record was shifted to reference GMT without daylight savings time adjustments. Finally, only salinity measurements during the period of interest for this study (later than approximately 1 Jan. 2011) were written to time series for comparison with model results.

A.3.2 ENCOS NAS Data

The ENCOS gages deployed during the 2011 field measurement campaign were also capable of measuring and recording salinity levels. Section 2.2.2 describes the rationale for the deployment and the specific gage locations. Salinity measured in PPT was also available at each of the locations given in Figure 2-3:. This data was processed into time series and written to text files for future use in salinity modeling.

A.4 All ENCOS Continuous Data

The following section gives plots of all the continuously-measured data received from ENCOS for this project. Each figure contains all the measured parameters at each NAS gage.

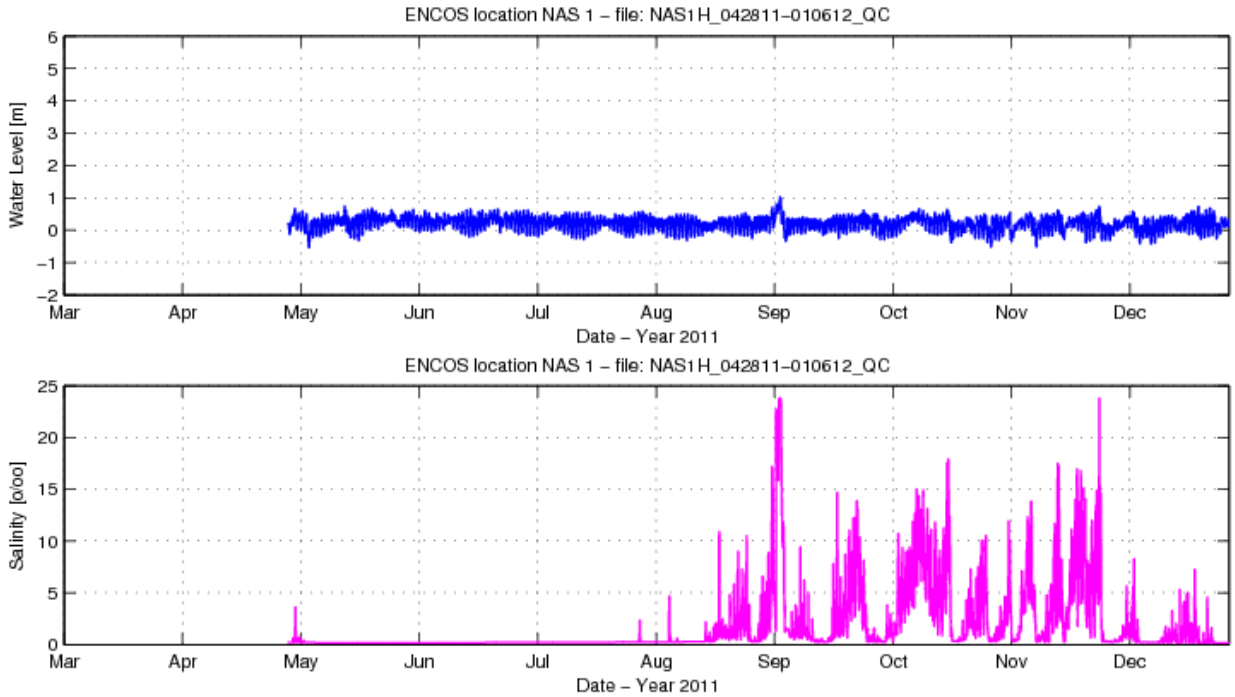

Figure A-6: NAS1H Measured Data

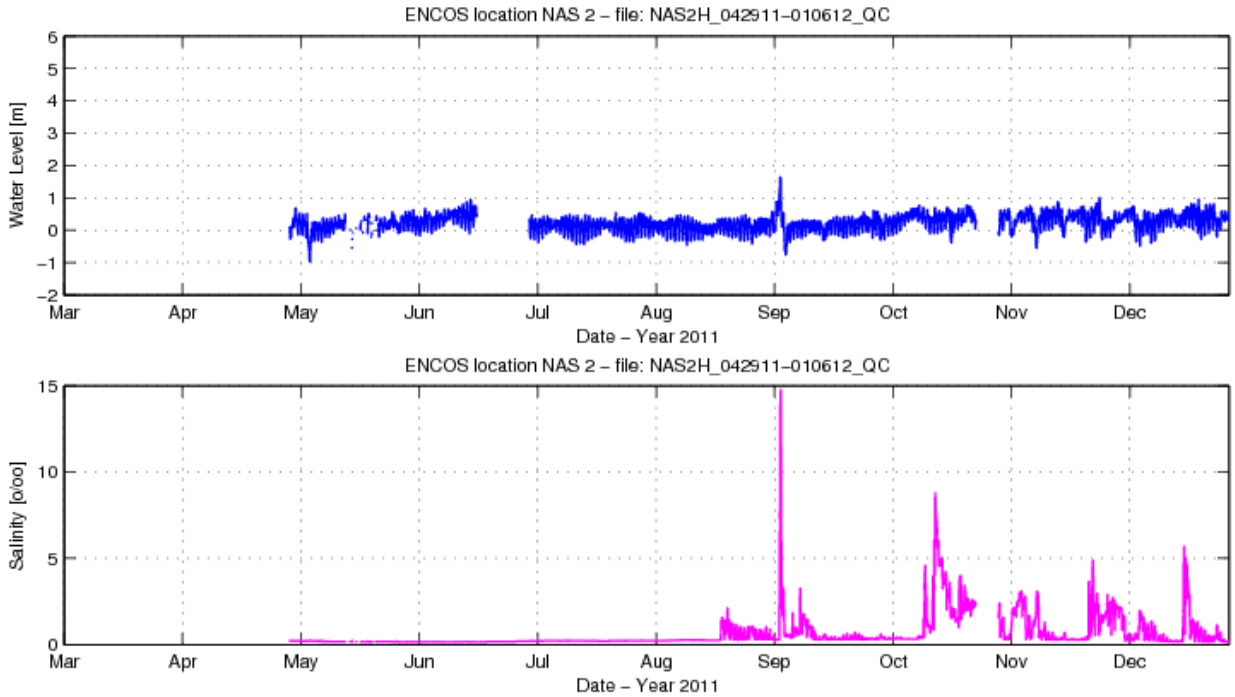

Figure A-7: NAS2H Measured Data

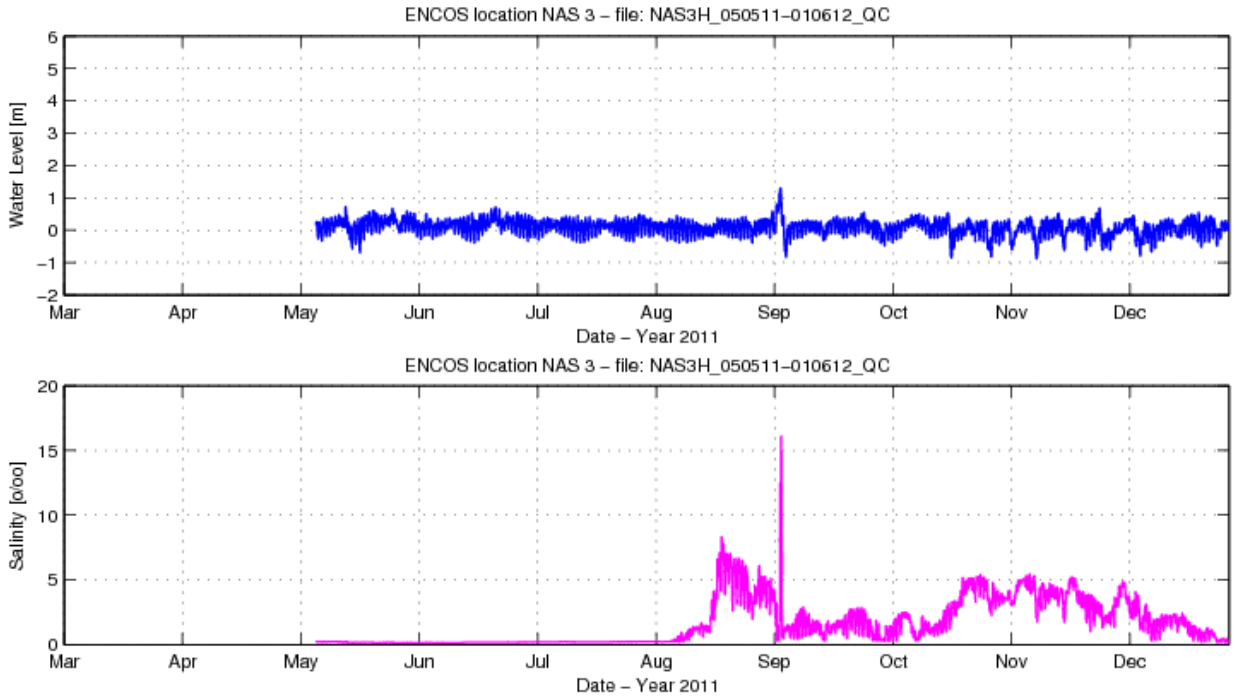

Figure A-8: NAS3H Measured Data

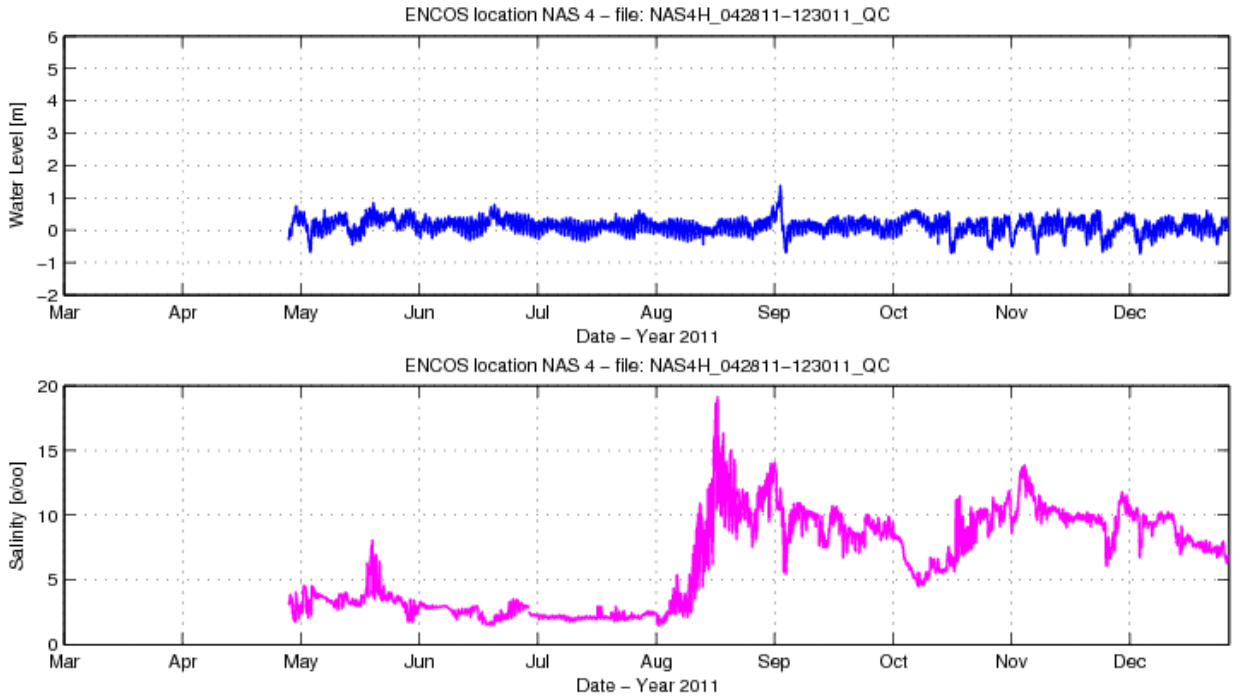

Figure A-9: NAS4H Measured Data

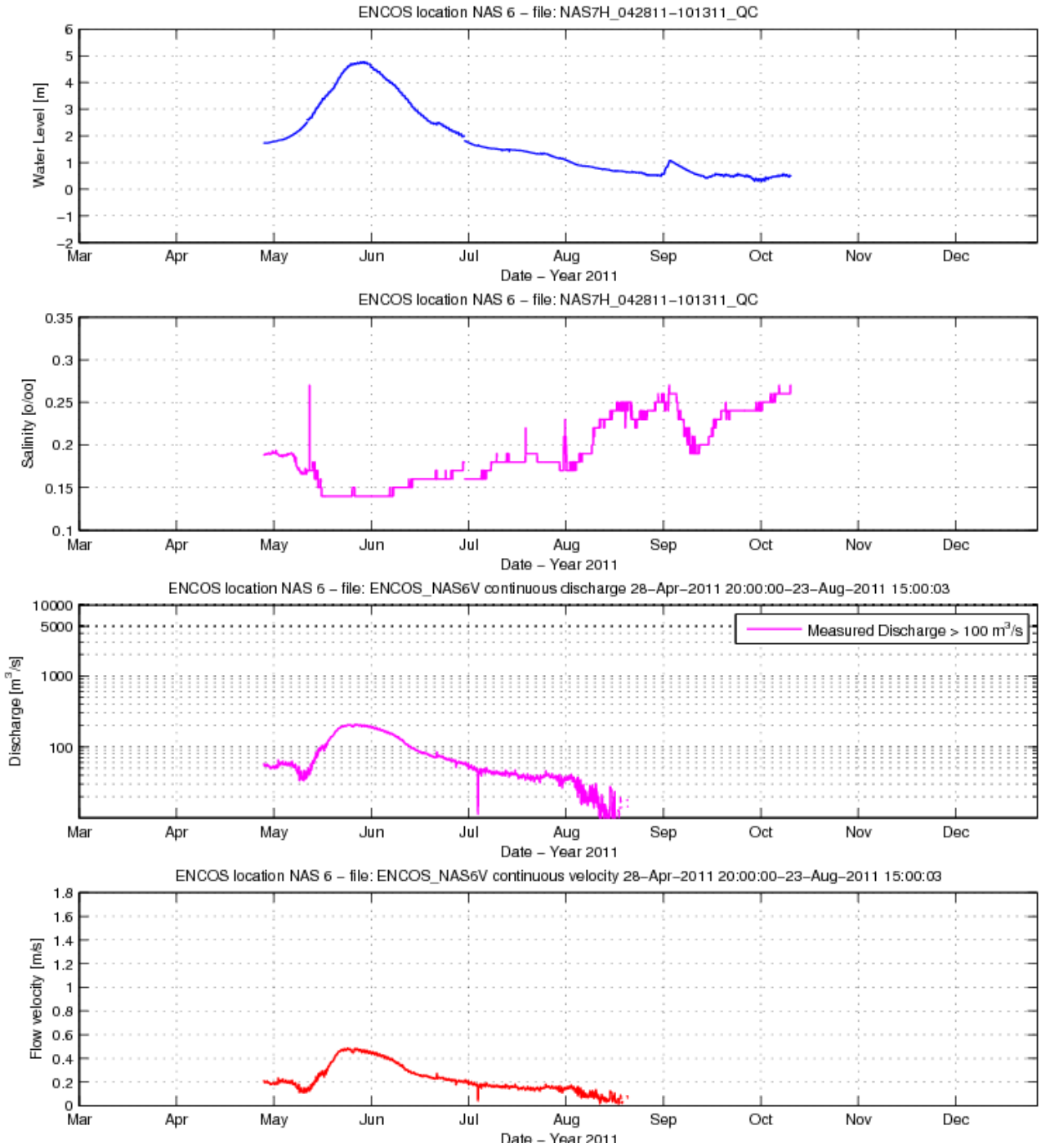

Figure A-10: NAS67 Measured Data

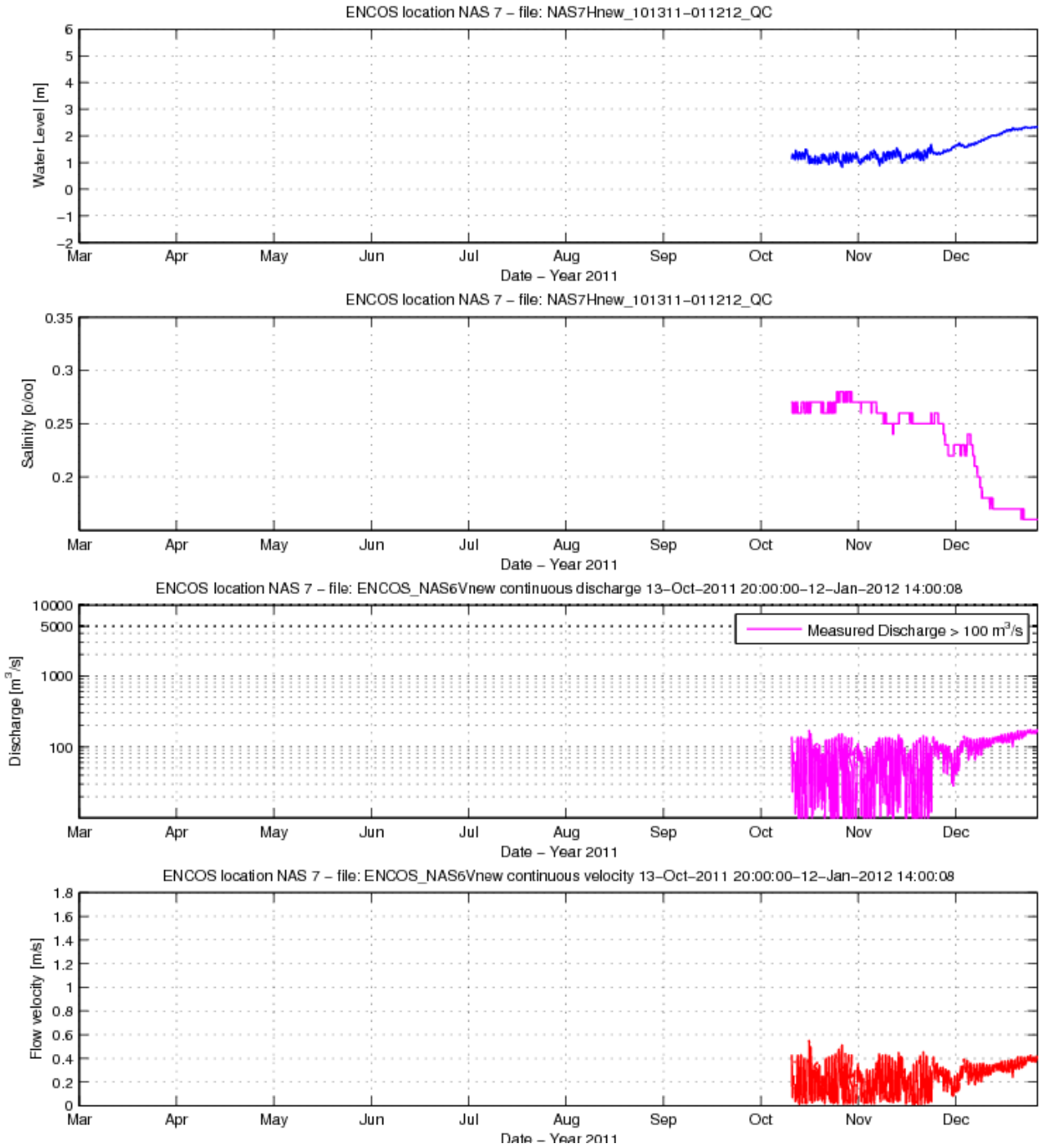

Figure A-11: NAS67new Measured Data

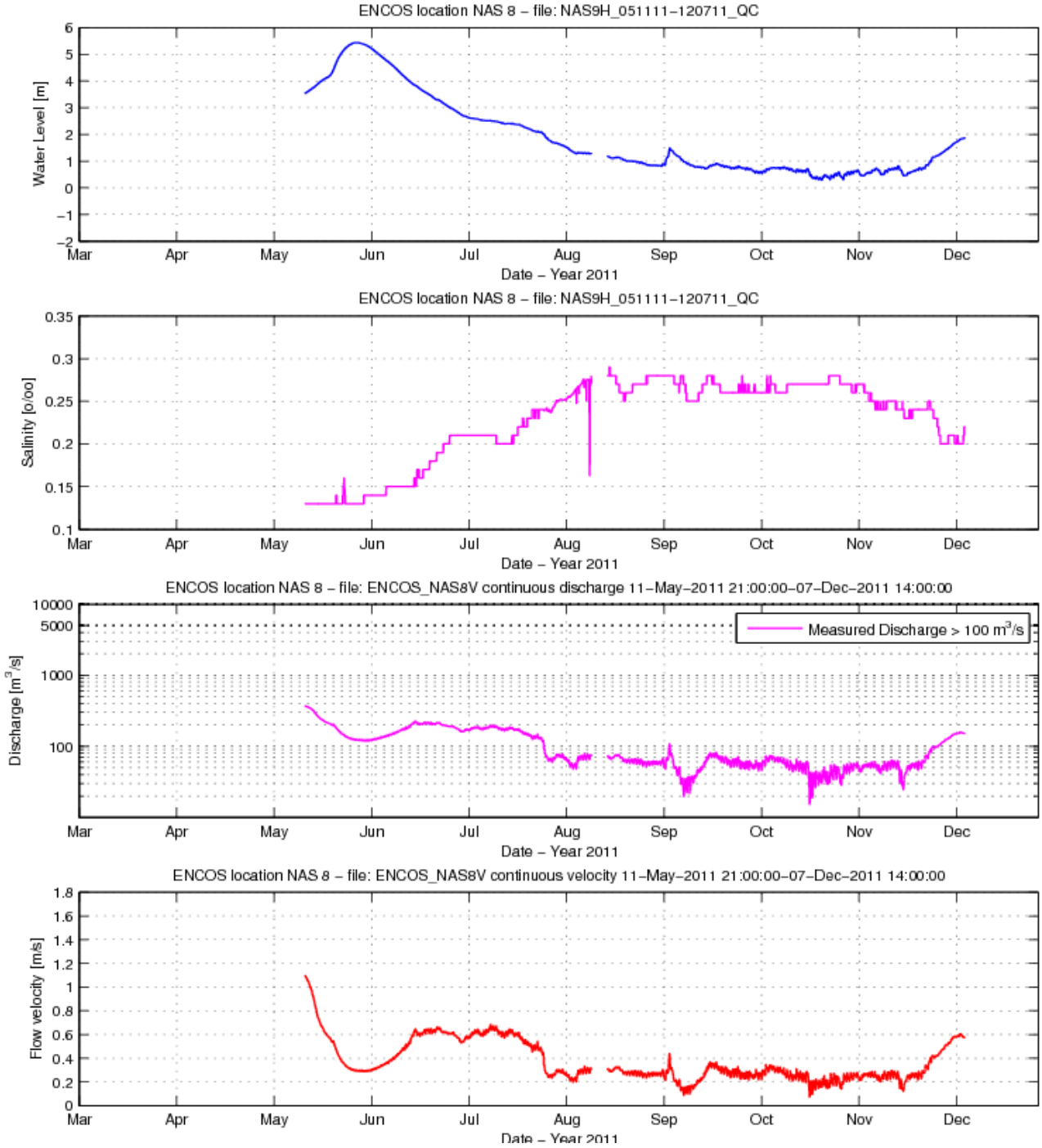

Figure A-12: NAS89 Measured Data

APPENDIX B

ATCHAFALAYA BASIN WATER MANAGEMENT UNITS

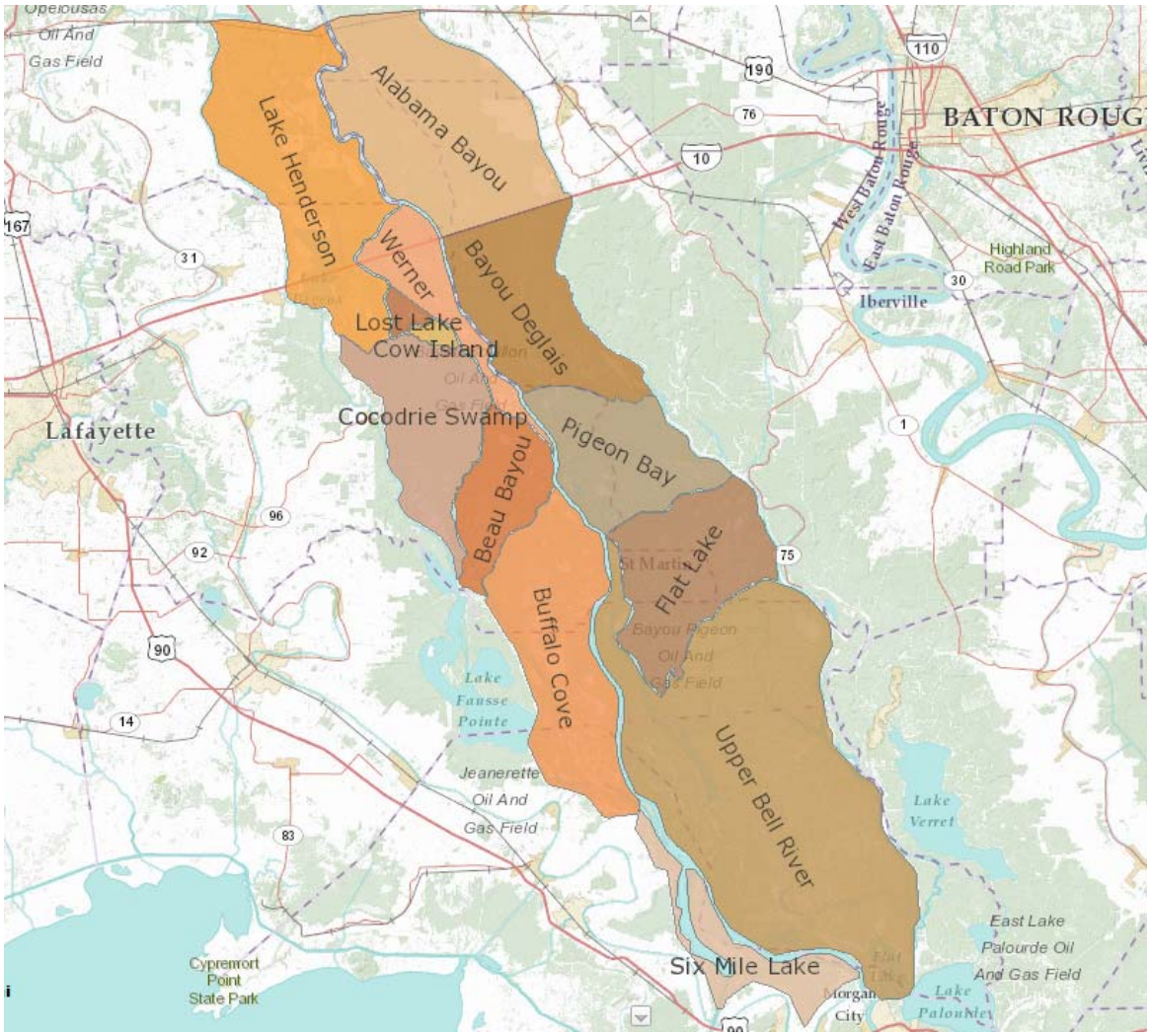

Figure B-1: Atchafalaya Basin Water Management Units (http://abp.cr.usgs.gov/Map.aspx)

APPENDIX C

MODEL CALIBRATION STATISTICS

Several statistical measured were used to help assess the model calibration and validation results. These include the mean error (ME), root mean square (RMS) error, normalized RMS error, correlation coefficient (R), time delay or lag (ΔT), mean absolute error (MAE), and index of agreement (d). These parameters are briefly described here. Let *x* and *y* be the measured and calculated data respectively. Then the following statistics can be calculated:

Mean error (ME):

$$ME = \bar{x} - \bar{y}$$

where "bar" denotes the sample mean.

Root-mean-squared (RMS) error:

$$\varepsilon_{\mathrm{RMS}} = \sqrt{\overline{(\mathrm{x} - \mathrm{y})^2}}$$

To reduce an effect of measurement error and possible outliers, a 12 hour low-pass filter was applied to the measured data and a trend x_f is determined. Then a normalized error is calculated as

$$\varepsilon_{norm} = \frac{\varepsilon_{RMS}}{x_{f,max} - x_{f,min}} * 100\%$$

where $x_{f,max}$ and $x_{f,min}$ are the maximum and minimum values of the trend x_f.

Correlation coefficient *R* was calculated using standard method and represents a non-squared value.

Time delay ΔT shows possible time difference between corresponding events in measured and calculated data. To estimate the delay, the cross-correlation function between measured and calculated data is computed and the smallest time lag at which a maximum of function occurs is determined. Because the cross-correlation function is calculated from discrete data, the resulting time resolution may not be sufficient to accurately define a maximum. Therefore, computed values of the cross-correlation function were interpolated with a piecewise polynomial of 5th order, which was then used to determine the extremum.

Mean absolute error (MAE):

$$MAE = \overline{|x - y|}$$

Model prediction capability was estimated with an index of agreement between measured and calculated data (after Willmott, 1982 and Willmott et al., 1985):

$$d = 1 - \frac{\overline{(x-y)^2}}{\overline{(|x-\overline{x}| - |y-\overline{x}|)^2}}\ , 0 \leq d \leq 1$$

A Hydrodynamic Model of the Atchafalaya Basin

moffatt & nichol

One American Place
301 Main Street, Suite 800
Baton Rouge, LA 70825

August 2012